

UiO • **University of Oslo**

Alexandra Zaputlyeva

**Fluid Geochemistry and Migration Processes
at the Lusi Mud Eruption, Indonesia**

Thesis submitted for the degree of Philosophiae Doctor

The Centre for Earth Evolution and Dynamics
Department of Geosciences
Faculty of Mathematics and Natural Sciences

September 2020



© Alexandra Zaputlyeva, 2020

*Series of dissertations submitted to the
Faculty of Mathematics and Natural Sciences, University of Oslo
No. 2327*

ISSN 1501-7710

All rights reserved. No part of this publication may be
reproduced or transmitted, in any form or by any means, without permission.

Cover: Hanne Baadsgaard Utigard.
Print production: Representralen, University of Oslo.

Principal supervisor:

Dr. Adriano Mazzini

Centre for Earth Evolution and Dynamics, University of Oslo

Subsidiary supervisor:

Dr. Henrik Hovland Svensen

Centre for Earth Evolution and Dynamics, University of Oslo

"If you think you are too small to make a difference, try sleeping with a mosquito."
His Holiness the 14th Dalai Lama.

Preface

This thesis is submitted in partial fulfilment of the requirements for the degree of Philosophiae Doctor at the University of Oslo. The study was carried out at the Centre for Earth Evolution and Dynamics at the Department of Geosciences of University of Oslo, during 2016 - 2020. The research was supported by a 3-year doctoral fellowship from the Department of Geosciences of University of Oslo, European Research Council under the European Union's Seventh Framework Programme Grant agreement n°308126 (LUSI LAB project, PI A. Mazzini), and Research Council of Norway through its Centres of Excellence funding scheme (Project 223272, CEED).

This PhD project focuses on the fluid geochemistry and fluid-rock interaction in the southern part of the East Java sedimentary basin. The study area is neighbouring the Arjuno-Welirang volcanic complex and hosts the world largest ongoing onshore mud eruption Lusi, which activity commenced in May 2006. Approximately half of the studied sample material (rock clasts, oil, gas) was collected during the research expedition to Java in March 2017. The other samples (rock clasts and mud erupted between 2006-2016) were collected earlier and provided by the principal supervisor Dr. Adriano Mazzini. Laboratory work was performed using the facilities of the organic geochemistry laboratory at the Department of Geosciences, University of Oslo and during several research visits to the National Institute of Geophysics and Volcanology (INGV, Palermo, Italy) and to the Federal Institute for Geosciences and Natural Resources (BGR, Hannover, Germany).

The thesis consists of two parts: introduction and scientific contributions. The former part provides the background information on the studied topic, the motivation for the work, description of the applied methods, summary of the papers and the future outlook. The latter part represents a collection of three manuscripts, prepared during the PhD project. The first manuscript, titled “Mantle-derived fluids in the East Java sedimentary basin, Indonesia” (published in the *Journal of Geophysical Research: Solid Earth*) highlights the distribution and migration pathways of the mantle-derived volatiles in the southern part of the East Java sedimentary basin, based on the gas data from the hydrocarbon fields surrounding Lusi. The second manuscript “Recent magmatism drives hydrocarbon generation in north-east Java, Indonesia”, (published in *Scientific Reports*) describes the ongoing hydrocarbon generation driven by the magmatic activity below Lusi. The third manuscript “Extensive oil discharge ongoing at the Lusi mud eruption, Indonesia” (currently in preparation) aims to calculate the amount of erupted mud breccia and oil vented from the Lusi crater during 13 years of its eruptive activity.

The papers were written in collaboration with scientists from several research institutions, including: University of Oslo, Norway, National Institute of Geophysics and Volcanology (INGV), Italy, Federal Institute for Geosciences and Natural Resources (BGR), Germany, and Utrecht University, Netherlands.

The results from this thesis were presented at several international conferences and meetings, including Bubbles International Training School in Tromsø, Norway (2017), General Assembly of DEEP Research School in Geilo (2017) and Bergen (2018), Norway, EGU General Assembly in Vienna, Austria (2018, 2019), International Meeting on Organic Geochemistry in Gothenburg, Sweden (2019), Nordic Geological Winter Meeting in Oslo, Norway (2020).



Field view of the Lusi mud eruption, March 2017

Acknowledgements

“In union there is strength” Aesop

I am sincerely grateful to many people for their direct or indirect contribution and help during my PhD journey, which otherwise would make pursuing a PhD degree unattainable.

I would like to thank my supervisors and particularly the first and foremost **Adriano**. Thank you for guiding me through all these years and sharing your knowledge about geology and beyond. Your incredible enthusiasm, creativity and passion for geosciences always amazed me. Every time I thought something would be impossible, your simple “Just do it!” helped me to move forward! Thank you for organizing amazing fieldtrips and being available nearly 24/7 no matter which day of the week and which continent and time zone you were in. **Henrik**, thank you for your interesting questions and ideas that always helped me to look at scientific problems from a different angle. Discussions with you were always enlightening.

I would also like to thank my collaborators, who happily shared their knowledge with me and helped me with data acquisition and interpretation. **Antonio**, thank you for opening the world of volcanoes to me. Thank you for the warm welcome in INGV and arranging the labwork, for long discussions about noble gases, science, history, and life, as well as for your patience answering myriads of my questions. **Martin and Georg**, thank you for organizing the labwork in the BGR, guiding me in the field of organic geochemistry, and being always so prompt with your help and support. **Alessandra**, thank you for teaching me various field methods and your positive attitude in any situation. **Kristian**, I wish I met you earlier and spent more time in the lab at Geo. Thank you for helping me with all the equipment and all the scientific and non-scientific discussions, it was always a pleasure. **Morgan**, thank you for providing your expertise on mercury geochemistry and help with text editing. **Wolfram**, thank you for introducing me to the world of palynology. I also would like to acknowledge **Jolanta** for sharing the knowledge about organic petrography.

I would like to thank **Giorgio, Isabella, and Kiki** who made my stay in INGV so warm, **Monika** for the cheerful atmosphere, inspiration, and help in the lab in the BGR.

Dear CEEDlings, thank you for the nice social environment. I especially would like to thank **Evgeniy** for the lovely tea breaks and **Sergey** for sharing candies and other carbohydrates. **Sruthi**, thank you for the long discussions and your care. **Vanja**, thank you for your cheerful energy, I wish you were still working at CEED. **Marine**, thank you for your support and sharing your ideas about the Lusi project. **Reidar**, thank you for being so thoughtful and caring all the time. **Trine-Lise**, your particular skill to arrange things the way that everything works smoothly at CEED is amazing! Thank you for the help with all administrative questions and regular nice brief conversations we had on the first floor. **Carmen**, thank you for your support during my years at CEED.

Pursuing the PhD degree would have been impossible without several people from my alma mater - Lomonosov Moscow State University. Dear ladies from 619, **Lenochki and Natalya Petrovna**, thank you for introducing me to the world of the organic geochemistry, you clearly got me addicted to it. **Grigory Georgievich**, you were the first to introduce Lusi to me back in 2011. Then I could have never imagined that I would spend 4 years working on that exciting site later on. Thank you for that first acquaintance and arranging the TTR-18 research cruise, that definitely left a remarkable trace in my life. **Sergey Vladimirovich**, thank you for involving me in many challenging research projects and sharing that constant calmness and confidence that I am doing things right. You were the one who told me that you expect a “book” sent to you in few years when I had zero plans on my future career. How did you predict?

I would also like to take the opportunity to cherish my friendship with dear people outside academic world. **Sunil**, thank you for inspiring me to pursue a PhD degree, believing in me more than I do and for being there anytime I needed no matter what. Your calm nature and wise solutions are priceless. My girls from the Women chat: **Dasha, Galya, Jenya, Nelya, and Tanya**, I am so grateful for your cheering, support and our continuous chats! Although some of you are as far as Canberra, I still feel that we are connected as 10 years ago in MSU! **Masha and Dasha**, ladies you are precious, thank you for being with me last 3 years here in Oslo and sharing laughs and tears. **Sasha**, thank you for the constant boost and inspiration, the weekend breakfast club, dinners, cycling trips, and our endless discussions. I do not know how I would have survived this long quarantine without you. I would also like to note **Karina, Albina, Imane**, and **Sydney**, dears, you are so inspiring!

My dear salsa family, I am not going to try naming all of the bright, warm, interesting, funny, and creative people I have met during last 4 years, otherwise this section would be longer than all next ones. Meeting you, training, and dancing with you, smiling, laughing, travelling – was always recharging and helping me to carry on with my PhD project.

Finally, my dear parents, without your unending love and care I would not be able to go so far on this path. Thank you for your constant support.

Alexandra

07.09.2020

Contents

Preface	1
Acknowledgements	3
Contents	5
Part I Introduction	7
1.1 Aim and scope of the thesis	7
1.2 Large Igneous Provinces	9
1.3 Sediment-hosted geothermal systems	12
1.4 Lusi SHGS	15
1.5 Organic matter, petroleum composition and generation	20
1.6 Organic matter maturation and contact metamorphism	24
1.7 Analytical methods for the study case	25
1.8 Summary of the articles	29
1.9 Outlook	31
References	35
Part II Scientific Contributions	43
Manuscript 1: Mantle-derived fluids in the East Java sedimentary basin, Indonesia	43
Manuscript 2: Recent magmatism drives hydrocarbon generation in north-east Java, Indonesia.	61
Manuscript 3: Extensive oil discharge ongoing at the Lusi mud eruption, Indonesia	89

Part I Introduction

1.1 Aim and scope of the thesis

This study was performed in the framework of an ERC start up grant to study Lusi (the LUSILAB project) - the world largest active mud venting site on Earth. Over ten research institutions in Europe and Indonesia, including CEED-University of Oslo, were actively collaborating in the framework of LUSILAB. This multidisciplinary project aimed to explore the interaction between the erupting Lusi system, the adjacent active Arjuno-Welirang volcanic complex, and the frequent seismicity in the region.

The Lusi mud eruption is located in the southern part of the East Java sedimentary basin (Indonesia) and connected to the Arjuno-Welirang volcanic complex through a system of faults (Mazzini et al., 2009; Mazzini et al., 2012; Fallahi et al., 2017; Moscariello et al., 2018; Obermann et al., 2018) (Figure 1). The continuous Lusi activity is driven by the magmatic intrusion and associated hydrothermal fluid migration within organic-rich deposits at ~4.5 km depth below the vent (Mazzini et al., 2012; Fallahi et al., 2017; Malvoisin et al., 2018; Svensen et al., 2018). Induced high temperature anomaly resulted in carbon-rich gas generation (mainly CO₂ and CH₄), which consequently led to anomalously high pressures at ~4.5 km depth. The reactivation of a pre-existing fault system was followed by the Lusi birth in May 2006. During the last 14 years Lusi has been continuously venting boiling water, mud breccia, oil and gas (Mazzini et al., 2007; Mazzini et al., 2009; Miller and Mazzini, 2018).

Lusi is defined as a sediment-hosted geothermal (hydrothermal) system. It represents a rare modern analogue of the paleo-hydrothermal vent complexes associated with Phanerozoic Large Igneous Provinces (LIPs). The largest paleo-vent systems, documented in the North Atlantic, South Africa, and Siberia, are associated with Paleocene-Eocene, Early Jurassic and end-Permian magmatism, respectively (Jamtveit et al., 2004; Svensen et al., 2004; Svensen et al., 2009). The activity of these systems is supposedly driven by mechanisms similar to one observed at Lusi: vigorous gas generation in contact metamorphic zone resulted in the overpressure build-up and occurrence of the piercement structures. The vast release of greenhouse and toxic gases could have led to rapid climate and environmental perturbations, some of which coincide with known mass extinctions events (Vogt, 1972; Racki et al., 2020 and refs. therein). Therefore, understanding the proper mechanisms and physiochemical processes driving these plumbing systems has major implications for assessing the

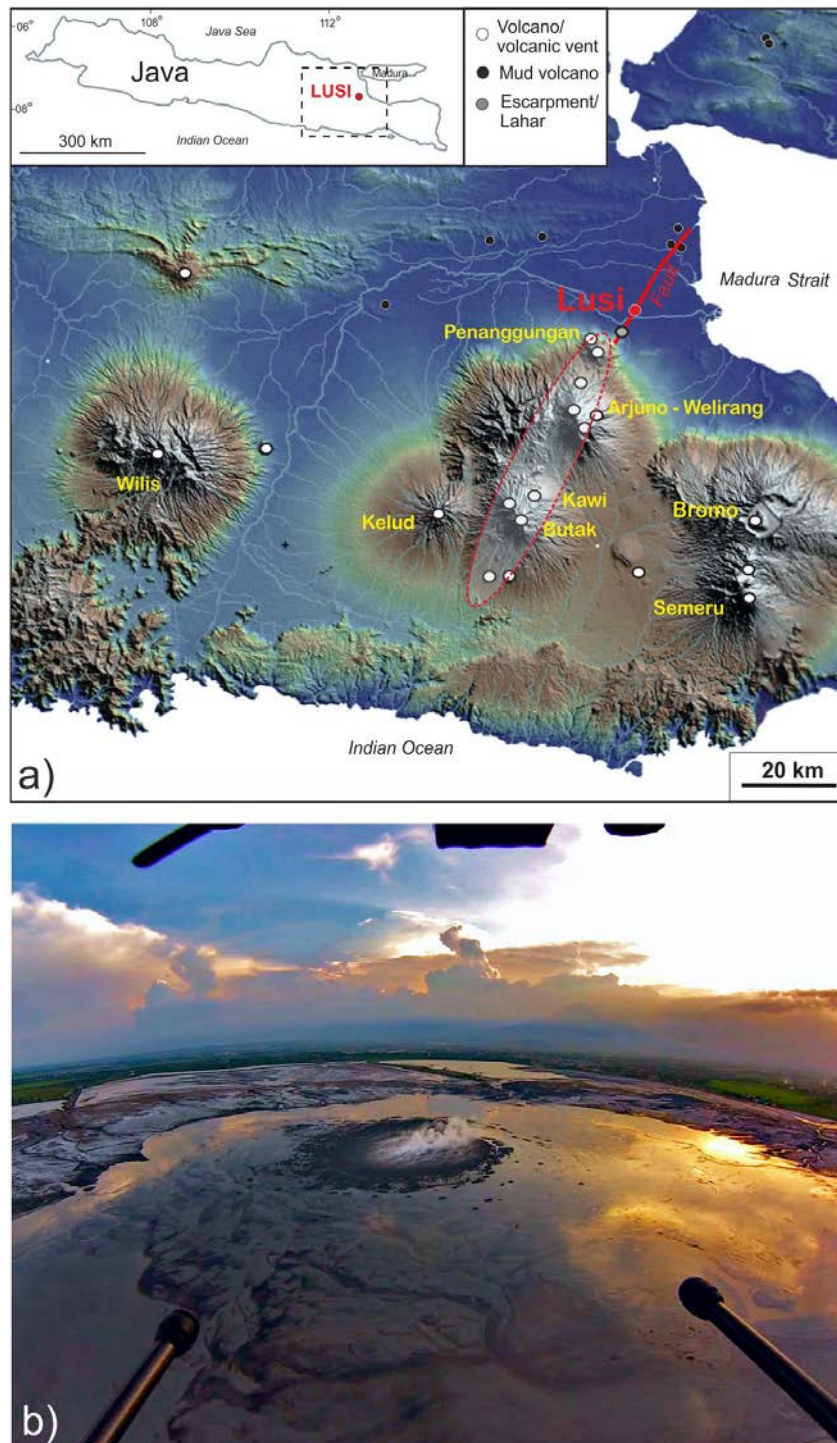


Figure 1. a) Elevation map of the eastern part of Java Island, showing the position of Lusi, some known mud volcanoes, volcanic complexes and vents, and Watukosek fault system. Note the NE-SW orientation of the volcanic complexes (outlined in red) and the Watukosek fault system, hosting a large escarpment, Lusi, and several mud volcanoes (Mazzini et al., 2012). The position of the elevation map is shown in the small Java map inset. b) Drone image of the Lusi site, note the main active bubbling crater in the centre, white vapour plume, black oil slicks on the surface. The volcanic complex is visible in the background (Di Stefano et al., 2018).

budget of greenhouse and toxic volatile release, global carbon cycle, modelling climate changes, and biodiversity perturbations. During the last decade, numerous studies were carried out on Lusi and the adjacent areas in the fields of engineering, geochemistry, geophysics, geology and numerical modelling (Davies et al., 2008; Plumlee et al., 2008; Mazzini, 2009 and refs. therein; Vanderkluisen et al., 2014; Mazzini, 2018 and refs. therein). However, several aspects of the Lusi system still remain uncertain. This PhD thesis tries to tackle some of them, specifically: 1) investigate the maturation of the organic-rich sedimentary rocks associated with magmatism; 2) explore the potential propagation of the mantle-derived volatiles towards the East Java sedimentary basin; 3) define the oil composition and its origin; 4) study the hydrocarbon migration pathways in the southern part of the East Java basin; 5) estimate the total volume of the erupted unconsolidated mud breccia and oil during first 13 years of activity.

1.2 Large Igneous Provinces

A large igneous province (LIP) is defined by the voluminous ($> 0.1 \text{ Mkm}^3$), laterally extensive ($> 0.1 \text{ Mkm}^2$) rapid (from 10k years to several million years) emplacement of the igneous rocks, unrelated to seafloor spreading (Coffin and Eldholm, 1992; Bryan and Ernst, 2008; Bryan and Ferrari, 2013; Self et al., 2015a). LIPs can essentially be divided in three groups: a) oceanic plateaus, e.g. Kerguelen Plateau, and Ontong Java Plateau; b) flood basalts along volcanic rifted margins, e.g., the North Atlantic Igneous Province; c) intra-continental flood basalt, e.g., Karoo-Ferrar LIP, Siberian Traps (Svensen et al., 2019 and refs. therein). All three groups are composed of intrusive and extrusive domains. The origin of LIPs is still debated. Some researches link the cause of LIPs with deep plume generation zones and core mantle boundary anomalies (Torsvik and Burke, 2015). Alternative hypothesis links the LIPs occurrence with the passive lithosphere extension, decompression, and basaltic-enriched mantle melting (Foulger et al., 2007).

Many of the volcanic basins on Earth are associated with LIPs (Figure 2) (Jerram, 2015; Planke et al., 2018). On the regional scale, magmatic activity may significantly affect sedimentary and volcanic basin development. Magma propagation in the form of dykes, sills, and flood basalts can locally increase the regional heat flow and hence enhance the maturation of organic matter in sedimentary rocks and initiate (or increase) hydrocarbon generation. Fractured intrusive bodies may also act as hydrocarbon reservoirs, while

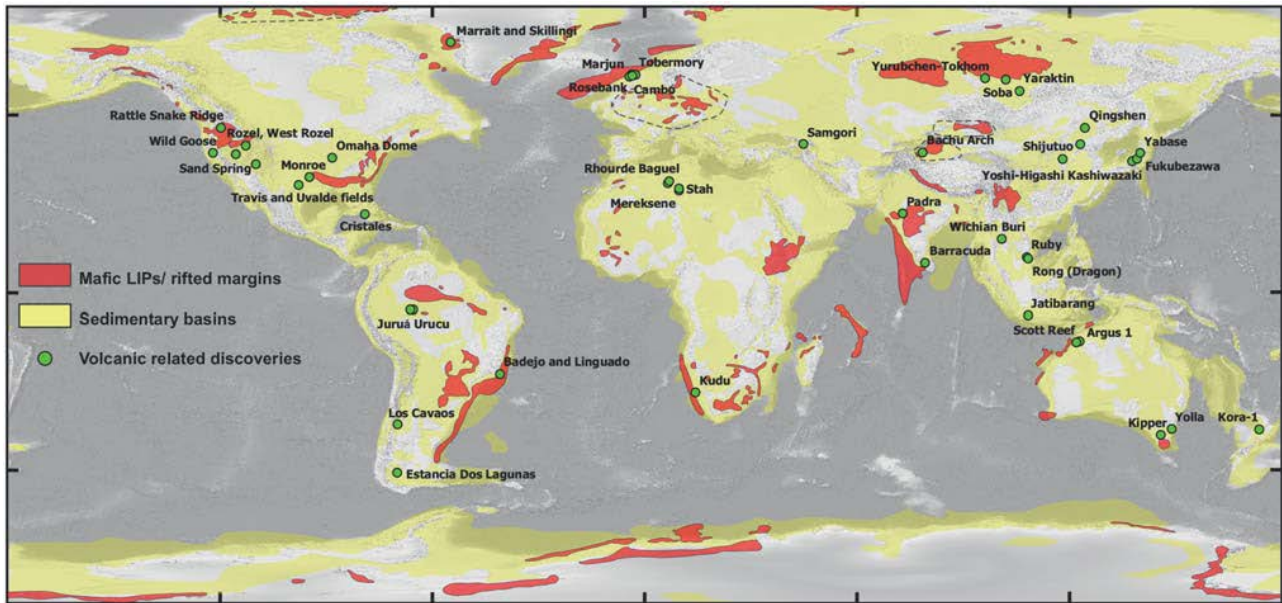


Figure 2. Global distribution of Large Igneous Provinces (LIPs), sedimentary basins, and notable volcanic related discoveries (from Senger et al., 2017).

impermeable intrusions form efficient seals and even structural traps. Intrusions may also compartmentalize reservoirs and/or source rocks, hampering hydrocarbon migration and hydrocarbon traps charging, or even destroy existing conventional traps (Jerram, 2015; Senger et al., 2017 and refs. therein; Planke et al., 2018).

On the global scale, magmatic activity, associated with LIPs, has important environmental and climate impacts due to: a) the release of large masses of volcanic aerosols (primarily CO_2 , SO_2 , Cl, F) from basaltic magma and explosive volcanism; b) the release of the gases generated due to contact metamorphism of the magma with sedimentary rocks (mainly H_2O , CO_2 , CH_4 , SO_2) (Figure 3) (Svensen et al., 2004; Self et al., 2005; Aarnes et al., 2011; Aarnes et al., 2015; Aiuppa, 2015; Platt and Bobrowski, 2015; Self et al., 2015b; Svensen et al., 2015). The type of the generated gas is in principle defined by the host-rock type. Intruded shales and coals largely produce CH_4 and CO_2 , whereas limestones may yield CO_2 , and evaporates can release SO_2 and halogens, e.g. CH_3Cl (Svensen et al., 2015). Massive release of these two types of volatiles can lead to significant environmental perturbations, such as temperature changes (short-term cooling and long-term warming), ocean acidification and marine anoxia, ozone depletion, acid rain, or/and sea-level decrease (Wignall, 2001; Svensen et al., 2004; Self et al., 2005; Bond et al., 2014). These drastic perturbations, may result in ecosystem collapse and significant loss of biodiversity during a relatively short period

of time, commonly termed a mass extinction (Wignall, 2001; Courtillot and Renne, 2003; Aarnes et al., 2010; Bond et al., 2014).

Massive gas generation, triggered by the emplacement of high-temperature (up to 1200 °C) intrusive rocks into sedimentary basins, leads to overpressure build-up in the system (Aarnes et al., 2010). Generated gas is often released through pipes, fissures and/or hydrothermal vent complexes (Jamtveit et al., 2004; Svensen et al., 2004; Svensen et al., 2007b; Berndt et al., 2016) (Figure 3). Although these systems are typically linked to the LIPs, there are modern analogues, usually referred to as sediment-hosted geothermal (hydrothermal) systems.

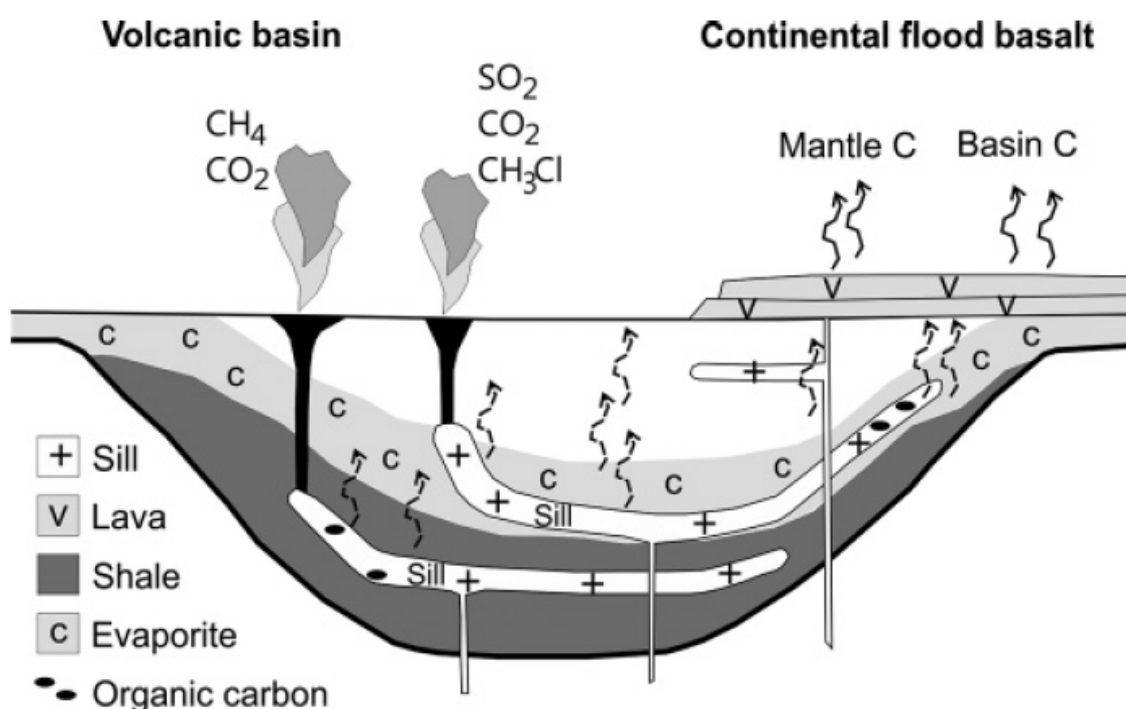


Figure 3. Schematic model of a volcanic basin, showing sedimentary sequence, magmatic intrusions in the form of sills, dykes, flood basalts, and gas pipes (hydrothermal vent complexes). The composition of the released gas formed during contact metamorphism largely depends on the lithological type of the host-rock (Svensen et al., 2015).

1.3 Sediment-hosted geothermal systems

The term sediment-hosted geothermal system (SHGS) defines a geological phenomenon where the released carbon-bearing gases are produced by the interaction between igneous and sedimentary domains (Procesi et al., 2019). The authors highlight that the gas is usually dominated by abiogenic CO₂ and variable amounts of biogenic gases (CH₄, its homologues, and CO₂). Typically, they occur in the tectonically active regions (back-arc basins, rift zones, foredeeps) with anomalously high heat flow (> 50 mW/m²). These systems' activity is driven by emplacement of the magmatic intrusions into thick sequences of the organic-rich sediments (Figure 4).

Some SHGSs display mud discharge from their crater and could be mistakenly referred to as mud volcanoes. Mud volcanism is instead solely related to sedimentary basins hosting active petroleum systems. Mud volcanoes are piercement structures that occur in basins, characterized by high sedimentation rate that results in thick sedimentary sequences of semi-lithified clastic rocks. The activity of mud volcanoes is usually driven by gravitative instability of these buoyant and deeply buried units as well as by hydrocarbon generation within organic-rich deposits (Mazzini and Etiope, 2017). These plumbing systems usually emit CH₄-dominated gas, that has biogenic (thermogenic/microbial) origin (Etiope et al., 2009a; Etiope et al., 2009b; Nuzzo et al., 2009). Temperatures at mud volcanoes are usually monitored in the localized small crater seepage sites (pools, gryphons, salsa lakes), active during dormancy intervals. The temperatures are typically low (~ 30 °C) during dormant stage. Unfortunately, temperature records during eruption do not exist mainly due to the unpredictable nature of explosions. The maximum measured temperature is 75 °C, defined at the flank of the Lokbatan mud volcano after the 2001 eruption (Mukhtarov et al., 2003; Mazzini and Etiope, 2017). Higher temperatures are typically attributed to the SHGSs.

In addition, some SHGSs may be confused with geothermal (hydrothermal) systems, that are exclusively related to the sub-volcanic activity, which occur in modern continental rifts, deep active fault systems or at the crater or flanks of the volcano and form moffets, bubbling pools, and muddy geysers (Sano and Fischer, 2013; Caracausi et al., 2015; Lee et al., 2016; Caracausi and Sulli, 2019). These systems are usually releasing CO₂-dominated gas, largely of abiogenic origin.

The reason for these misinterpretations is intrinsically related to the hybrid nature of SHGSs. These phenomena feature some characteristics that could be attributed to

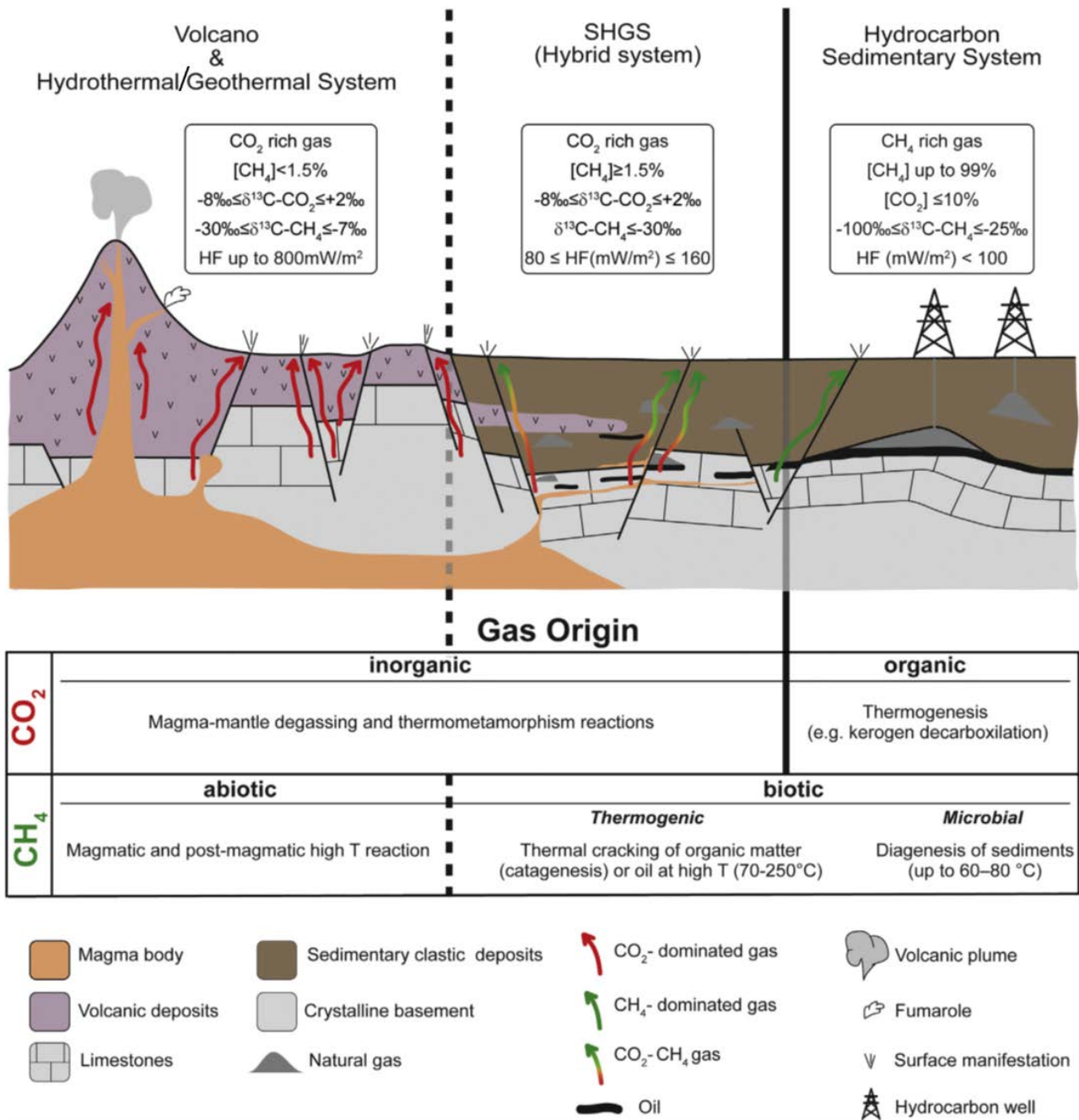


Figure 4. Geological sketch depicting the main geological features and gas origin of the hydrothermal/geothermal systems, hybrid sediment-hosted geothermal systems, and hydrocarbon sedimentary systems (Procesi et al., 2019).

either mud volcanoes or hydrothermal vent complexes, since they outgas a mixture of high temperature fluids of both biotic and abiotic origin. Some SHGSs may release mud breccia, oil, hydrocarbon gases, and may display geysering activity.

To date, 38 SHGS have been identified in various locations worldwide: in the Guaymas Basin and Salton Sea in California, within Tiber Delta in central Italy, Songliao Basin in China, NE Java, Indonesia and more in the USA, Italy, Hungary, Slovenia, Poland, Taiwan-China, Thailand, China, and New Zealand (Procesi et al., 2019 and refs. therein). The SHGSs of the Guaymas Basin and Salton Sea have been extensively studied for more than 50 years. Below is a brief description of these active systems.

Guaymas Basin is a young seafloor spreading system, part of the East Pacific Rise in the central part of the Gulf of California (Lizarralde et al., 2007). The basin is characterized by rapid sedimentation (> 2 m/1000 yr) and shallow emplacement of the dolerite sill intrusions into organic-rich sediments and associated hydrothermal activity and hydrocarbon generation (Einsele et al., 1980; Simoneit et al., 1984). Numerous hydrothermal mounds, rising 20-30 m above the rift floor and discharging high temperature fluids (up to 315 °C), were detected in the basin, both on- and off- spreading axis (Lonsdale and Becker, 1985; Berndt et al., 2016; Teske et al., 2019). The vented gas is dominated by CO₂ (~90 vol.%) with carbon isotope composition suggesting magmatic or carbonate thermo-metamorphic origin ($\delta^{13}\text{C}_{\text{CO}_2}$ ranges between -6 and $+2.7\%$, VPDB (Procesi et al., 2019 and refs. therein). About 10 vol.% is represented by fossil CH₄ ($\delta^{13}\text{C}_{\text{CH}_4}$ ranges between -51 and -15% , VPDB). The isotopic ratio of the injected helium ($^3\text{He}/^4\text{He}$) is >7.7 Ra, where Ra= $^3\text{He}/^4\text{He}$ of air, 1.4×10^{-6} (Lupton, 1979; Berndt et al., 2016). Collected mound sediments often contain hydrothermal petroleum. The petroleum content varies from 1 to 550 mg/g sediment (Simoneit, 2018). The recovered oil has high concentrations of polar compounds, exceeding those in conventional petroleums. The alkane distribution ranges from methane to $n\text{-C}_{40+}$ with no carbon number predominance, suggesting oil window maturity. Various biomarker ratios indicate high oil maturity and biomarkers are generally mature and, along with the ^{14}C age data, show that hydrocarbon generation was induced by rapid and intense heating (Simoneit, 2018 and refs. therein).

Other well-known SHGS is Salton Sea, located in the Salton Trough in Southern California. Salton Sea is a pull-apart basin, occurred in the transition zone of the East Pacific Rise and transform boundary of the San Andreas fault system. The activity of the geothermal system is linked to the Quaternary magmatic intrusions into the fluvial-lacustrine deposits at ~ 1400 m depth, resulting in high temperatures exceeding 350 °C at this depth (Younker et al., 1982; Svensen et al., 2007a). The area has numerous water-, mud-, gas-, and petroleum-bearing seeps. The released gas is dominated by CO₂ (~98 vol. %) of magmatic or thermo-metamorphic origin ($\delta^{13}\text{C}_{\text{CO}_2}$ ranges between -5.4 and $+0.4\%$). CH₄ concentrations can reach 1.9 vol.% and heavier hydrocarbons are less

than 0.5 vol.%. Mazzini et al. (2011) suggest mixed thermogenic and abiotic origin of the methane ($\delta^{13}\text{C}_{\text{CH}_4}$ ranges between -32 and -17.6% , VPDB). High helium isotope ratio ($\text{R/Ra} > 6$) suggests a significant contribution of mantle-derived fluids (Mazzini et al., 2011). Petroleum from the water-dominated springs contain 53% saturated compounds, 35% aromatic and 12% polar compounds. Unlike the oils in the Guaymas Basin, the Salton Sea oil is immature and biodegraded, displaying high unresolved complex mixture (UCM) and biomarker (BMH) humps on the alkane distribution (Svensen et al., 2007a).

1.4 Lusi SHGS

The Lusi eruptive activity commenced in May 2006 with several gas and mud eruptions along a lineament that extended for more than 1 km in the Sidoarjo district in East Java, Indonesia. Several boiling mud vents soon focused into one main vent. Lusi is continuously bursting mud, water, gases, oil, and rock clasts with a mean flow rate of $64,000 \text{ m}^3/\text{day}$. The initial eruption flooded with mud more than 7 km^2 area of Sidoarjo regency within a short time, forcing more than 60,000 people to relocate (Figure 5). This event resulted in severe social and economic consequences in the area. The continuous eruptive activity, on the other hand, provided a unique opportunity for the geoscientists to study the dynamics and evolution of a new-born active sedimentary erupting system. To date, Lusi is recognized as the world's largest active SHGS.

Lusi is located within the Cenozoic back-arc East Java basin. The back-arc was formed due to northward-directed subduction of oceanic crust, attached to the leading edge of the Indian-Australian Plate, beneath the continental Sunda Plate. Subduction resulted in formation of the E-W trending volcanic arc (Hall, 2002). The Lusi eruption occurred on the south-western tip of the back-arc basin and the northernmost part of the adjacent large Arjuno-Welirang volcanic complex, 10 km NE from Penanggungan volcano. The plumbing system is connected with the volcanic complex by a major tectonic feature: the Watukosek fault system (Istadi et al., 2009; Mazzini et al., 2009; Fallahi et al., 2017; Moscariello et al., 2018; Sciarra et al., 2018). The sedimentary section of the East Java Basin, overlying the pre-Tertiary basement, comprises more than 5 km-thick deposits spanning from Eocene through Recent (Kusumastuti, 1999; Hall et al., 2011). The sedimentary sequence at Lusi contains (from bottom to top, Figure 6): Middle Eocene-Lower Oligocene organic-rich black shales of the Ngimbang Fm. ($>3800 \text{ m}$), Upper Oligocene-Lower Miocene carbonates of the Kujung Fm. (from ~ 3800 to $\sim 3250 \text{ m}$),



Figure 5. Google Earth images of Lusi, showing the changes in morphology from July 2006 till July 2019.

Lower-Upper Miocene marls and shales of the Tuban Fm. (from ~3250 to ~2830 m), Upper Pliocene-Pleistocene Upper Kalibeng Fm. containing tight volcanic and volcanoclastic units in the lower part (~2830 to 1870 m) and bluish grey shales and marls in the upper part (1870-900 m), Pleistocene altering volcanoclastic shales and sands of the Pucangan Fm. (900-290 m), and recent alluvial sediments (290-0 m) (Mazzini et al., 2007; Samankassou et al., 2018). The upper part of the sedimentary section, comprising the Upper Kalibeng and Pucangan formations, is characterized by high sedimentation rates (0.7 km/Ma), which resulted in fast burial and preservation of the semi-lithified deposits.

The Lusi system erupts boiling mud (~100°C) consisting of ~60% of water and 40% of siliciclastic material (Mazzini et al., 2007). Based on measurements from the neighbouring hydrocarbon exploration well Banjarpanji-1 (BJP-1, ~200 m away the active vent), the geothermal gradient prior to the eruption was 42°C/km. Mud samples collected from the eruption site are composed by a mixture of kaolinite, smectite and illite (Mazzini et al., 2007). A significant portion of the clayey fraction is likely to originate from the poorly lithified Upper Kalibeng Fm.

The gas erupted from Lusi consists of water vapour (98%), and CO₂ and CH₄, ~1.5 % and ~0.5% respectively (Mazzini et al., 2012; Vanderkluyzen et al., 2014). The gas from satellite seeps is CH₄-dominated (up to 97%) (Mazzini et al., 2012; Sciarra et al., 2018). However, the gas composition at Lusi varies through time. Geochemical analyses of the emitted hydrocarbon gases show thermogenic signature ($\delta^{13}\text{C}_{\text{CH}_4}$ varies from -35.7 to -51.8 ‰), and an inferred origin from the Ngimbang Formation buried at more than 3.8 km depth (Mazzini et al., 2012).

The expelled water is Cl- and Na-dominated, originating from altered formation waters (Mazzini et al., 2018). In addition, the water is enriched in Li and B, which is common for hydrothermal waters. The waters are enriched in ¹⁸O ($\delta^{18}\text{O}$ =9.0 ‰ in the crater and 3.7‰ far from crater) compared to sea water and normal pore fluids from sedimentary basins (Mazzini et al., 2018). Overall, several sources of water are suggested: a) shallow meteoric fluids (< 300 m depth); b) formation water, entrapped during burial of the clays of the Upper Kalibeng Fm (>1870 m); c) fluids resulting from the illitization of the clays of the Up. Kalibeng and Ngimbang Fm. (>1870 m); d) water originating from carbonates of the Kujung Fm (3200-3800 m); e) hydrothermal fluids, originating from the high temperature fluid-rock interaction at ~4.5 km depth.

Visual field and camera observations show that since its outbreak, Lusi had a cyclical erupting geysering activity (Karyono et al., 2017; Lupi et al., 2018). More specifically

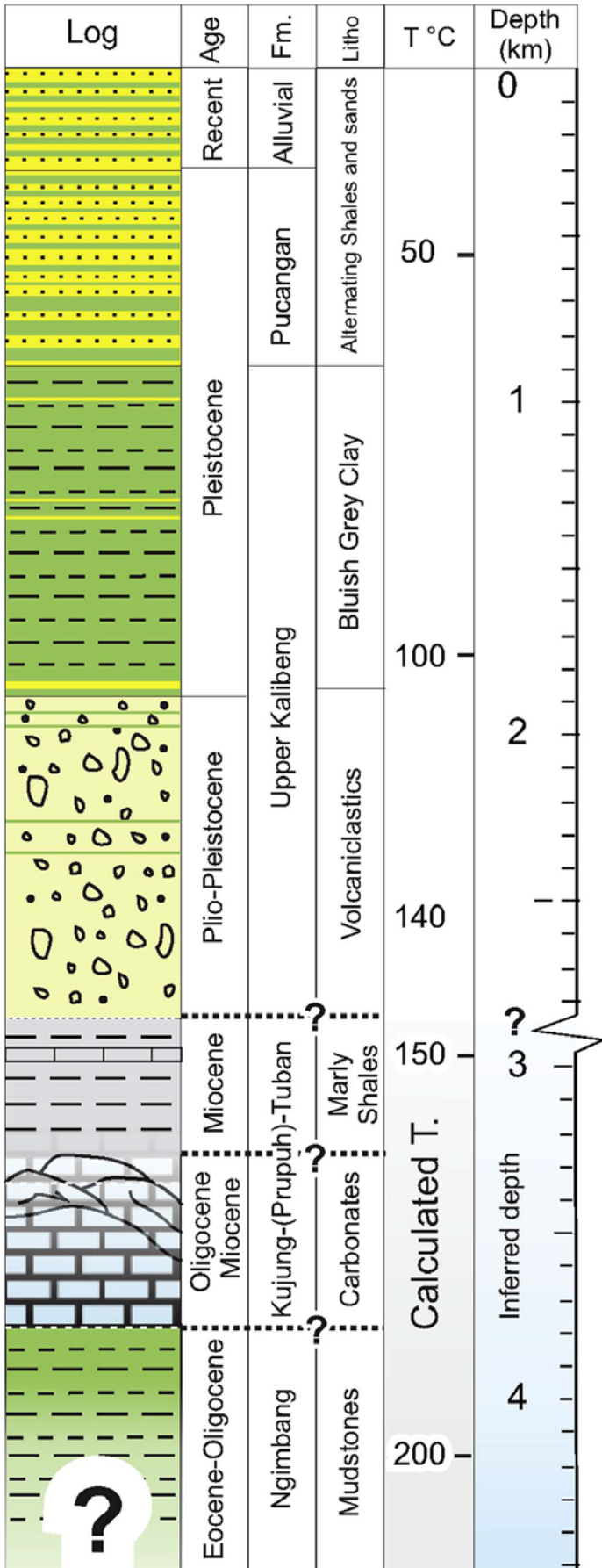


Figure 6. Summarising lithostratigraphic section below Lusi, based on the results of BJP-1 well drilling with the total depth below sea floor 2833 m. The section is constrained by the regional geological knowledge, various exploration drillings, seismic surveys, and dating of the clasts erupted at Lusi. Question marks and dashed lines refer to uncertainties of the formation boundary locations (Samankassou et al., 2018).

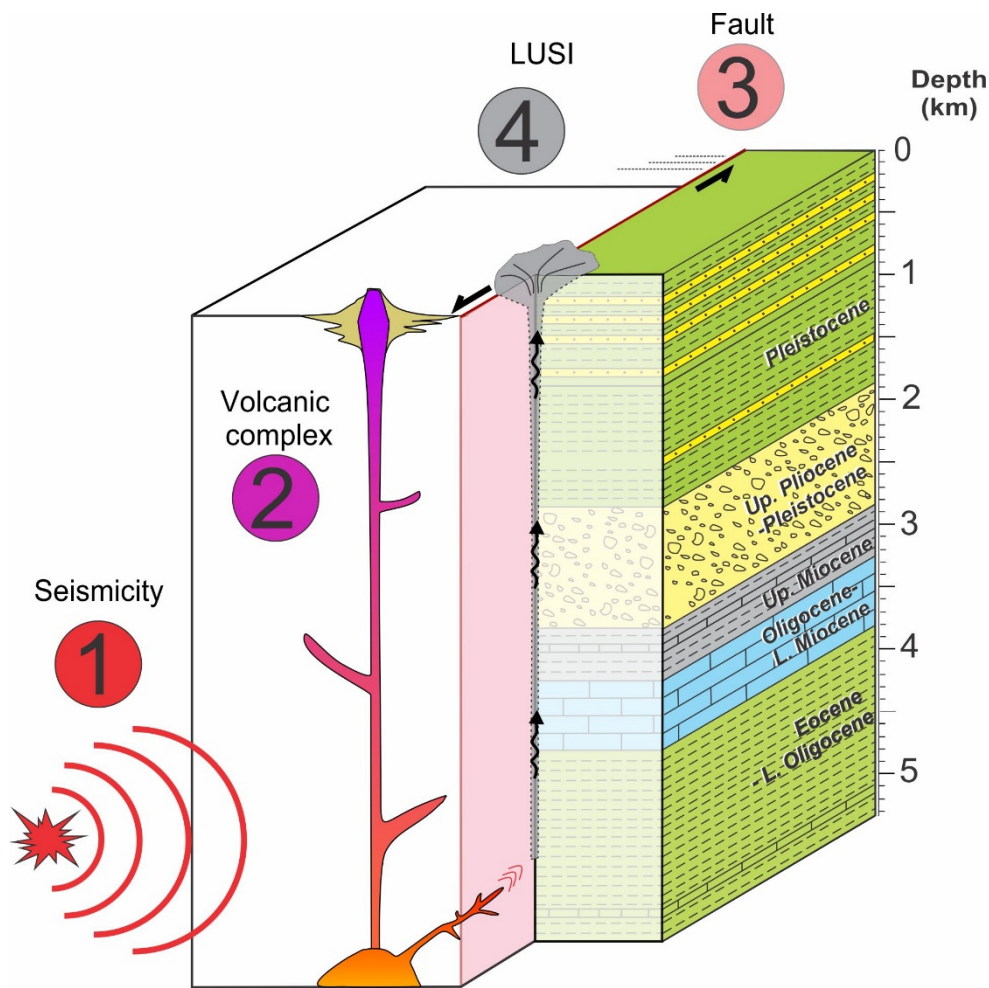


Figure 7. Three-dimensional conceptual model of the Lusi system, highlighting several major factors, that may affect the Lusi activity: (1) high seismicity, (2) volcanic activity, magmatic intrusion and magmatic/hydrothermal fluid propagation, (3) Watukosek fault reactivation, (4) Lusi outbreak. Figure prepared by A. Mazzini and A. Zaputlyeva.

the activity is characterized by 4 phases: 1) regular bubbling activity (lasts 5-10 minutes); 2) enhanced bubbling and mud bursts (lasts ~ 0.5 minute); 3) enhanced bubbling with intense vapour (lasts 2-10 minutes); 4) quiescent phase (lasts 2-10 minutes). Regular bubbling activity is associated with constant mud breccia eruption and water release in liquid and gaseous state. Enhanced bubbling and mud bursts may form mud bubbles 5-10 m in diameter and height. Enhanced bubbling and intense vapour phase feature noisy and vigorous degassing, forming dense vapour plumes up to 100 m above the ground. The quiescent phase highlights the end of the venting activity during which no significant gas/mud emissions were observed (Karyono et al., 2017).

The triggering mechanism of the Lusi eruption is yet debated. Some researches link the origin of the mud eruption with drilling of the BJP-1 well, whereas the others argue that Lusi is a natural geohazard triggered by the high magnitude earthquake 250 km away (Davies et al., 2007; Mazzini et al., 2007; Mazzini et al., 2009; Sawolo et al., 2009). In May 2006, the BJP-1 well was being drilled, targeting carbonate reservoir of the Kujung Fm., located at >3 km depth. On May 28th, a pressure kick was recorded in the well, when the well had already reached 2800 m depth. The situation was under control within 3 hours, according to the published drilling reports (Sawolo et al., 2010). The latest study by Tingay et al. (2018) suggests that the observed pressure kick in the well was associated with the underground blowout, that consequently triggered the Lusi inception. The drilling-triggered scenario was evolving through time. For more information I refer readers to a plentiful literature (e.g. Davies et al. (2007); Davies et al. (2008); Davies et al. (2011); Tingay et al. (2018)). An alternative scenario suggests that Lusi eruption is related to the reactivation of the Watukosek fault system following the 6.3 M earthquake that struck Java 2 days prior to the Lusi birth. This hypothesis is supported by the following lines of evidence: 1) Lusi is intersected by the NE-SW oriented Watukosek fault, which originates from the Arjuno-Welirang volcanic complex and was reactivated prior to the eruption (Mazzini et al., 2007) (Figure 7); 2) volcanic vents and multiple mud volcanoes in East Java are all located along this fault system; 3) Lusi responded to seismic activity in numerous observed cases with sudden bursts, increase in flow rate and rupture of the embankment, surrounding the eruption site; 4) the pressure monitoring within the BJP-1 well did not reveal any pressure loss after the Lusi eruption started (Istadi et al., 2009), suggesting that the well bore is intact; 5) mud vents appeared at ~ 200 m distance from the BJP-1 well site. However, regardless the trigger mechanism, Lusi is a complex active system, offering an unprecedented opportunity for studying the geological processes that take place below its surface expression.

1.5 Organic matter, petroleum composition and generation

Hydrocarbons stored within sedimentary basins are predominantly of biotic origin, i.e. they originate from the thermal or bacterial decomposition of organic matter (Sherwood Lollar et al., 2002). Organic matter is a complex material, comprised of molecules derived directly or indirectly from the organic part of the living organisms, such as algae, phytoplankton, bacteria, and plants (Vassoevitch, 1972; Tissot and Welte, 1984). Photosynthesis is a key process for organic matter formation. The type of organic matter

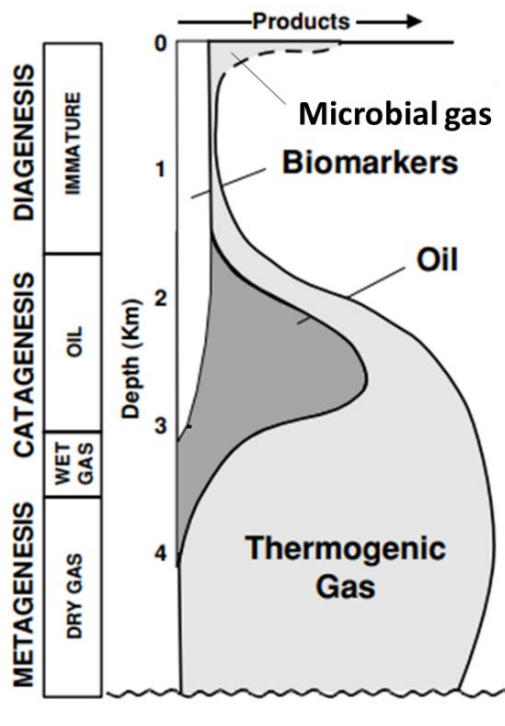


Figure 8. Generalized evolution of the organic matter with burial and major stages of petroleum formation (from Peters et al, 2005).

largely depends on the depositional environment (lacustrine, marine, fluvio-deltaic) and the stage of ecosystem evolution over geologic time.

Only a small portion of the synthesized organic matter is usually preserved in the sediments (< 0.1 %) and undergoes the diagenetic alteration. Microbial gas production by specific microbial communities (mainly by Archaea) commonly occurs during diagenesis at temperatures below 60-80 °C (Figure 8). Methane is the main gas produced by microbial activity, accessory amounts of ethane and trace of propane are usually present (Formolo, 2010).

The amount and type of organic matter, remaining after the diagenesis, define the hydrocarbon potential of the rocks. Commonly, the assessment is based on the Rock-Eval pyrolysis parameters: Total Organic Carbon (TOC) and generative potential (S_2). Organically lean/poor rocks contain TOC < 0.5 wt.% and generative potential S_2 < 2.5 mg HC/g rock (Peters et al., 2005). Organic-rich rocks (commonly shales and carbonates) that could generate or have already generated petroleum are often termed as petroleum (hydrocarbon) source rocks.

At the end of diagenesis, organic matter comprises kerogen and bitumen. Kerogen is insoluble in organic solvents part of organic matter, consisting of macerals and reconstituted products of organic matter, formed during diagenesis (Peters and Cassa, 1994). Macerals are petrographically and geochemically distinct remains of different

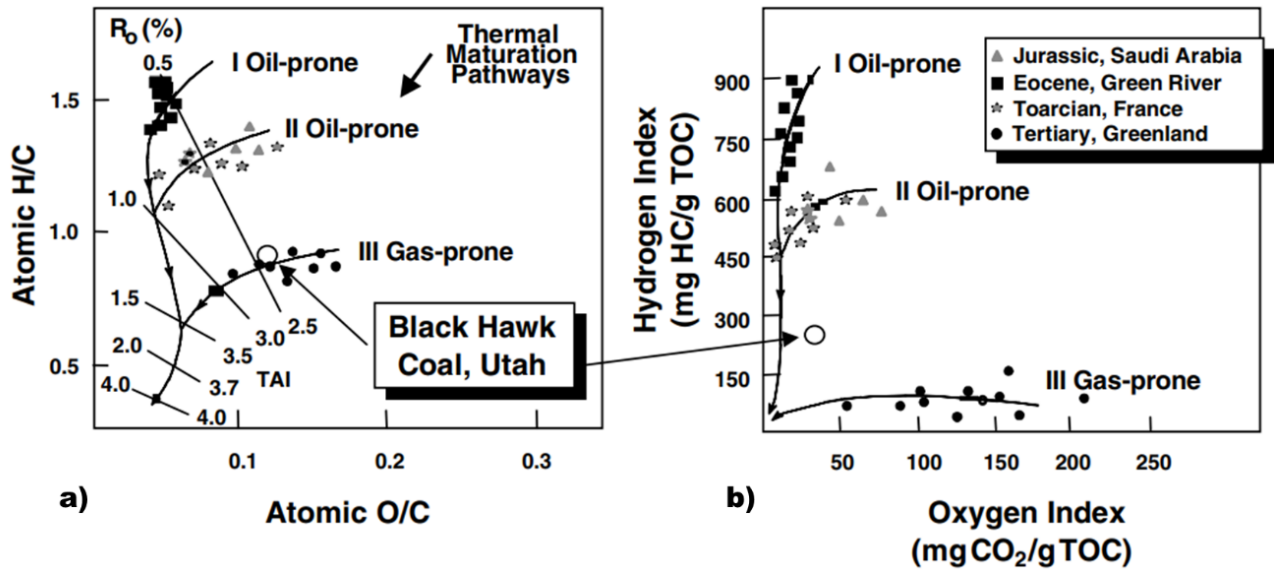


Figure 9. Diagrams characterizing source rock types, based on the a) elemental analysis of kerogen (Van Krevelen diagram); b) Rock-Eval pyrolysis of whole rock sample (modified van Krevelen diagram). Thermal maturity increases along the converging maturation pathways, the top right samples are the least mature. R_o , vitrinite reflectance; TAI, thermal alteration index of spores and pollen. Development of the Rock-Eval pyrolysis method showed, that hydrogen (HI) and oxygen (OI) indices were directly proportional to H/C and O/C ratios (Peters et al., 2005).

types of organic matter. Principle maceral groups are liptinites, exinites, vitrinites, and inertines. Kerogen can have different types based on the depositional environment of the initial organic matter, commonly defined by the H/C and O/C proportions, or hydrogen (HI) and oxygen (OI) indices, derived from the source rock Rock-Eval pyrolysis ($HI = S_2 / (TOC \times 100)$, $OI = S_3 / (TOC \times 100)$), where S_3 represent the amount of CO₂ yield during pyrolysis up to 390 °C (Figure 9). Depending on the kerogen type, source rocks can be oil-prone or gas-prone. Bitumen is a fraction of organic matter that is soluble in organic solvents (Tissot and Welte, 1984). While small amounts of bitumen originate from lipid components in once-living organisms, most of it is formed during a thermo-cracking process from kerogen.

With increased burial depth and temperatures conditions (greater than ~ 60 °C) organic-rich sediments reach the so-called *oil window zone*, where microbial gas generation is overtaken by active oil and gas generation via thermal cracking of kerogen (Figure 8) (Vassoevitch et al., 1969; Tissot and Welte, 1984; Hunt, 1996). This process typically takes place at significant burial depth (~1.5-4 km) and requires millions of years (Peters et al., 2005). Further increase of the temperature to more than ~150°C, leads to extensive

gas generation in the *gas window zone*, comprising wet gas generation (methane and its homologues) and dry gas generation (only methane). Additionally, at temperatures >200 °C, methane forms due to secondary cracking of the generated petroleum remained in the source rocks or stored in the reservoirs (Prinzhofer and Huc, 1995; Schenk et al., 1997). Due to complexity of organic matter composition, oil and gas window zones do not have precise temperature limits. The thermal alteration stage of sedimentary organic matter (source rock) is commonly termed as maturity (Peters and Cassa, 1994). Organic matter is *immature* when the source rocks were affected by diagenesis and did not enter the oil window zone. Thermally *mature* when it is (or was) in the oil window zone. Thermally *post-mature* (also called over mature) organic matter is in the wet and dry gas zones.

Maturation rank		% Volatiles in coal (d.a.f.)*	Max. paleo Temp. °C	Microscopic parameters						Geochemical parameters														
Kerogen	Coal			Vitrin refl. %R _o	TAI	SCI	Conodont alteration index	Fluorescence		CPI	R.-Ev.Pyrol.		C (wt%)	H (wt%)	HC (wt%)	Hydro-carbon products								
								Color of alginite	λ _{max} (nm)		T _{max}	P.I.												
Diagenesis	Peat	60	0.2	1 Yellow	1	1 Yellow	Blue green	500	5	400	0.1	67	8	1.5	Bacterial gas									
	Lignite		0.3				2					Golden yellow	2	425	70	8	1.4	Immature heavy oil						
	Sub-bituminous C		0.4				3					2 Orange	3	2 Dull yellow	600	1.5	435	0.2	80	7	1.1	Wet gas and oil		
Sub-bituminous B	0.5	4	2 Light brown	4	640	1.2	450	0.3	85	6	0.85													
Sub-bituminous A	0.6	5										3	3	Orange	640	1.0	475	0.4	87	5	0.7	Condensate		
Catagenesis	High volatile bituminous C	46	0.7	2 Orange	4	2 Light brown	680	1.5	435	0.2	80	7	1.1	Wet gas and oil										
	High volatile bituminous B		0.8												3 Brown	5	Red	680	1.0	450	0.3	85	6	0.85
	High volatile bituminous A		0.9																					
	Medium volatile bituminous		1.0												7	3	3	Red	680	1.0	475	0.4	87	5
Low volatile bituminous	1.3	8	3	3	Nonfluorescent	680	1.5	475	0.4	87	5	0.7	Condensate											
Sem-anthrac.	1.5	8	4	4										Dark brown	500	90	4	0.5	Dry gas					
Metagenesis	Anthracite	13	2.0	4 Brown/black	9	4 Dark brown	Nonfluorescent	680	1.5	475	0.4	87	5	0.7	Condensate									
	Anthracite		2.5													5 Black	10	5 Black	550	90	4	0.5	Dry gas	
	Anthracite		3.0																					5 Black
Meta-anthrac.	4.0	5	5	5	550	90	4	0.5	Dry gas															
Meta-anthrac.	5.0	4	5.0	5	5	5	5	5	5	5	96	2	0.25											

* Dry ash free

Figure 10. Compilation of several microscopic and geochemical parameters to estimate the maturity of the organic matter. TAI - thermal alteration index, SCI- Spore Coloration Index, λ_{max} - fluorescence intensity, CPI - carbon preference index, P.I.- production index, HC- hydrocarbons (Philp, 2014).

Multiple methods exist to estimate thermal maturity, including vitrinite reflectance (%Ro), Rock-Eval pyrolysis (T_{\max} parameter), biomarker analysis, spore and pollen colour (thermal alteration index, thermal alteration scale, spore coloration index), fluorescence changes, carbon preference index, carbon isotope composition (see chapter 1.7). In conventional sedimentary basins (i.e. with relatively gradual burial history), organic matter maturation lasts for millions of years and maturity-related parameters typically change coherently (Figure 10).

Generated petroleum represents a complex mixture that contains thousands of unique compounds, largely represented by hydrocarbons, with minor amount of nonhydrocarbons. Nonhydrocarbons contain nitrogen, oxygen, and sulfur in addition to carbon and hydrogen (often called heterocyclic compounds), and trace amount of metals (V, Ni, Cr). Crude oil can have various classifications, including those based on distillation properties (boiling temperatures), oil phase behaviour in the reservoir (using pressure, volume, temperature (PVT) dependencies of the oil), API gravity, sulfur content, compound classes (saturated compounds, aromatic, resins, and asphaltenes) (Tissot and Welte, 1984; Hunt, 1996).

1.6 Organic matter maturation and contact metamorphism

Emplacement of magmatic intrusions in a sedimentary basin can significantly alter its thermal history. High temperatures of intrusive bodies (up to 1200 °C), in combination with the release of latent heat of crystallisation, cause rapid heat transfer into relatively cold host-rocks that induce or enhance maturation of the organic matter, often leading to immense hydrocarbon generation. The volatile loss takes place from the aureole zone that often corresponds to ~ 200% of the sill thickness (100% above and 100% below). However, in some cases it may reach up to 1000% of the intrusion thickness (Aarnes et al., 2011). The thickness of the aureole zone and the generated amount of hydrocarbons in the organic-rich strata depend on multiple factors, including sill thickness and spatial clustering, host-rock composition, its porosity, permeability, and water saturation degree, heating rate, depth and rate of penetration, time of the emplacement, initial temperature and pressure regime, organic matter content, and initial maturation level (Raymond and Murchison, 1988; Galushkin, 1997; Aarnes et al., 2010; Rahman and Rimmer, 2014; Aarnes et al., 2015; Wang and Manga, 2015; Quaderer et al., 2016; Sydnes et al., 2018).

The alteration of the organic matter in the aureole zone is characterized by the increased vitrinite reflectance (%Ro), loss of organic carbon, elevated aromatisation, enrichment in ^{13}C from the edge of the aureole towards the contact zone (Peters et al., 1983; Clayton and Bostick, 1986; Bishop and Abbott, 1995; Meyers and Simoneit, 1999). Maturation in this type of geological setting has geologically instant character, therefore, the organic matter transformation path can vary from that observed at conventional slow thermal burial. Furthermore, the standard geochemical approaches to evaluate the maturity may reveal the discrepancies or may not be correlated with the actual in-place temperatures (Raymond and Murchison, 1992; Hubred, 2006; Rahman and Rimmer, 2014; Mißbach et al., 2016; Spacapan et al., 2018).

1.7 Analytical methods for the study case

A multidisciplinary approach was used in order to characterize the fluid-rock interaction at Lusi and the surrounding area. Depending on the sample type, two groups of laboratory methods were used for: 1) gas characterisation; 2) oils and hydrocarbon source rock characterisation. This chapter aims to provide a general overview of applied methods and their implication. The specification of the utilised equipment can be found in the Part II (Scientific Contributions) of the thesis, in the “Methods” sections of the articles.

Applied methods for gas characterisation

Gas chromatography is a common technique, used to assess gas molecular composition, where a gas mixture is heated at a specific rate and separated within chromatographic column. At the end of the column several detectors (usually Flame Ionization Detector and Thermal Conductivity Detector) measure the arrival of the different compounds to a signal processing system. The final output is a gas chromatogram where the various components of the analysed gas sample appear as peaks as a function of time.

Stable isotope (carbon and hydrogen) composition of the CO_2 , CH_4 and its homologues (C_2H_6 ethane, C_3H_8 propane, etc.) is a principal tool to evaluate the origin of gas and potential secondary processes that may have altered the original fluid composition (Bernard et al., 1977; Etiope, 2015; White, 2015; Milkov and Etiope, 2018) (Figure 11). This method analyses isotopic ratios of principal compounds (C, H) and allows to distinguish between abiotic and biotic nature of CO_2 and gaseous

hydrocarbons, as well as temperature range of gas generation, and potential secondary alteration processes that could have affected the gas, i.e. biodegradation, mixing, migration and oxidation. Laboratory analyses are performed on Isotope Ratio Mass Spectrometers. Variations in stable isotope ratios are typically expressed in the parts per thousand range and usually reported as permil variations (δ) from a universally accepted standard. Carbon isotope variations ($^{13}\text{C}/^{12}\text{C}$ or $\delta^{13}\text{C}$) are generally reported in permil deviations from Vienna Pee Dee Belemnite standard (VPDB), $^2\text{H}/^1\text{H}$ ratios are reported as δD with respect to Vienna Standard Mean Ocean Water (VSMOW) or VPDB (White, 2015). The genetic diagrams are empirical. The reliable interpretation of the gas origin should comprise comprehensive geological and geochemical data evaluation.

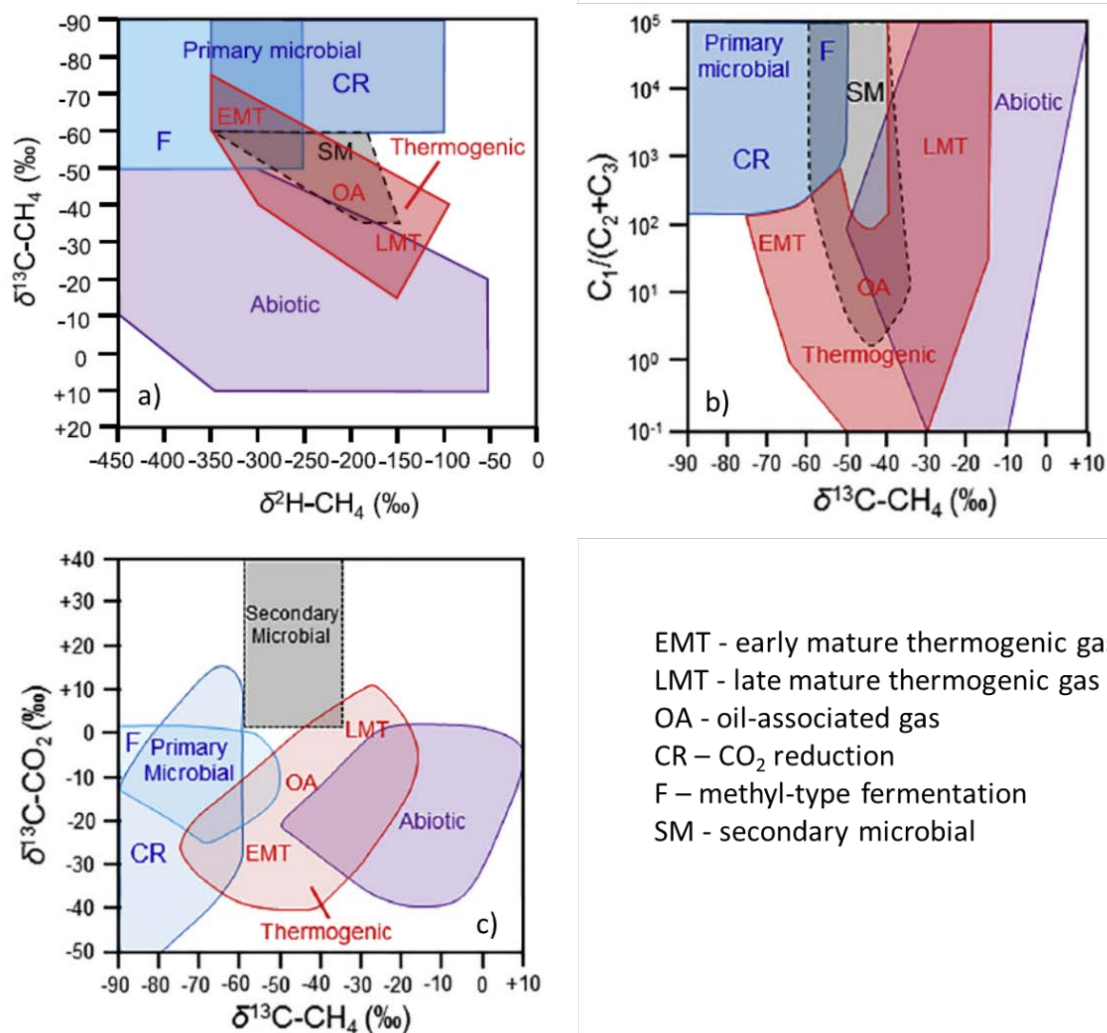


Figure 11. Empirical gas genetic diagrams based on molecular and isotope composition: a) $\delta^{13}\text{C}_{\text{CH}_4}$ and $\delta\text{D}_{\text{CH}_4}$; b) gas dryness $C_1/(C_2+C_3)$ and $\delta^{13}\text{C}_{\text{CH}_4}$; c) $\delta^{13}\text{C}_{\text{CO}_2}$ and $\delta^{13}\text{C}_{\text{CH}_4}$ (Milkov and Etiope, 2018).

Noble gas geochemistry (especially the helium isotopic composition) is used to elucidate a broad range of Earth science topics, including origin and evolution of the Earth, geochronology, subsurface CO₂ migration, hydrothermal systems, mantle processes, magmatic degassing, and volcanic activity (Burnard et al., 2013). Helium is an inert, highly mobile and volatile element with two isotopes: ⁴He is mostly radiogenic (from U and Th decay chains) and ³He which is primordial. Three major near-surface He reservoirs are the atmosphere (³He/⁴He= 1.4 ×10⁻⁶ = 1 Ra), the continental crust (0.01 Ra) and the asthenospheric mantle, which is the source of mid-ocean ridge basalts (~8 Ra). The Solar system primordial He-isotope composition is probably about 120 Ra (the Jupiter ratio), and plume-related primitive basalts in large igneous provinces and modern oceanic islands record a range of 5 to 50 Ra (Ozima and Podosek, 2002; White, 2015). In this thesis, noble gas geochemistry was applied to constrain the source of the helium and trace the migration pathways of the mantle-derived volatiles.

Applied methods for oil and hydrocarbon source rock characterization

Palynological study was aimed at estimating the stratigraphical age of the sampled sedimentary rock, erupted from Lusi by analysis of spore and pollen communities that advanced through time during Earth evolution. The colour of the species reflects the maturation (alteration temperature) of the organic matter: light yellow corresponds to immature organic matter OM (< 65 °C), different shades of orange and brown correspond to the low to high maturation level (65<T<170 °C), and black to overmature stage (>170 °C) (Batten, 1996).

Vitrinite reflectance measurement is among the most common and reliable methods to estimate the maturity of organic matter. Vitrinite macerals represent the remains of woody material in coals and shales. Their reflectance in incident light in polished rock samples changes with the maturation of the rock, i.e. with increasing temperature (Burnham and Sweeney, 1989; Taylor et al., 1998) (Figure 10).

Organic carbon content analysis is a basic method to distinguish organic-rich sediments within the investigated interval of sedimentary rocks. Commonly, organic carbon content is estimated by burning a small amount of decalcified crushed rock material in an oxygen atmosphere. The amount of carbon content is recalculated from the amount of CO₂ gas released during combustion. Leco Instrument or Rock-Eval pyrolysis are commonly used to measure the organic carbon content.

Pyrolysis Rock-Eval 6 is an efficient method to evaluate the potential for oil and gas generation of organic matter in the sedimentary rocks. The method is based on the heating of the crushed sedimentary rock in tiny crucibles starting from 300 °C with a fixed heating rate of 25 °C/min up to 650 °C (Espitalié et al., 1977; Lafargue et al., 1998). A flame ionization detector (FID) is used to trace the pyrolyzed product. Measurements of the amount of released gases at particular temperature intervals characterize the generative potential of the sedimentary rock, i.e. the amount of hydrocarbons, which was already generated by the source rock (peak S₁ on the pyrogram) and could potentially be generated if the rock experienced elevated temperatures and pressures during progressive burial (peak S₂). The pyrolysis is also used to assess the thermal maturity of the organic-rich sedimentary rocks (T_{max} parameter), estimate the amount of organic carbon content (TOC, wt.%), and define the organic matter type (lacustrine/marine/terrestrial/mixed) based on hydrogen and oxygen indices (HI and OI, where $HI=S_2/(TOC \times 100)$ and $OI=S_3/(TOC \times 100)$).

Bitumen extraction allows a separation of the generated and/or migrated hydrocarbons (or so-called “free oil”) from the rock matrix. The extraction is usually performed on a crushed rock using a solvent mixture (commonly dichloromethane-methanol or trichloromethane). The measured weight of the extractable organic matter (EOM) characterizes the amount of generated or trapped hydrocarbons in the analysed rock sample. The EOM is commonly used for further geochemical studies, particularly biomarker analysis and isotope composition.

Biomarker analysis is a broad method focused on the investigation of the complex organic compounds that contain carbon, hydrogen, and other elements and have a molecular structure inherited fully or partially from their biological precursors (i.e. parent organic molecules in living organisms). Biomarkers provide important information about oil and source rocks, including type of organic matter, its maturity (i.e. alteration stage and temperature), depositional environment, and secondary alteration processes (e.g. biodegradation) (Peters et al., 2005). The most common methods for biomarker analysis are gas chromatography coupled with flame ionization detector (GC-FID) and gas-chromatography-mass spectrometry (GC-MS). Analysis of oils and bitumen via GC-FID is commonly used to identify the most abundant molecules present in a sample (e.g. *n*-alkanes and *iso*-alkanes). In order to investigate the presence and distribution of more specific compounds (e.g. hopanes and steranes), samples are analyzed using a GC-MS. This technique allows to select characteristic molecular masses or mass fragments to perform selective scanning of targeted biomarkers. The key idea of the GC-MS technique relies on the fact that compounds are ionized and

fragmented in a certain manner, depending on the structure of the investigated compound. Modern mass-spectrometers can either collect the complete mass spectra of every compound (full-scan mode) or perform the selective scanning of the targeted mass fragments. Two largely investigated classes of the biomarkers, steranes and terpanes, fragment forming the most stable masses m/z 217 and 191, respectively. Using selected ion monitoring, only ions with the selected masses are monitored.

Mercury content analysis is a useful tool to define periods of volcanic activity during sediment deposition. Mercury (Hg) is one of the most toxic elements, and its large input to the atmosphere is a result of volcanic emissions and coal combustion (Sanei et al., 2012). The highest abundances are usually in organic-rich rocks within sedimentary sections (Outridge et al., 2007). Therefore, elevated Hg/TOC ratios are often used as a proxy for enhanced volcanic activity during deposition (Percival et al., 2015; Jones et al., 2019).

The following laboratory analyses have been performed by the candidate: gas chromatography, stable isotopes (carbon and hydrogen) composition, pyrolysis Rock-Eval-6, bitumen extraction, biomarker analysis. Palynology, noble gas isotope composition, vitrinite reflectance measurement, and mercury content were performed by the co-authors of the manuscripts, the candidate participated in the data interpretation.

1.8 Summary of the articles

This thesis is composed of three scientific manuscripts. The first two papers focus on the deep fluid generation and migration in the southern part of the East Java sedimentary basin. The third paper investigates the Lusi flow rate and the amount of erupted oil throughout thirteen years of monitoring.

Manuscript 1. “*Mantle-derived fluids in the East Java sedimentary basin, Indonesia.*”

This study investigates the gas geochemistry of the hydrocarbon fields located 3–36 km away from the Lusi site. The analysed gas was sampled from the shallow (200–1000 m) reservoirs of the Pleistocene Pucangan Fm. that are currently being produced. Methane is a major constituent (up to 98%) with minor amount of its higher molecular homologues (ethane, propane, butane). CH_4 and CO_2 carbon isotopes and the oil

presence in the deeper layers of the Pucangan Fm. suggest that this gas has thermogenic origin, but was altered by biodegradation processes. Molecular gas composition in the hydrocarbon fields differs from that at the Lusi site. In contrast, similar helium isotope ratios were recorded in the gas from reservoirs, Lusi and the fumaroles from the adjacent (25 km) Arjuno-Welirang volcanic complex. This indicates a broad migration of mantle-derived volatiles from the volcanic complex towards the sedimentary basin. Available seismic profiles show that the fault system (the Watukosek fault system) extending from the volcanic complex towards the sedimentary basin, promoted the ideal pathways for the fluid migration. These results provide additional evidence of the connection between the back-arc volcanic activity and the Lusi hybrid system.

Manuscript 2. *“Recent magmatism drives hydrocarbon generation in north-east Java, Indonesia.”*

This paper describes a rare example of a large-scale hydrocarbon generation that is ongoing below a sediment-hosted geothermal system (i.e. Lusi). This multidisciplinary study examined the erupted rock clasts and oil films from the Lusi crater and compared them with the oils sampled from the hydrocarbon fields in the vicinity to the eruption site. The results indicate that hydrocarbons vented at Lusi have different geochemical properties compared to those sampled from the adjacent hydrocarbon reservoirs. This suggests that these field accumulations do not feed the Lusi plumbing system. Subsurface paleotemperature estimates were conducted on a suite of erupted clasts. Discrepancies of at least 100 °C were observed depending on the method used. These are interpreted as the result of heterogeneity of the organic matter and the uneven maturation rate of its particles under a geologically short heat impact. The set of data is used to propose a geological model for hydrocarbon migration pathways at a regional scale. This study highlights the importance of the application of specific methods for temperature estimations in sedimentary basins affected by volcanic activity.

Manuscript 3. *“Extensive oil discharge ongoing at the Lusi mud eruption, Indonesia”*

The manuscript reports the amount of mud breccia and oil erupted from Lusi. Flow rate measurements performed at the Lusi site since its birth, suggest that ~ 0.3 km³ of liquid mud breccia were erupted during the first 13 years of activity with an average rate of 64,000 m³/day. Hydrocarbon extraction from mud samples collected yearly reveals that the dry bulk mud contains 0.2–0.4 vol.% of hydrocarbons. Geochemical analyses suggest two organic matter sources of the hydrocarbons. The major part (60–80%)

consists of the migrated oil from the Ngimbang Fm., the minor 20–40% is derived from the immature bitumen of the Up. Kalibeng Fm. (the main mud constituent). Total discharged amount of the hydrocarbons is 0.28–0.36 Mt, with 0.24–0.30 Mt of the oil for the first 13 years of Lusi activity. This study highlights the elevated oil release rate through time and its potentially hazardous impact on the ecosystems of the neighbouring Porong River and the coastal area of the Madura Strait.

1.9 Outlook

A wide body of research dedicated to the Lusi phenomenon was carried out in order to understand its nature and driving mechanisms, many questions and interesting hypothesis remain still pending.

Calculation of the gas emission

Lusi continuously emits a significant amount of carbon dioxide and methane that are powerful greenhouse gases. Several geochemical field surveys showed that the gases are being discharged from the main crater zone (visible plume) and also within the 7 km² region inside the embankment from the fractured zones, satellite seeps and soil (invisible microseepage). Estimates of the gas output (natural geological methane + carbon dioxide) from Lusi may be used to calibrate basin modelling previously proposed by Svensen et al. (2018). Furthermore, constrained degassing volumes at Lusi may be used to estimate of the potential greenhouse gas release from the analogous palaeo systems that were triggered during the emplacement of the large igneous provinces in sedimentary basins. The activity of these hydrothermal vents is suggested to have contributed to trigger rapid climate change and extinction events since 260 Ma.

Hydrocarbon gas monitoring

Lusi gas composition changed during 13 years of activity. The recent gas samples contain methane enriched in ¹³C, compared to older gas analyses. This may suggest that the maturation of Ngimbang Fm. (major hydrocarbon source rock) increased through time or, alternatively, that mixing with potentially shallower gas sources (of i.e. microbial origin) ceased. Given the relatively easy access to the system and the means of sampling gases remotely (e.g. using the designed LUSI drone that can perform the

sampling), we have the opportunity to perform systematic monitoring. In addition, targeted analyses of methane clumped isotopes of methane (CH_4 molecule with two or more heavy isotope substitutions of C and/or H atoms) may provide insights regarding the temperature of methane formation (Douglas et al., 2017).

Seismicity, flow rate

It was previously reported that the Lusi activity and its flow rate are affected by several external factors, such as seismicity (regional and major teleseismic earthquakes), volcanic eruptions, and fault displacement (Miller and Mazzini, 2018). To identify the potential seismicity impact on the Lusi activity, we have calculated potential ground motion at Lusi, derived from the regional and teleseismic earthquakes and compared those with the changes in flow rate. We have used USGS (United States Geological Survey) and BMKG (Indonesian Meteorological, Climatological, and Geophysical agency) seismicity databases to get the earthquake coordinates, magnitude, and focal depth. Regional earthquakes were filtered in a radius of 350 km away from Lusi. Overall, 707 earthquakes were registered within this radius in the period between the end of May 2006 till February 2019. Ground motions were estimated using regional seismic attenuation relationship described in Davies et al. (2008). Calculated peak ground velocities (PGV) varied from 0.0001 to 5.8 cm/s. Teleseismic earthquakes were filtered with the magnitude greater than 6.5. Overall, 673 events were registered within the study period (2006-2019). PGVs for the teleseismic events were calculated using the formula from Agnew and Wyatt (2014). Resulting PGVs varied from 0.0001 to 0.7 cm/s. Similar study was carried out for the Campi Flegrei caldera in the southern Italy by Lupi et al. (2017). The authors suggested that regional earthquakes affect on the uplift activity of the caldera. The observed thresholds of the PGVs, that could result in significant impact on the Campi Flegrei system are 0.01 cm/s for the teleseismic earthquakes and 0.1 cm/s for the regional earthquakes. In our database 12 regional earthquakes and 100 teleseismic events fulfil these criteria. Calculated PGVs were plotted together with flow rate data (Fig.12). Many earthquakes with PGVs greater than the specific thresholds described above coincide with the flow rate increase. However, in some cases the flow rate increases independently from the seismicity. However, the analysis is largely complicated by the frequency of the flow rate measurements. The latter were performed sparsely between 2006-2016, on average weekly, occasionally monthly. The analysis of the flow rate and seismicity is currently ongoing. More detailed study including thorough statistics implementation is required in order to identify the patterns of the potential seismicity impact on the Lusi flow rate variation.

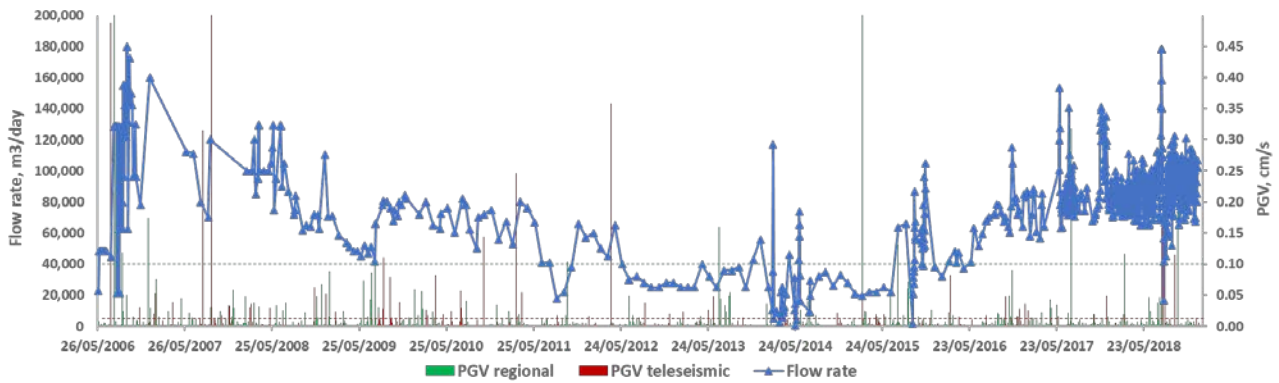


Figure 12. Flow rate variations and calculated peak ground velocities (PGV) from the regional (<350 km away) and teleseismic ($M > 6.5$) earthquakes. Green and red dashed lines are thresholds for the PGVs from regional and teleseismic earthquakes, respectively, that are suggested to have an impact on the uplift activity of the Campi Flegrei caldera (Lupi et al., 2017).

Flow rate and water composition

Previous studies monitored water composition of wells in Iceland and Kamchatka and revealed geochemistry changes associated with regional seismicity (Kingsley et al., 2001; Claesson et al., 2004). Similarly a potential link between the erupted Lusi water composition and seismicity could also exist. In order to test this hypothesis we have completed a set of anions, cations, and stable isotope analyses on a large suite of samples collected weekly at the Lusi site during past 4 years. The dataset was partially acquired during my research stay in INGV (Palermo, Italy fall 2018). An in depth interpretation of these data may reveal if e.g. water geochemical variations may represent precursors of seismic activity or whether the fluid composition changes after these events.

Noble gas monitoring

Previous studies revealed that the helium isotope ratio measured in the hydrocarbon fields near Lusi is similar to that of fumaroles at the Arjuno-Welirang volcanic complex (Inguaggiato et al., 2018). This suggests a broad migration of the mantle-derived volatiles from the volcanic complex towards the sedimentary basin in north-east Java, Indonesia (Zaputlyeva et al., 2019). Monitoring the gas from the hydrocarbon fields in the vicinity of Lusi is a logistically simple way to observe the patterns in perturbations in the magma chamber that can characterize the activity of the Arjuno-Welirang volcanic complex.

Bledug Kuwu SHGS

The Bledug Kuwu mud eruption site, located in central Java, 200 km to the west of Lusi, is supposedly a similar, yet smaller, active analogue of Lusi (Mazzini et al., 2014). It is worth performing a similar fluid sampling from this vent and carry out a set of similar geochemical analysis. So far there are only a few comprehensive studies performed on SHGS. A better understanding of these systems provide constrains to improve our estimates of methane and carbon dioxide emissions from the natural geological sources.

Environmental monitoring

Large amount of mud and oil discharged from the Lusi vent are currently released into the Porong River and ultimately reach the Madura Strait. The available chemical water studies from Lusi and the Porong River indicate elevated concentrations of several toxic elements (including arsenic, selenium, mercury, phenols), decreased water quality due to high suspended solids, particulate organic carbon and ammonium input (Plumlee et al., 2008; Jennerjahn et al., 2013; Hidayati et al., 2019). A detailed chemical survey in the Porong River and coastal area of the Madura Strait is necessary to assess Lusi's environmental hazard potential.

References

- Aarnes, I., Planke, S., Trulsvik, M. and Svensen, H., 2015. Contact metamorphism and thermogenic gas generation in the Vøring and Møre basins, offshore Norway, during the Paleocene–Eocene thermal maximum. *Journal of the Geological Society*, 172(5): 588.
- Aarnes, I., Svensen, H., Connolly, J.A.D. and Podladchikov, Y.Y., 2010. How contact metamorphism can trigger global climate changes: Modeling gas generation around igneous sills in sedimentary basins. *Geochimica et Cosmochimica Acta*, 74(24): 7179-7195.
- Aarnes, I., Svensen, H., Polteau, S. and Planke, S., 2011. Contact metamorphic devolatilization of shales in the Karoo Basin, South Africa, and the effects of multiple sill intrusions. *Chemical Geology*, 281(3): 181-194.
- Agnew, D.C. and Wyatt, F.K., 2014. Dynamic Strains at Regional and Teleseismic Distances. *Bulletin of the Seismological Society of America*, 104(4): 1846-1859.
- Aiuppa, A., 2015. Volcanic-gas monitoring. In: A. Schmidt, K. Fristad and L. Elkins-Tanton (Editors), *Volcanism and Global Environmental Change*. Cambridge University Press, Cambridge, pp. 81-96.
- Batten, D., 1996. Palynofacies and petroleum potential. In: J. Jansonius and D.C. McGregor (Editors), *Palynology: principles and applications*. American Association of Stratigraphic Palynologists Foundation, pp. 1065-1084.
- Bernard, B., Brooks, J.M. and Sackett, W.M., 1977. A geochemical model for characterization of hydrocarbon gas sources in marine sediments, 9th Annual OTC Conference, pp. 435–438.
- Berndt, C., Hensen, C., Mortera-Gutierrez, C., Sarkar, S., Geilert, S., Schmidt, M., Liebetrau, V., Kipfer, R., Scholz, F., Doll, M., Muff, S., Karstens, J., Planke, S., Petersen, S., Böttner, C., Chi, W.-C., Moser, M., Behrendt, R., Fiskal, A., Lever, M.A., Su, C.-C., Deng, L., Brennwald, M.S. and Lizarralde, D., 2016. Rifting under steam—How rift magmatism triggers methane venting from sedimentary basins. *Geology*, 44(9): 767-770.
- Bishop, A.N. and Abbott, G.D., 1995. Vitrinite reflectance and molecular geochemistry of Jurassic sediments: the influence of heating by Tertiary dykes (northwest Scotland). *Organic Geochemistry*, 22(1): 165-177.
- Bond, D.P.G., Wignall, P.B., Keller, G. and Kerr, A.C., 2014. Large igneous provinces and mass extinctions: An update, *Volcanism, Impacts, and Mass Extinctions: Causes and Effects*. Geological Society of America, pp. 29-55.
- Bryan, S.E. and Ernst, R.E., 2008. Revised definition of Large Igneous Provinces (LIPs). *Earth-Science Reviews*, 86(1): 175-202.
- Bryan, S.E. and Ferrari, L., 2013. Large igneous provinces and silicic large igneous provinces: Progress in our understanding over the last 25 years. *GSA Bulletin*, 125(7-8): 1053-1078.
- Burnard, P., Zimmermann, L. and Sano, Y., 2013. The Noble Gases as Geochemical Tracers: History and Background. In: P. Burnard (Editor), *The Noble Gases as Geochemical Tracers*. Springer Berlin Heidelberg, Berlin, Heidelberg, pp. 1-15.
- Burnham, A.K. and Sweeney, J.J., 1989. A chemical kinetic model of vitrinite maturation and reflectance. *Geochimica et Cosmochimica Acta*, 53(10): 2649-2657.
- Caracausi, A., Paternoster, M. and Nuccio, P.M., 2015. Mantle CO₂ degassing at Mt. Vulture volcano (Italy): Relationship between CO₂ outgassing of volcanoes and the time of their last eruption. *Earth and Planetary Science Letters*, 411: 268-280.
- Caracausi, A. and Sulli, A., 2019. Outgassing of mantle volatiles in compressional tectonic regime away from volcanism: the role of continental delamination. *Geochemistry, Geophysics, Geosystems*.
- Claesson, L., Skelton, A., Graham, C., Dietl, C., Mörth, M., Torssander, P. and Kockum, I., 2004. Hydrogeochemical changes before and after a major earthquake. *Geology*, 32(8): 641.

- Clayton, J.L. and Bostick, N.H., 1986. Temperature effects on kerogen and on molecular and isotopic composition of organic matter in Pierre Shale near an igneous dike. *Organic Geochemistry*, 10(1): 135-143.
- Coffin, M.F. and Eldholm, O., 1992. *Volcanism and continental break-up: a global compilation of large igneous provinces*. Geological Society, London, Special Publications, 68(1): 17.
- Courtillot, V.E. and Renne, P.R., 2003. On the ages of flood basalt events. *Comptes Rendus Geoscience*, 335(1): 113-140.
- Davies, R., Manga, M., Tingay, M. and Swarbrick, R., 2011. Fluid transport properties and estimation of overpressure at the Lusi mud volcano, East Java Basin (Tanikawa et al., 2010). *Engineering Geology*, 121(1-2): 97-99.
- Davies, R.J., Brumm, M., Manga, M., Rubiandini, R., Swarbrick, R. and Tingay, M., 2008. The East Java mud volcano (2006 to present): An earthquake or drilling trigger? *Earth and Planetary Science Letters*, 272(3-4): 627-638.
- Davies, R.J., Swarbrick, R.E., Evans, R.J. and Huuse, M., 2007. Birth of a mud volcano: East Java, 29 May 2006. *GSA Today*, 17(2): 4.
- Di Stefano, G., Romeo, G., Mazzini, A., Iarocci, A., Hadi, S. and Pelphrey, S., 2018. The Lusi drone: A multidisciplinary tool to access extreme environments. *Marine and Petroleum Geology*, 90: 26-37.
- Douglas, P.M.J., Stolper, D.A., Eiler, J.M., Sessions, A.L., Lawson, M., Shuai, Y., Bishop, A., Podlaha, O.G., Ferreira, A.A., Santos Neto, E.V., Niemann, M., Steen, A.S., Huang, L., Chimiak, L., Valentine, D.L., Fiebig, J., Luhmann, A.J., Seyfried, W.E., Etiope, G., Schoell, M., Inskeep, W.P., Moran, J.J. and Kitchen, N., 2017. Methane clumped isotopes: Progress and potential for a new isotopic tracer. *Organic Geochemistry*, 113: 262-282.
- Einsele, G., Gieskes, J.M., Curray, J., Moore, D.M., Aguayo, E., Aubry, M.-P., Fornari, D., Guerrero, J., Kastner, M., Kelts, K., Lyle, M., Matoba, Y., Molina-Cruz, A., Niemitz, J., Rueda, J., Saunders, A., Schrader, H., Simoneit, B. and Vacquier, V., 1980. Intrusion of basaltic sills into highly porous sediments, and resulting hydrothermal activity. *Nature*, 283(5746): 441-445.
- Espitalié, J., Laporte, J.L., Madec, M., Marquis, F., Leplat, P., Paulet, J. and Boutefeu, A., 1977. Méthode rapide de caractérisation des roches mères, de leur potentiel pétrolier et de leur degré d'évolution. *Rev. Inst. Fr. Pét.*, 32(1): 23-42.
- Etiope, G., 2015. *Natural Gas Seepage*. Springer International Publishing.
- Etiope, G., Feyzullayev, A. and Baciu, C.L., 2009a. Terrestrial methane seeps and mud volcanoes: A global perspective of gas origin. *Marine and Petroleum Geology*, 26(3): 333-344.
- Etiope, G., Feyzullayev, A., Milkov, A.V., Waseda, A., Mizobe, K. and Sun, C.H., 2009b. Evidence of subsurface anaerobic biodegradation of hydrocarbons and potential secondary methanogenesis in terrestrial mud volcanoes. *Marine and Petroleum Geology*, 26(9): 1692-1703.
- Fallahi, M.J., Obermann, A., Lupi, M., Karyono, K. and Mazzini, A., 2017. The Plumbing System Feeding the Lusi Eruption Revealed by Ambient Noise Tomography. *Journal of Geophysical Research: Solid Earth*, 122(10): 8200-8213.
- Formolo, M., 2010. The Microbial Production of Methane and Other Volatile Hydrocarbons. In: K.N. Timmis (Editor), *Handbook of Hydrocarbon and Lipid Microbiology*. Springer Berlin Heidelberg, Berlin, Heidelberg, pp. 113-126.
- Foulger, G.R., Foulger, G.R. and Jurdy, D.M., 2007. The "plate" model for the genesis of melting anomalies, Plates, Plumes and Planetary Processes. Geological Society of America, pp. 0.
- Galushkin, Y.I., 1997. Thermal effects of igneous intrusions on maturity of organic matter: A possible mechanism of intrusion. *Organic Geochemistry*, 26(11): 645-658.

- Hall, R., 2002. Cenozoic geological and plate tectonic evolution of SE Asia and the SW Pacific: computer-based reconstructions, model and animations. *Journal of Asian Earth Sciences*, 20(4): 353-431.
- Hall, R., Cottam, M.A. and Wilson, M.E.J., 2011. Australia–SE Asia collision: plate tectonics and crustal flow In: M.A.C. R. Hall, M.E.J. Wilson (Editor), *The SE Asian gateway: history and tectonics of Australia-Asia collision*. Geological Society of London Special Publication.
- Hidayati, D., Sulaiman, N., Ismail, B.S., Jadid, N. and Muchamad, L.S., 2019. Volcanic mud contamination in the river ecosystem: The case study of Lusi mud volcano, Indonesia. *Nature Environment and Pollution Technology*, 18(1): 31-40.
- Hubred, J.H., 2006. *Thermal Effects of Basaltic Sill Emplacement in Source Rocks on Maturation and Hydrocarbon Generation*, University of Oslo, 290 pp.
- Hunt, J.M., 1996. *Petroleum Geochemistry and Geology*. W.H. Freeman, New York, 743 pp.
- Inguaggiato, S., Mazzini, A., Vita, F. and Sciarra, A., 2018. The Arjuno-Welirang volcanic complex and the connected Lusi system: Geochemical evidences. *Marine and Petroleum Geology*, 90: 67-76.
- Istadi, B.P., Pramono, G.H., Sumintadireja, P. and Alam, S., 2009. Modeling study of growth and potential geohazard for LUSI mud volcano: East Java, Indonesia. *Marine and Petroleum Geology*, 26(9): 1724-1739.
- Jamtveit, B., Svensen, H., Podladchikov, Y.Y. and Planke, S., 2004. Hydrothermal vent complexes associated with sill intrusions in sedimentary basins. *Geological Society, London, Special Publications*, 234(1): 233.
- Jennerjahn, T.C., Jänen, I., Propp, C., Adi, S. and Nugroho, S.P., 2013. Environmental impact of mud volcano inputs on the anthropogenically altered Porong River and Madura Strait coastal waters, Java, Indonesia. *Estuarine, Coastal and Shelf Science*, 130: 152-160.
- Jerram, D.A., 2015. *Hot Rocks and Oil: Are Volcanic Margins the New Frontier?* Elsevier R&D, Solutions for Oil & Gas.
- Jones, M.T., Percival, L.M.E., Stokke, E.W., Frieling, J., Mather, T.A., Riber, L., Schubert, B.A., Schultz, B., Tegner, C., Planke, S. and Svensen, H.H., 2019. Mercury anomalies across the Palaeocene–Eocene Thermal Maximum. *Clim. Past*, 15(1): 217-236.
- Karyono, K., Obermann, A., Lupi, M., Masturyono, M., Hadi, S., Syafri, I., Abdurrokhim, A. and Mazzini, A., 2017. Lusi, a clastic-dominated geysering system in Indonesia recently explored by surface and subsurface observations. *Terra Nova*, 29(1): 13-19.
- Kingsley, S., Biagi, P., Piccolo, R., Capozzi, V., Ermini, A., Khatkevich, Y. and Gordeev, E., 2001. Hydrogeochemical precursors of strong earthquakes: a realistic possibility in Kamchatka. *Physics and Chemistry of the Earth, Part C: Solar, Terrestrial & Planetary Science*, 26(10-12): 769-774.
- Kusumastuti, A., Darmoyo, A.B., Suwarlan, W., Sosromihardjo, S.P.C., 1999. The Wunut field: Pleistocene volcanoclastic gas sands in East Java. *Proceedings, Indonesian Petroleum Association, Twenty Seventh Annual Convention & Exhibition, October 1999*.
- Lafargue, E., Marquis, F. and Pillot, D., 1998. Rock-Eval 6 Applications in Hydrocarbon Exploration, Production, and Soil Contamination Studies. *Rev. Inst. Fr. Pét.*, 53(4): 421-437.
- Lee, H., Muirhead, J.D., Fischer, T.P., Ebinger, C.J., Kattenhorn, S.A., Sharp, Z.D. and Kianji, G., 2016. Massive and prolonged deep carbon emissions associated with continental rifting. *Nature Geoscience*, 9(2): 145-149.
- Lizarralde, D., Axen, G.J., Brown, H.E., Fletcher, J.M., González-Fernández, A., Harding, A.J., Holbrook, W.S., Kent, G.M., Paramo, P., Sutherland, F. and Umhoefer, P.J., 2007. Variation in styles of rifting in the Gulf of California. *Nature*, 448(7152): 466-469.
- Lonsdale, P. and Becker, K., 1985. Hydrothermal plumes, hot springs, and conductive heat flow in the Southern Trough of Guaymas Basin. *Earth and Planetary Science Letters*, 73(2): 211-225.

- Lupi, M., Frehner, M., Weis, P., Skelton, A., Saenger, E.H., Tisato, N., Geiger, S., Chiodini, G. and Driesner, T., 2017. Regional earthquakes followed by delayed ground uplifts at Campi Flegrei Caldera, Italy: Arguments for a causal link. *Earth and Planetary Science Letters*, 474: 436-446.
- Lupi, M., Mazzini, A., Sciarra, A., Collignon, M., Schmid, D.W., Husein, A., Romeo, G., Obermann, A. and Karyono, K., 2018. Enhanced hydrothermal processes at the new-born Lusi eruptive system, Indonesia. *Journal of Volcanology and Geothermal Research*, 366: 47-57.
- Lupton, J.E., 1979. Helium-3 in the Guaymas Basin: Evidence for injection of mantle volatiles in the Gulf of California. *84(B13): 7446-7452*.
- Malvoisin, B., Mazzini, A. and Miller, S.A., 2018. Deep hydrothermal activity driving the Lusi mud eruption. *Earth and Planetary Science Letters*, 497: 42-49.
- Mazzini, A., 2009. Mud volcanism: Processes and implications. *Marine and Petroleum Geology*, 26(9): 1677-1680.
- Mazzini, A., 2018. 10 years of Lusi eruption: Lessons learned from multidisciplinary studies (LUSI LAB). *Marine and Petroleum Geology*, 90: 1-9.
- Mazzini, A. and Etiope, G., 2017. Mud volcanism: An updated review. *Earth-Science Reviews*, 168: 81-112.
- Mazzini, A., Etiope, G. and Svensen, H., 2012. A new hydrothermal scenario for the 2006 Lusi eruption, Indonesia. Insights from gas geochemistry. *Earth and Planetary Science Letters*, 317-318: 305-318.
- Mazzini, A., Hadi, S., Etiope, G. and Inguaggiato, S., 2014. Tectonic Control of Piercement Structures in Central Java, Indonesia, American Geophysical Union, Fall Meeting 2014.
- Mazzini, A., Neramoen, A., Krotkiewski, M., Podladchikov, Y., Planke, S. and Svensen, H., 2009. Strike-slip faulting as a trigger mechanism for overpressure release through piercement structures. Implications for the Lusi mud volcano, Indonesia. *Marine and Petroleum Geology*, 26(9): 1751-1765.
- Mazzini, A., Scholz, F., Svensen, H.H., Hensen, C. and Hadi, S., 2018. The geochemistry and origin of the hydrothermal water erupted at Lusi, Indonesia. *Marine and Petroleum Geology*, 90: 52-66.
- Mazzini, A., Svensen, H., Akhmanov, G.G., Aloisi, G., Planke, S., Malthe-Sørensen, A. and Istadi, B., 2007. Triggering and dynamic evolution of the LUSI mud volcano, Indonesia. *Earth and Planetary Science Letters*, 261(3-4): 375-388.
- Mazzini, A., Svensen, H., Etiope, G., Onderdonk, N. and Banks, D., 2011. Fluid origin, gas fluxes and plumbing system in the sediment-hosted Salton Sea Geothermal System (California, USA). *Journal of Volcanology and Geothermal Research*, 205(3-4): 67-83.
- Meyers, P.A. and Simoneit, B.R.T., 1999. Effects of extreme heating on the elemental and isotopic compositions of an Upper Cretaceous coal. *Organic Geochemistry*, 30(5): 299-305.
- Milkov, A.V. and Etiope, G., 2018. Revised genetic diagrams for natural gases based on a global dataset of >20,000 samples. *Organic Geochemistry*, 125: 109-120.
- Miller, S.A. and Mazzini, A., 2018. More than ten years of Lusi: A review of facts, coincidences, and past and future studies. *Marine and Petroleum Geology*, 90: 10-25.
- Mißbach, H., Duda, J.P., Lünsdorf, N.K., Schmidt, B.C. and Thiel, V., 2016. Testing the preservation of biomarkers during experimental maturation of an immature kerogen. *International Journal of Astrobiology*, 15(3): 165-175.
- Moscariello, A., Do Couto, D., Mondino, F., Booth, J., Lupi, M. and Mazzini, A., 2018. Genesis and evolution of the Watukosek fault system in the Lusi area (East Java). *Marine and Petroleum Geology*, 90: 125-137.
- Mukhtarov, A.S., Kadirov, F.A., Guliyev, I.S., Feyzullayev, A. and Lerche, I., 2003. Temperature evolution in the Lokbatan mud volcano crater (Azerbaijan) after the eruption of 25 October 2001. *Energy Exploration and Exploitation*, 21(3): 187-207.

- Nuzzo, M., Hornibrook, E.R.C., Gill, F., Hensen, C., Pancost, R.D., Haeckel, M., Reitz, A., Scholz, F., Magalhães, V.H., Brückmann, W. and Pinheiro, L.M., 2009. Origin of light volatile hydrocarbon gases in mud volcano fluids, Gulf of Cadiz — Evidence for multiple sources and transport mechanisms in active sedimentary wedges. *Chemical Geology*, 266(3): 350-363.
- Obermann, A., Karyono, K., Diehl, T., Lupi, M. and Mazzini, A., 2018. Seismicity at Lusi and the adjacent volcanic complex, Java, Indonesia. *Marine and Petroleum Geology*, 90: 149-156.
- Outridge, P.M., Sanei, H., Stern, G.A., Hamilton, P.B. and Goodarzi, F., 2007. Evidence for Control of Mercury Accumulation Rates in Canadian High Arctic Lake Sediments by Variations of Aquatic Primary Productivity. *Environmental Science & Technology*, 41(15): 5259-5265.
- Ozima, M. and Podosek, F.A., 2002. *Noble Gas Geochemistry* Cambridge University Press.
- Percival, L.M.E., Witt, M.L.I., Mather, T.A., Hermoso, M., Jenkyns, H.C., Hesselbo, S.P., Al-Suwaidi, A.H., Storm, M.S., Xu, W. and Ruhl, M., 2015. Globally enhanced mercury deposition during the end-Pliensbachian extinction and Toarcian OAE: A link to the Karoo–Ferrar Large Igneous Province. *Earth and Planetary Science Letters*, 428: 267-280.
- Peters, K.E. and Cassa, M.R., 1994. *Applied source rock geochemistry: Chapter 5: Part II. Essential elements*.
- Peters, K.E., Walters, C.C. and Moldowan, J.M., 2005. *The Biomarker Guide*. Cambridge University Press.
- Peters, K.E., Whelan, J.K., Hunt, J.M. and Tarafa, M.E., 1983. Programmed Pyrolysis of Organic Matter from Thermally Altered Cretaceous Black Shales1. *AAPG Bulletin*, 67(11): 2137-2146.
- Philp, R.P., 2014. 9.9 - Formation and Geochemistry of Oil and Gas. In: H.D. Holland and K.K. Turekian (Editors), *Treatise on Geochemistry (Second Edition)*. Elsevier, Oxford, pp. 233-265.
- Planke, S., Rabbel, O., Galland, O., Millett, J.M., Manton, B., Jerram, D.A., Palma, O.J. and Spacapan, J.B., 2018. Seismic imaging and petroleum implications of igneous intrusions in sedimentary basins constrained by outcrop analogues and seismic data from the Neuquen Basin and the NE Atlantic, 10^o Congreso de Exploración y Desarrollo de Hidrocarburos, Mendoza, Argentina.
- Platt, U. and Bobrowski, N., 2015. Quantification of volcanic reactive halogen emissions. In: A. Schmidt, K. Fristad and L. Elkins-Tanton (Editors), *Volcanism and Global Environmental Change*. Cambridge University Press, Cambridge, pp. 115-132.
- Plumlee, G.S., Casadevall, T.J., Wibowo, H.T., Rosenbauer, R.J., Johnson, C.A., Breit, G.N., Lowers, H., Wolf, R.E., Hageman, P.L., Goldstein, H.L., Anthony, M.W., Berry, C.J., Fey, D.L., Meeker, G.P. and Morman, S.A., 2008. Preliminary analytical results for a mud sample collected from the LUSI Mud Volcano, Sidoarjo, East Java, Indonesia. 2008-1019, Reston, VA.
- Prinzhofer, A.A. and Huc, A.Y., 1995. Genetic and post-genetic molecular and isotopic fractionations in natural gases. *Chemical Geology*, 126(3): 281-290.
- Procesi, M., Ciotoli, G., Mazzini, A. and Etiope, G., 2019. Sediment-hosted geothermal systems: Review and first global mapping. *Earth-Science Reviews*, 192: 529-544.
- Quaderer, A., Mastalerz, M., Schimmelmann, A., Drobniak, A., Bish, D.L. and Wintsch, R.P., 2016. Dike-induced thermal alteration of the Springfield Coal Member (Pennsylvanian) and adjacent clastic rocks, Illinois Basin, USA. *International Journal of Coal Geology*, 166: 108-117.
- Racki, G., Adatte, T., Bond, D.P.G. and Keller, G., 2020. Volcanism as a prime cause of mass extinctions: Retrospectives and perspectives, *Mass Extinctions, Volcanism, and Impacts: New Developments*. Geological Society of America, pp. 0.

- Rahman, M.W. and Rimmer, S.M., 2014. Effects of rapid thermal alteration on coal: Geochemical and petrographic signatures in the Springfield (No. 5) Coal, Illinois Basin. *International Journal of Coal Geology*, 131: 214-226.
- Raymond, A.C. and Murchison, D.G., 1988. Development of organic maturation in the thermal aureoles of sills and its relation to sediment compaction. *Fuel*, 67(12): 1599-1608.
- Raymond, A.C. and Murchison, D.G., 1992. Effect of igneous activity on molecular-maturation indices in different types of organic matter. *Organic Geochemistry*, 18(5): 725-735.
- Samankassou, E., Mazzini, A., Chiaradia, M., Spezzaferri, S., Moscariello, A. and Do Couto, D., 2018. Origin and age of carbonate clasts from the Lusi eruption, Java, Indonesia. *Marine and Petroleum Geology*, 90: 138-148.
- Sanei, H., Grasby, S.E. and Beauchamp, B., 2012. Latest permian mercury anomalies. *Geology*, 40(1): 63-66.
- Sano, Y. and Fischer, T.P., 2013. The Analysis and Interpretation of Noble Gases in Modern Hydrothermal Systems. In: P. Burnard (Editor), *The Noble Gases as Geochemical Tracers*. Springer Berlin Heidelberg, Berlin, Heidelberg, pp. 249-317.
- Sawolo, N., Sutriyono, E., Istadi, B.P. and Darmoyo, A.B., 2009. The LUSI mud volcano triggering controversy: Was it caused by drilling? *Marine and Petroleum Geology*, 26(9): 1766-1784.
- Sawolo, N., Sutriyono, E., Istadi, B.P. and Darmoyo, A.B., 2010. Was LUSI caused by drilling? – Authors reply to discussion. *Marine and Petroleum Geology*, 27(7): 1658-1675.
- Schenk, H.J., Di Primio, R. and Horsfield, B., 1997. The conversion of oil into gas in petroleum reservoirs. Part 1: Comparative kinetic investigation of gas generation from crude oils of lacustrine, marine and fluviodeltaic origin by programmed-temperature closed-system pyrolysis. *Organic Geochemistry*, 26(7): 467-481.
- Sciarra, A., Mazzini, A., Inguaggiato, S., Vita, F., Lupi, M. and Hadi, S., 2018. Radon and carbon gas anomalies along the Watukosek Fault System and Lusi mud eruption, Indonesia. *Marine and Petroleum Geology*, 90: 77-90.
- Self, S., Coffin, M.F., Rampino, M.R. and Wolff, J.A., 2015a. Chapter 24 - Large Igneous Provinces and Flood Basalt Volcanism. In: H. Sigurdsson (Editor), *The Encyclopedia of Volcanoes* (Second Edition). Academic Press, Amsterdam, pp. 441-455.
- Self, S., Glaze, L.S., Schmidt, A. and Mather, T.A., 2015b. Volatile release from flood basalt eruptions: understanding the potential environmental effects. In: A. Schmidt, K. Fristad and L. Elkins-Tanton (Editors), *Volcanism and Global Environmental Change*. Cambridge University Press, Cambridge, pp. 164-176.
- Self, S., Thordarson, T. and Widdowson, M., 2005. Gas Fluxes from Flood Basalt Eruptions. *Elements*, 1(5): 283-287.
- Senger, K., Millett, J., Planke, S., Ogata, K., Eide, C.H., Festøy, M., Galland, O. and Jerram, D.A., 2017. Effects of igneous intrusions on the petroleum system: a review. *First Break*, 35(6): 47-56.
- Sherwood Lollar, B., Westgate, T.D., Ward, J.A., Slater, G.F. and Lacrampe-Couloume, G., 2002. Abiogenic formation of alkanes in the Earth's crust as a minor source for global hydrocarbon reservoirs. *Nature*, 416(6880): 522-524.
- Simoneit, B.R.T., 2018. Hydrothermal Petroleum. In: H. Wilkes (Editor), *Hydrocarbons, Oils and Lipids: Diversity, Origin, Chemistry and Fate*. Springer International Publishing, Cham, pp. 1-35.
- Simoneit, B.R.T., Philp, R.P., Jenden, P.D. and Galimov, E.M., 1984. Organic geochemistry of Deep Sea Drilling Project sediments from the Gulf of California—hydrothermal effects on unconsolidated diatom ooze. *Organic Geochemistry*, 7(3): 173-205.
- Spacapan, J.B., Palma, J.O., Galland, O., Manceda, R., Rocha, E., D'Odorico, A. and Leanza, H.A., 2018. Thermal impact of igneous sill-complexes on organic-rich formations and implications

- for petroleum systems: A case study in the northern Neuquén Basin, Argentina. *Marine and Petroleum Geology*, 91: 519-531.
- Svensen, H., Fristad, K.E., Polozov, A.G. and Planke, S., 2015. Volatile generation and release from continental large igneous provinces. In: A. Schmidt, K. Fristad and L. Elkins-Tanton (Editors), *Volcanism and Global Environmental Change*. Cambridge University Press, Cambridge, pp. 177-192.
- Svensen, H., Karlsen, D.A., Sturz, A., Backer-Owe, K., Banks, D.A. and Planke, S., 2007a. Processes controlling water and hydrocarbon composition in seeps from the Salton Sea geothermal system, California, USA. *Geology*, 35(1): 85-88.
- Svensen, H., Planke, S., Chevallier, L., Malthe-Sørenssen, A., Corfu, F. and Jamtveit, B., 2007b. Hydrothermal venting of greenhouse gases triggering Early Jurassic global warming. *Earth and Planetary Science Letters*, 256(3): 554-566.
- Svensen, H., Planke, S., Malthe-Sørenssen, A., Jamtveit, B., Myklebust, R., Rasmussen Eidem, T. and Rey, S.S., 2004. Release of methane from a volcanic basin as a mechanism for initial Eocene global warming. *Nature*, 429(6991): 542-545.
- Svensen, H., Planke, S., Polozov, A.G., Schmidbauer, N., Corfu, F., Podladchikov, Y.Y. and Jamtveit, B., 2009. Siberian gas venting and the end-Permian environmental crisis. *Earth and Planetary Science Letters*, 277(3): 490-500.
- Svensen, H.H., Iyer, K., Schmid, D.W. and Mazzini, A., 2018. Modelling of gas generation following emplacement of an igneous sill below Lusi, East Java, Indonesia. *Marine and Petroleum Geology*, 90: 201-208.
- Svensen, H.H., Jerram, D.A., Polozov, A.G., Planke, S., Neal, C.R., Augland, L.E. and Emeleus, H.C., 2019. Thinking about LIPs: A brief history of ideas in Large igneous province research. *Tectonophysics*, 760: 229-251.
- Sydnes, M., Fjeldskaar, W., Løtveit, I.F., Grunnaleite, I. and Cardozo, N., 2018. The importance of sill thickness and timing of sill emplacement on hydrocarbon maturation. *Marine and Petroleum Geology*, 89: 500-514.
- Taylor, G.H., Teichmüller, M., Davis, A., Diessel, C.F.K., Littke, R. and Robert, P., 1998. *Organic petrology*. Gebrüder Borntraeger Berlin.
- Teske, A., McKay, L.J., Ravelo, A.C., Aiello, I., Mortera, C., Núñez-Useche, F., Canet, C., Chanton, J.P., Brunner, B., Hensen, C., Ramírez, G.A., Sibert, R.J., Turner, T., White, D., Chambers, C.R., Buckley, A., Joye, S.B., Soule, S.A. and Lizarralde, D., 2019. Characteristics and Evolution of sill-driven off-axis hydrothermalism in Guaymas Basin – the Ringvent site. *Scientific Reports*, 9(1): 13847.
- Tingay, M., Manga, M., Rudolph, M.L. and Davies, R., 2018. An alternative review of facts, coincidences and past and future studies of the Lusi eruption. *Marine and Petroleum Geology*, 95: 345-361.
- Tissot, B.P. and Welte, D.H., 1984. *Petroleum Formation and Occurrence*. Springer Berlin Heidelberg.
- Torsvik, T.H. and Burke, K., 2015. Large igneous province locations and their connections with the core–mantle boundary. In: A. Schmidt, K. Fristad and L. Elkins-Tanton (Editors), *Volcanism and Global Environmental Change*. Cambridge University Press, Cambridge, pp. 30-46.
- Vanderkluyzen, L., Burton, M.R., Clarke, A.B., Hartnett, H.E. and Smekens, J.-F., 2014. Composition and flux of explosive gas release at LUSI mud volcano (East Java, Indonesia). *Geochemistry, Geophysics, Geosystems*, 15(7): 2932-2946.
- Vassoevitch, N., 1972. Source matter for oil and gas (In Rus.) *Ishodnoye veschestvo dlya nefi i gasa*, Oil and gas origin and field formation. Nedra, Moscow, pp. 39-70.
- Vassoevitch, N., Korchagina, Y., Lopatin, N. and Chernyshev, V., 1969. Principal phase of oil formation. *Moscow Univ. Vestnik* 6, pps 3-27 (In Russian). *Engl Translation in Geol. Rev.* (1970), 12: 1276-1296.

- Vogt, P.R., 1972. Evidence for Global Synchronism in Mantle Plume Convection, and Possible Significance for Geology. *Nature*, 240(5380): 338-342.
- Wang, D. and Manga, M., 2015. Organic matter maturation in the contact aureole of an igneous sill as a tracer of hydrothermal convection. *Journal of Geophysical Research: Solid Earth*, 120(6): 4102-4112.
- White, W.M., 2015. *Isotope geochemistry*. John Wiley & Sons.
- Wignall, P.B., 2001. Large igneous provinces and mass extinctions. *Earth-Science Reviews*, 53(1): 1-33.
- Younker, L.W., Kasameyer, P.W. and Tewhey, J.D., 1982. Geological, geophysical, and thermal characteristics of the Salton Sea Geothermal Field, California. *Journal of Volcanology and Geothermal Research*, 12(3): 221-258.
- Zaputlyeva, A., Mazzini, A., Caracausi, A. and Sciarra, A., 2019. Mantle-derived fluids in the East Java sedimentary basin, Indonesia. *Journal of Geophysical Research: Solid Earth*, 124: 7962–7977.

Part II Scientific Contributions

Manuscript 1: Mantle-derived fluids in the East Java sedimentary basin, Indonesia

A. Zaputlyeva, A. Mazzini, A. Caracausi, and A. Sciarra

Published in the *Journal of Geophysical Research: Solid Earth*, 124.

<https://doi.org/10.1029/2018JB017274>



RESEARCH ARTICLE

10.1029/2018JB017274

Mantle-Derived Fluids in the East Java Sedimentary Basin, Indonesia

Alexandra Zaputlyaeva¹ , Adriano Mazzini¹ , Antonio Caracausi² , and Alessandra Sciarra^{3,4}

¹Centre for Earth Evolution and Dynamics (CEED), University of Oslo, Oslo, Norway, ²Istituto Nazionale di Geofisica e Vulcanologia (INGV), Palermo, Italy, ³Istituto Nazionale di Geofisica e Vulcanologia (INGV), Rome, Italy, ⁴Consiglio Nazionale delle Ricerche—Istituto di Geologia Ambientale e Geoingegneria, Rome, Italy

Key Points:

- Advective migration of mantle-derived volatiles occurs through faults and fractures in the sedimentary basin
- Mantle-derived volatiles are trapped within shallow hydrocarbon accumulations
- Biodegradation processes in the hydrocarbon reservoirs and gas dissolution in the formation water mask the abiogenic carrier gas

Correspondence to:

A. Zaputlyaeva, alexandra.zaputlyaeva@geo.uio.no

Citation:

Zaputlyaeva, A., Mazzini, A., Caracausi, A., & Sciarra, A. (2019). Mantle-derived fluids in the East Java sedimentary basin, Indonesia. *Journal of Geophysical Research: Solid Earth*, 124, 7962–7977. <https://doi.org/10.1029/2018JB017274>

Received 29 DEC 2018
 Accepted 8 JUL 2019
 Accepted article online 16 JUL 2019
 Published online 14 AUG 2019
 Corrected 18 NOV 2019

This article was corrected on 18 NOV 2019. See the end of the full text for details.

Abstract The Tertiary back-arc sedimentary basin in East Java (Indonesia) hosts a large variety of piercement structures and hydrocarbon fields. Some of the latter (Wunut, Tanggulangin, Carat, Watudakon) are located a few kilometers away from the Arjuno-Welirang volcanic complex and neighboring Lusi, the largest active sediment-hosted hydrothermal system on Earth. In order to investigate interactions between volcanic and sedimentary settings, we performed gas sampling on these four shallow (200- to 1,000-m depth) petroleum fields. The fields around Lusi are dominated by thermogenic gas that was altered during biodegradation processes. The helium isotope ratios (³He/⁴He) are as high as 6.7 R_A, which is remarkably similar to those measured at the fumaroles of the adjacent volcanic complex (R = 7.3 R_A) and at the Lusi site (up to 6.5 R_A). This highlights the pervasive outgassing of mantle-derived fluids in the sedimentary basin. Despite these two systems sharing the same mantle-derived helium source, their hydrocarbons have two different genetic histories: Lusi hydrocarbon gas has been more recently generated and is less molecularly and isotopically fractionated, while the gas trapped in the reservoirs is older and more altered. Unlike Lusi, the hydrocarbon fields contain small amounts of CO₂ resulting from biodegradation processes. The Watukosek fault system, originating from the Arjuno-Welirang volcanic complex and extending toward the northeast of Java, intersects Lusi and the hydrocarbon fields. This network of faults controls the migration of mantle-derived fluids within the sedimentary basin, feeding the focused venting at the Lusi site and promoting the slower and pervasive migration in the reservoirs.

Plain Language Summary The East Java sedimentary basin is located to the north of the E-W trending chain of active volcanoes that transects the Java Island. The basin hosts numerous oil and gas fields, as well as buried diapirs and active mud eruption sites. This study focuses on gas geochemical analyses from the surface seeps and four shallow petroleum fields located around Lusi, the largest active mud eruption on Earth. Comparative results show that the biodegraded thermogenic gas in the reservoirs differs from the thermogenic gas vented at Lusi and its surrounding seeps. In contrast, helium gas analysis from the hydrocarbon reservoirs, the Lusi eruption and satellite seeps, and from the fumaroles at the neighboring Arjuno-Welirang volcanic complex share a common mantle-derived component. Available seismic data from the region confirm that a system of faults (Watukosek fault system), extending from the volcanic complex toward the sedimentary basin, promotes the migration of mantle-derived fluids through a broad area in the East Java sedimentary basin. These results confirm that the Lusi system is fueled by the lateral migration of mantle-derived fluids that trigger reactions within the organic rich formations in the sedimentary basin.

1. Introduction

The presence of mantle-derived volatiles is typically associated with degassing of volcanic plumes, diffuse emissions around volcanic edifices, mid-ocean ridges, modern continental rifts, or deep active fault systems (e.g., Caracausi et al., 2015; Caracausi & Sulli, 2019; Halldórsson et al., 2013; Lee et al., 2016; Sano & Fischer, 2013). These systems are commonly dominated by water and CO₂ and contain trace amounts of noble gases with specific isotopic compositions that indicate a mantle-derived origin (Moreira & Kurz, 2013). Some sedimentary basins have been documented to host hydrocarbon (HC) reservoirs containing mantle-derived volatiles, for example, Green Tuff Basin in Japan, Okinawa Trough in East China Sea,

©2019. The Authors. This is an open access article under the terms of the Creative Commons AttributionNonCommercialNoDerivs License, which permits use and distribution in any medium, provided the original work is properly cited, the use is noncommercial and no modifications or adaptations are made.

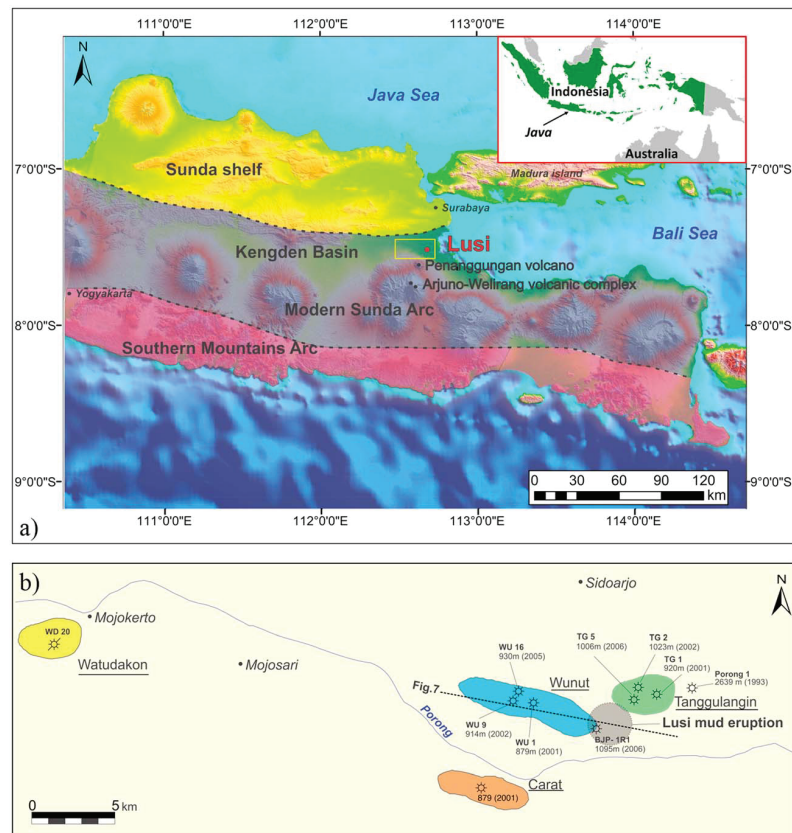


Figure 1. (a) Digital elevation model of the central and eastern Java with main tectonic zones (redrawn and modified after Istadi et al., 2009; Smyth et al., 2008); the yellow rectangle indicates the study area depicted at (b); inset map of Indonesia; (b) location of the sampled wells in the Wunut, Tanggulangin, Carat, Watudakon fields, bottom hole depth, and drilling year. Dashed line indicates the location of the seismic profile, shown at Figure 7.

Sacramento Basin and Escanaba Trough in California, and multiple basins distributed in New Zealand, Thailand, Indonesia, Philippines, Taiwan, and Kamchatka peninsula (Ishibashi et al., 2002; Jenden et al., 1993; Kamenskiy et al., 1971; Poreda et al., 1986; Sakata et al., 1997; Xu et al., 1995). Thermogenic gas produced at these localities ($\delta^{13}\text{C}_{\text{CH}_4}$ between -30‰ and -60‰) was mainly generated by the thermal cracking of organic matter. Helium (hereafter He) isotope compositions at these reservoirs indicate the presence of mantle-derived volatiles ($R = 0.2\text{--}7.7 R_A$, where $R = {}^3\text{He}/{}^4\text{He}$ of the sample, $R_A = {}^3\text{He}/{}^4\text{He}$ of air (1.4×10^{-6})).

A setting similar to those described above is encountered in the Tertiary-aged East Java sedimentary basin, north of the volcanic Sunda Arc, formed by the subduction of the Indo-Australian plate beneath the Eurasian continental plate (Hall, 2002; Figure 1a). The basin is characterized by high sedimentation rates, deposition of organic-rich sediments, and volcanoclastic and carbonate traps, resulting in the formation of a HC province with numerous oil and gas fields and diffused surface and subsurface piercement structures (Istadi et al., 2012; Mazzini et al., 2018; Mazzini et al., 2007; Moscariello et al., 2018; Satyana & Purwaningsih, 2003a, 2003b). The basin bordered to the south by the Penanggungan, Arjuno-Welirang, and Bromo volcanoes and represents an ideal opportunity to investigate the relationship between mantle-derived volatiles and HC fluids in oil and gas reservoirs.

This region is also of particular interest because of the Lusi piercement, the world's largest active mud eruption neighboring the Holocene Penanggungan and Arjuno-Welirang volcanoes, situated, respectively, at 10 and 25 km to the southwest (Figures 1b and 2). Lusi (named after LUMpur, meaning mud in Indonesian, and Sidoarjo, the Local Regency) started its eruptive activity on the 29 May 2006 and has since been continuously

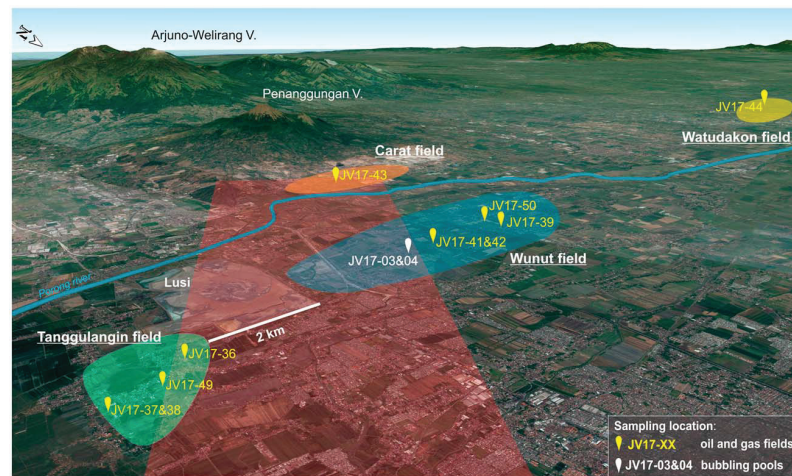


Figure 2. 3-D Google Earth view of the study area with indicated location of the oil and gas fields (color shaded areas), the sampling stations, and the Watukosek fault system (red shaded area).

bursting boiling water, gas, mud, oil, and rock clasts (Van Noorden, 2006). A set of targeted field campaigns has been completed since the beginning of the eruption to investigate the origin of the erupted fluids and the subsurface plumbing system (Miller & Mazzini, 2018, and references therein). Results revealed that outgassing boiling fluids at the Lusi surface contain evidence of hydrothermal waters and a mix of inorganic and organic gases, including geothermal (thermo-metamorphic and mantle-derived) and biotic (i.e., thermogenic methane) gases (Mazzini et al., 2012; Mazzini et al., 2018). Ambient noise tomography revealed a connection between the Arjuno-Welirang magma chamber and the Lusi conduit at around 4.5-km depth, indicating the migration of magmatic and hydrothermal fluids toward the sedimentary basin (Fallahi et al., 2017). These results confirmed that Lusi is indeed not a mud volcano but rather a sediment-hosted geothermal system (Mazzini & Etiope, 2017; Procesi et al., 2019). Sampling from the fumaroles of the Arjuno-Welirang volcanic complex provided further evidence of the connection between these two eruptive systems (Inguaggiato et al., 2018). The authors revealed that both the fumaroles of the Arjuno-Welirang and gas at the Lusi site contain magmatic volatiles with high ^3He abundance ($R = 7.3$ and $6.5 R_A$, respectively). Furthermore, the Watukosek fault system (WFS), extending toward the northeast of the island from the Arjuno-Welirang volcanic complex (Figure 2), hosts Lusi and several mud volcanoes (Fallahi et al., 2017; Mazzini et al., 2009; Mazzini et al., 2012; Moscariello et al., 2018; Obermann et al., 2018; Sciarra et al., 2018). The authors indicate that this sinistral strike-slip system provides an ideal pathway for the propagation of the deep overpressured hydrothermal fluids toward the sedimentary basin and further to the surface.

This complex plumbing system and tectonic structures are largely controlling the past and present migration of fluids. Lusi is surrounded by three shallow oil and gas fields (Figures 1b and 2) that reflect the paleo-migration of HCs in the basin. Despite the obvious proximity between Lusi and these HC reservoirs, no dedicated studies have yet been conducted to investigate (1) if the HC gas currently erupted at Lusi is the same as that stored in the reservoirs, (2) if any correlation represents a potential connection between these two systems, and (3) whether the WFS could also provide a migration pathway for the mantle-derived fluids to the shallow reservoirs. This study aims to characterize the composition and origin of the gas trapped in the subsurface and to unravel the above questions by analyzing targeted samples.

2. Geological Setting

The East Java Basin is located on the southeastern margin of the Sunda plate, bounded to the south by the northward subduction of the Indian-Australian Plate. The subduction initiated in the Middle Eocene and resulted in the formation of two volcanic arcs: the Southern Mountain Arc (active between ca. 45 and

20 Ma) and Sunda Arc (active since ca. 12–10 Ma; Hall, 2013; Smyth et al., 2008). The axis of the Sunda Arc is located 50 km to the north from the older Southern Mountain Arc. The Arjuno-Welirang volcanic complex consists of Holocene stratovolcanoes, located in the eastern part of the Sunda Arc. Penanggungan is the northeasternmost volcano of this complex and is in the vicinity (~10 km) of the Lusi mud eruption and the studied oil and gas fields. The most recent recorded eruptive activity occurred at the Welirang volcano in 1952 (Global Volcanism Program, 2013). Currently, the crater is characterized by solfataric fields, with several hydrothermal seeps distributed on the flanks (Inguaggiato et al., 2018; Mazzini et al., 2012; Mazzini et al., 2018).

The East Java Basin comprises a complex of northeast to southwest trending troughs, developed during Late Eocene to Early Miocene due to the extensional regime of the Sunda plate (Doust & Noble, 2008). The sedimentary section contains more than 5 km of deposits, spanning in age from Eocene to recent, overlying the pre-Tertiary basement, with the maximum sediment thickness of 8–10 km in the Kengden graben (Hall et al., 2011; Kusumastuti et al., 1999; Martha et al., 2017). In the study area, the lithostratigraphic section is constrained by drilled boreholes, analyzed clasts erupted at the Lusi site, and by seismic surveys from the 1990s–2000s (Istadi et al., 2009; Malvoisin et al., 2018; Mazzini et al., 2018; Mazzini et al., 2007; Moscarriello et al., 2018; Samankassou et al., 2018; Satyana & Purwaningsih, 2003b; Sharaf et al., 2005; Tingay, 2015). The sedimentary section constrained in the deepest well (BJP1, TVD 2,833 m) consists of (from top to down) the following:

1. recent alluvial sediments (intercalated sands, shales, and volcanoclastic sands and clays), 0–290 m;
2. volcanoclastic shales and sands of the Pucangan Formation, Pleistocene, 290–900 m;
3. bluish gray shales of the upper part of the Upper Kalibeng Formation, Pleistocene, 900–1,871 m; and
4. tight volcanic and volcanoclastic units of the lower part of the Upper Kalibeng Formation, Upper Pliocene-Pleistocene, 1,871 to at least ~2,833 m.

Lithostratigraphy below 2,833 m is based on regional studies, Lusi mud breccia analyses, and seismic data

1. marls and shales of the Tuban Formation, Lower-Upper Miocene, from >2,833 to ~3,250 m;
2. reefal and platform carbonates of the Kujung Formation, Upper Oligocene-Lower Miocene, from ~3,250 to ~3,800 m; and
3. organic-rich black shales of the Ngimbang Formation, Middle Eocene-Lower Oligocene, >3,800 m.

The basin is characterized by high sedimentation rates (0.7 km/Ma) since Late Pliocene, which resulted in fast burial and preservation of the semilithified deposits.

3. Petroleum System of the East Java Basin

The East Java Basin is a petroleum province with a total reserve volume of 1,830 Million Barrels of Oil Equivalent (Doust & Noble, 2008). The HC accumulations in the basin are confined to shallow volcanoclastic Pleistocene reservoirs (Pucangan Fm.), Miocene sands of the Ngrayong and Woncolo Formations, Upper Oligocene-Lower Miocene reefal carbonates of the Kujung Fm., and carbonates and sands of the Ngimbang Formation (Doust & Noble, 2008; Satyana & Purwaningsih, 2003b).

The main HC source rock is suggested to be the Middle Eocene-Lower Oligocene organic-rich shales, coals, and coaly shales of the Ngimbang Fm. (Devi et al., 2018; Satyana & Purwaningsih, 2003a). These sediments were deposited in a fluvio-deltaic to near-shore marine environment. Organic-rich shales of the Ngimbang Fm. contain up to 5.7 wt.% Total Organic Carbon (TOC) and coal bearing interval with TOC up to 67 wt.% (Satyana & Purwaningsih, 2003a).

The study area is located in the southern part of the East Java Basin, to the north of the Arjuno-Welirang volcanic complex and in the neighborhood of the Lusi eruption site. Three production HC fields, Wunut, Tanggulangin, and Carat, surrounding Lusi site were targeted for investigation. Here producing reservoir intervals are confined to the Pucangan Fm., 200- to 1,000-m depth, that was deposited as a northeastward prograding, volcanoclastic sedimentary wedge (Istadi et al., 2009; Kusumastuti et al., 1999). The Pucangan Fm. consists of predominantly fine-grained material (up to 80% of net shales) and layers of sandstones, 3–47 m thick (Kusumastuti et al., 1999). The intercalating shales seal the HC accumulations. The traps

are four-way dip closures with multiple reservoir layers. The lower intervals of the Pucangan Fm. contain oil, while the shallower units are gas prone. The measured thermal gradient in the wells varies from 2.8 to 4.9 °C/100 m.

4. Sampling and Analytical Procedures

During spring 2017, a gas sampling campaign was conducted in northeast Java with the aim to obtain surface and subsurface gas samples of the southern part of the East Java Basin. Two main settings and localities have been targeted (Figures 1b and 2). The first set of samples (Group 1) was collected from several production wells of targeted gas fields (Wunut, Tanggulangin, and Carat). Surface seeping gas was collected from bubbling pools, located above the Wunut field (Group 2). In addition, the Watudakon gas field (~36 km west of the Lusi on the outskirts of the Arjuno-Welirang volcanic complex) was sampled (Group 3). Formation waters from the Wunut and Watudakon fields were also sampled to conduct dissolved gas analyses (Group 4). Finally, selected rock cuttings from the BJP1-R1 well, originally drilled in the outskirts of the Lusi eruption site (Sutrisna, 2009), were analyzed for the TOC content through the interval 543–884 m of the Pucangan Fm. and 900–993 m of the Up. Kalibeng Fm.

Gas samples were collected in two valve steel and glass samplers. Prior to sampling, the head well was routinely flushed for 20 min to reduce potential contamination of the sample. Bubbling seeps were sampled using a plastic funnel positioned upside-down and connected by silicone tubes to glass or steel tanks. Water was collected in crimped 245-ml glass water flasks.

The analyses of chemical composition of fluids were completed at the Istituto Nazionale di Geofisica e Vulcanologia (INGV-Palermo, Italy). Gas chromatography (GC) was performed using a gas chromatograph (Perkin Elmer Clarus 500) equipped with a double detector (thermal conductivity detector and a flame ionization detector with a methanizer) using Ar as the carrier gas and a 3-m packed column (Restek Shincarbon ST), with analytical errors of <3%.

Dissolved gas samples were extracted by the collected waters and analyzed by using the methodology proposed by Capasso and Inguaggiato (1998).

The carbon isotopic composition of CO₂ ($\delta^{13}\text{C}_{\text{CO}_2}$) was determined using a Thermo Delta XP Isotope Ratio Mass Spectrometer coupled with a Thermo Scientific™ TRACE™ Ultra Gas Chromatograph. Separation prior to analysis was done through a 30-m Q-plot column (i.e., of 0.32 mm). The resulting $\delta^{13}\text{C}_{\text{CO}_2}$ values are expressed in per mil notation with respect to the international Vienna Pee Dee Belemnite (VPDB) standard and analytical uncertainties of $\pm 0.15\%$.

The carbon and deuterium isotopic composition of CH₄ ($\delta^{13}\text{C}_{\text{CH}_4}$ and $\delta\text{D}_{\text{CH}_4}$) was determined using a Thermo TRACE GC interfaced to a Delta Plus XP gas source mass spectrometer and equipped with a Thermo GC/C III (for Carbon) and with GC/TC peripherals (for Hydrogen). The $^{13}\text{C}/^{12}\text{C}$ ratios are reported as $\delta^{13}\text{C}_{\text{CH}_4}$ values with respect to the VPDB standard, and $^2\text{H}/^1\text{H}$ ratios are reported here as $\delta\text{D}_{\text{CH}_4}$ values with respect to the Vienna Standard Mean Ocean Water (VSMOW) standard. The analytical uncertainty of the measurements was 0.1‰.

Carbon isotopes of the methane homologs were measured in the Isotech Labs Inc. (Illinois, USA) using three IRMS instruments: Delta Plus, Delta Plus XL, and Delta V Plus.

^3He , ^4He and ^{20}Ne , and the $^4\text{He}/^{20}\text{Ne}$ ratios were determined by separately injecting He and Ne into a split flight tube mass spectrometer (GVI-Helix SFT, for He analysis) and then into a multicollector mass spectrometer (Thermo-Helix MC plus, for Ne analysis), after standard purification procedures (Correale et al., 2012). The analytical error was generally less than 1%. The R/R_A values were corrected for atmospheric contamination based on the $^4\text{He}/^{20}\text{Ne}$ ratio (Sano & Wakita, 1985). The Ar-isotope composition was measured in a multicollector mass spectrometer (GVI Argus), for which the analytical uncertainty was 0.5%.

Measured He isotopes values are reported as R/R_A , where $R = ^3\text{He}/^4\text{He}$, measured in the sample, and $R_A = ^3\text{He}/^4\text{He}$ of air (1.4×10^{-6}). Helium concentrations in the analyzed samples range from 5 to 140 ppm. $^4\text{He}/^{20}\text{Ne}$ ratio is 120–1,690 times higher than that measured in air ($^4\text{He}/^{20}\text{Ne} = 0.318$), confirming very low air contamination and validating the accuracy of the results.

Table 1

Major Gas Components of the Sampled Free Gas (Group 1-3, in vol.%) and Dissolved Gas (Group 4, in cm³ per Liter at Standard Temperature and Pressure)

Sample ID	Group	Field	Well, sampling depth interval (m)	He	H ₂	O ₂	N ₂	CH ₄	CO	H ₂ S	CO ₂	C ₂ H ₆	C ₃ H ₈	C ₁ / (C ₂ + C ₃)	
JV17-36	1	Tanggulangin	Well TG5, 742–966	0.0008	nd	0.01	0.7	91.6	nd	nd	4.58	2.66	0.66	28	
JV17-37			Well TG1, 468–471	0.0013	nd	0.20	2.1	97.7	nd	nd	0.22	0.14	nd	698	
JV17-38			Well TG1SS, 417–425	0.0023	nd	0.11	2.6	96.9	nd	nd	0.06	0.05	nd	1,978	
JV17-49			Well TG2, 435–460	0.0026	0.0043	0.16	3.3	96.1	nd	nd	0.08	0.05	nd	2,056	
JV17-41			Wunut	Well WU-1ST, 218–246	0.0050	0.0005	1.13	6.9	91.0	nd	nd	0.05	0.03	nd	2,757
JV17-42				Well WU 1A-LS, 341–347	0.0046	0.0002	0.06	2.7	97.2	nd	nd	0.10	0.04	nd	2,745
JV17-50				Well WU9LS, 790–885	0.0005	0.0007	0.25	1.2	96.5	nd	nd	0.37	0.61	nd	158
JV17-39				Well WU16, 627–807 (?573?)	0.0015	0.0008	0.07	1.3	96.3	nd	nd	0.02	1.72	0.42	45
JV17-43			2	Carat	Well CA-1, 494–500	0.0012	0.0002	0.04	0.5	99.3	nd	nd	0.04	0.08	nd
JV17-03	Surface seep	Bubbling pool			0.0141	0.0043	0.33	7.0	85.2	nd	nd	1.10	3.88	1.60	16
JV17-04			Bubbling pool	0.0139	0.0040	0.28	6.9	83.4	nd	nd	1.18	3.86	1.68	15	
JV17-44	3	Watudakon	well WD20, ~350 m	0.0006	0.0011	0.01	1.2	98.7	nd	nd	0.06	0.09	nd	1,103	
JV17-46	4	Watudakon	well WD17, ~600 m	0.0004	0.0240	0.17	2.3	20.8	0.002	b.d.l.	8.28	b.d.l.	b.d.l.		
JV18-08			Wunut	well WU15, ~900 m	0.0002	0.00004	3.26	10.5	14.0	b.d.l.	b.d.l.	28.15	b.d.l.	b.d.l.	

Note. nd = not defined, b.d.l. = below detection limit.

TOC measurements were performed on the LECO CS-230, in the Federal Institute for Geosciences and Natural Resources (BGR), Germany. The method is described in Blumenberg et al. (2016).

5. Results

Gas geochemistry results obtained from the sampled localities are summarized in Tables 1 and 2. All sampled gases are methane-dominated (CH₄ > 91.6 vol.%). N₂ is present in variable concentrations (from 0.5 to 7.5 vol.%), and O₂ concentrations are up to 1.13 vol.%. The O₂/N₂ ratio in the collected gases is lower than 0.1 (except the sample JV17-50, 0.21), that is, lower than the same ratio in air (0.27) and in the air saturated water (0.53) showing that these fluids were not affected by strong air contamination.

More specifically, gas samples from the oil and gas production wells around Lusi (Group 1) contain methane ranging from 91 to 99 vol.% and higher methane homologs (ethane < 2.7 vol.% and propane < 0.7 vol.%). The gas dryness ratio C₁/(C₂ + C₃) varies from 28 to 2,757 and follows a general trend decreasing with the reservoir depth (Figure 3a). CO₂ concentrations are very low (average value 0.1 vol.%), except for the deepest producing units of TG5 well of Tanggulangin field (4.6 vol.%). The δ¹³C_{CH4} varies from −40.7‰ to −58.3‰ and δD_{CH4} from −201‰ to −177‰. The low CO₂ content present in the samples allowed the isotopic measurements to be performed in only two samples from Tanggulangin and Carat fields (18.9‰ and 22.8‰, respectively). He isotopes have a R/R_A ranging between 5.1 and 6.7, with the lowest values recorded in the deepest samples. Ar isotope composition (^{40/36}Ar) ranges between 303 and 435, higher than the same ratio in atmosphere (298.6; Ozima & Podosek, 2002).

Two gas samples from the bubbling pools above the Wunut field (Group 2, named surface seep in the Tables 1 and 2) revealed almost identical composition. Together with methane (average 84.3 vol.%) and CO₂ (average 1.14 vol.%), ethane and propane were also detected (3.9 and 1.6 vol.%, respectively). The average gas dryness ratio is 15.3, which is significantly lower than that measured for the Group 1 samples (Figure 3a). The isotopic analyses reveal δ¹³C_{CH4} = −42.5‰ and ranges of δD_{CH4} from −170‰ to −173‰, δ¹³C_{CO2} from 1.2‰ to 2.7‰, and R/R_A = 6.1 and ^{40/36}Ar from 330 to 357.

The gas sampled at the Watudakon gas field (Group 3) is also CH₄-dominated, with ethane abundance < 0.09 vol.%. Isotopic analyses revealed δ¹³C_{CH4} = −62.4‰ and δD_{CH4} = −190‰, while δ¹³C_{CO2} was not measured due to low CO₂ concentration (599 ppm).

Table 2
Isotopic Composition of the Sampled Free Gas

Sample ID	Group	Field	$\delta^{13}\text{C}_{\text{C1}}$	$\delta^{13}\text{C}_{\text{C2}}$	$\delta^{13}\text{C}_{\text{C3}}$	$\delta^{13}\text{C}_{\text{C4}}$	$\delta^{13}\text{C}_{\text{C5}}$	$\delta^{13}\text{C}_{\text{CH4}}$	$\delta^{13}\text{C}_{\text{CO2}}$	$\delta\text{D}_{\text{CH4}}$	R/ R_{A}	He	Ne	$^{4}\text{He}/^{20}\text{Ne}$	R/ R_{Ar}	$^{40}\text{Ar}/^{36}\text{Ar}$	^{40}Ar
JV17-36	1	Tanggulangin	-40.7	-25.7	-16.6	-22.6	-19.3	-21.8	-18.4	18.9	-181.5	7.3	0.04	194.3	5.9	435.0	18.7
JV17-37			-50.7							-200.9	5.9	13.8	0.09	147.6	5.9	323.2	83.8
JV17-38			-57.1							-196.9	6.6	22.7	0.17	130.1	6.6	308.9	181.1
JV17-49			-58.3							-198.4	6.2	25.4	0.66	38.4	6.2	303.4	288.9
JV17-41		Wunut	-48.5							-197.3	6.3	50.3	0.09	537.4	6.3	345.2	142.6
JV17-42			-47.8							-195.1	6.3	45.2	0.09	492.0	6.3	368.6	99.1
JV17-50			-57.7							-190.6	5.1	4.6	0.09	51.6	5.1	307.0	36.5
JV17-39			-41.8	-23.4	-16.1	-21.8	-18.1	-20.8		-176.8	5.9	14.9	0.18	81.6	5.9	357.0	40.6
JV17-43		Carat	-41.4							-195.6	6.7	11.2	0.03	371.4	6.7	313.8	84.3
JV17-03	2	Surface seep	-42.6	-27.1	-24.5	-25.7	-23.2	-23.8	22.8	-170.4	6.1	143.1	0.46	313.5	6.2	357.3	326.3
JV17-04			-42.5						2.7	-173.3	6.1	142.7	0.92	155.5	6.1	329.5	563.5
JV17-44	3	Watudakon	-62.4	-30.8					1.2	-190.1	2.1	5.8	0.10	56.5	2.1	300.5	83.1

Note. Isotopic data: $\delta^{13}\text{C}$ (‰ VPDB); δD (‰ VSMOW); R/ R_{A} = ($^{3}\text{He}/^{4}\text{He}$) sample / ($^{3}\text{He}/^{4}\text{He}$) atmosphere. He, Ne, and ^{40}Ar concentrations in parts per million.

The measurements of water-dissolved gases of the Watudakon gas field (Group 4) are CH₄-dominated (20.8-cm³/l Standard Temperature and Pressure (STP); Table 1) but with also high content of CO₂ (up to 8.28 cm³/l STP). This last value is 27 times higher than that measured in the Air Saturated Waters values (ASW = 0.31 cm³/l STP). Helium isotope composition revealed R/ R_{A} = 2.14 and $^{40}/^{36}\text{Ar}$ equals to 300.5‰. Water-dissolved gases at the Wunut field (Group 4) are CO₂-dominated (28.15 cm³/l STP, Table 1) with CH₄ content of 13.97 cm³/l STP.

Measured TOC in the cuttings of the Pucangan and Upper Kalibeng Formations from the BJP-R1 well resulted in 0.5 to 1.75 wt.% (average 0.9 wt.%).

6. Discussion

The acquired geochemical data set allowed to identify the origin of the gases that are trapped in the shallow HC reservoirs produced in the north-east Java. Furthermore, we combined the data in order to investigate if a possible connection exists between the neighboring Arjuno-Welirang volcanic complex and the reservoirs. This is described in detail in the following sections.

6.1. HC Origin and Alteration Processes in the Reservoirs

The origin of natural gases, trapped in the porous media, is commonly characterized using binary genetic diagrams of $\delta^{13}\text{C}_{\text{CH4}}$ versus $\delta\text{D}_{\text{CH4}}$, $\delta^{13}\text{C}_{\text{CH4}}$ versus $\text{C}_1/(\text{C}_2 + \text{C}_3)$, and $\delta^{13}\text{C}_{\text{CH4}}$ versus $\delta^{13}\text{C}_{\text{CO2}}$. These empirical diagrams were first proposed in 1970s–1980s (Bernard et al., 1977; Gutsalo & Plotnikov, 1981; Schoell, 1983; Whiticar et al., 1986) and have been more recently revised based on >690,000 data entries (Milkov & Etiope, 2018). This recent study highlights that the original molecular and isotopic composition of CH₄, its homologs, and CO₂ could be affected by several post-generation processes, including mixing, migration, biodegradation, thermochemical sulfate reduction, and oxidation. Therefore, a combined use of these plots is required to obtain distinctive conclusions in order to classify gases in natural systems.

Methane isotope composition of the gas from Group 1 ($\delta^{13}\text{C}_{\text{CH4}}$ range from -58.3‰ to -40.7‰ and $\delta\text{D}_{\text{CH4}}$ from -201‰ to -170‰) coupled to the ratio $\text{C}_1/(\text{C}_2 + \text{C}_3)$ indicates that the studied natural gases have mainly thermogenic origin (i.e., generated within organic-rich sediments due to thermal cracking of the kerogen), even if CH₄ from different reservoirs of the Group 1 shows a large variability of its isotopic composition (Figures 3b and 3c). These results are consistent with the migration of HCs from the organic-rich deep sited (>4 km) Middle Eocene-Lower Oligocene Ngimbang source rock (Kusumastuti et al., 1999). The HCs were presumably initially trapped in the Miocene reef carbonates of the Porong structure (located few kilometers to the east from the studied HC fields; see Figure 1b for location). After the collapse of the seal above this carbonate reservoir, HCs migrated through a system of faults to the shallow porous units of the Pucangan Fm during the Late Pleistocene-Holocene and migrated toward the west in the targeted reservoirs (Kusumastuti et al., 1999).

The positive carbon isotope ratio of the CO₂ ($\delta^{13}\text{C}_{\text{CO2}}$ +18.9‰ and +22.8‰) indicates that the HC reservoirs are affected by biodegradation processes (Figure 3d). Biodegradation is commonly taking place in

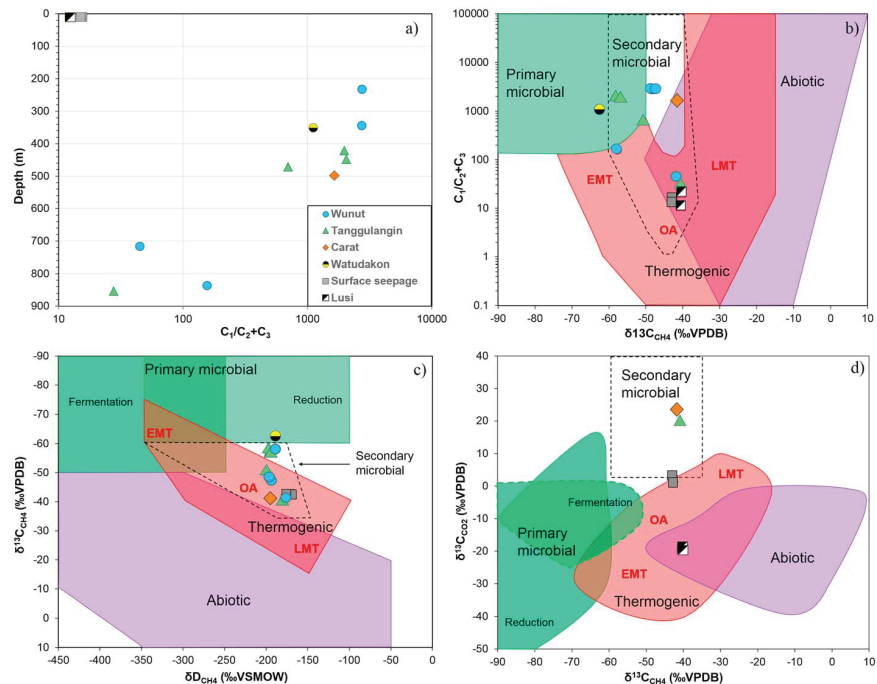


Figure 3. (a) The dryness plot of the sampled HC gases versus the reservoir depth reveals decreasing values at higher depths. The gas erupted at the Lusi surface, and adjacent seepages is wet. Gas genetic diagrams of (b) $C_1/(C_2 + C_3)$ versus $\delta^{13}C_{CH_4}$; (c) $\delta^{13}C_{CH_4}$ versus δD_{CH_4} ; (d) $\delta^{13}C_{CO_2}$ versus $\delta^{13}C_{CH_4}$; after Milkov and Etiope (2018). The genetic diagrams reveal the thermogenic origin of the gas sampled from the shallow HC reservoirs at Wunut, Tanggulangin, and Carat fields (Group 1) and the surface seepages (Group 2). The gas composition is altered by biodegradation processes, therefore mixed with secondary microbial gas. The gas sampled from the Watudakon field is of primary microbial origin. The majority of the sampled HC gas from the reservoirs is dry. HC gas from the Lusi crater (Mazzini et al., 2012), surface seepages, and two HC reservoirs (this study) is wet. EMT = Early Mature Thermogenic gas; LMT = Late Mature Thermogenic gas; OA = oil-associated gas; HC = hydrocarbon.

shallow HC reservoirs at temperatures below 80–90 °C (Head et al., 2003; Milkov, 2010, and references therein) and can be simplified in two main steps: 1) anaerobic oxidation of the thermogenic HCs followed by microbial CO_2 production, combined with (2) microbial (operated by methanogens) CH_4 generation via CO_2 reduction (Etiope et al., 2009; Milkov, 2018). Due to preferential selection by the methanogens of the ^{13}C -depleted CO_2 , the residue CO_2 is enriched in ^{13}C carbon isotope (Head et al., 2003; Milkov, 2011). Occurrence of biodegradation process in the reservoirs is also supported by the available carbon isotope analyses of the methane homologs (C_nH_{2n+2}) in the studied samples. The $\delta^{13}C$ measured on gaseous HCs formed due to thermocracking processes of, typically follows a regression trend (i.e., $\delta^{13}C_{CH_4} < \delta^{13}C_{C_2H_6} < \delta^{13}C_{C_3H_8} < \delta^{13}C_{C_4H_{10}}$, Chung et al., 1988; Schoell, 1983). An irregular trend is instead present in reservoirs with $T < 80$ – 90 °C affected by the HC biodegradation processes. This process occurs because of the selective preference of bacteria to use some homologs over others, that is propane and n-butane over ethane and isobutane (Wenger et al., 2002). Similarly to CO_2 microbial consumption, the bacteria favor the ^{13}C -depleted C_nH_{2n+2} , that is controlled by the bacterial enzymatic processes and C-C bond energies (Peters et al., 2005). As a result, the remaining C_nH_{2n+2} molecules are enriched in ^{13}C carbon. Our analyses, and the one described in Mazzini et al. (2012), reveal that the observed carbon isotope ratios trend (Figure 4) are consistent with the biodegradation processes described above.

A potential contribution of methane generated within the shales of the Pucangan and/or Kalibeng Formations cannot be excluded; however, this should be a limited amount given the relatively low TOC in this formation (TOC from 0.5 to 1.75 wt.%, average 0.9 wt.%).

The natural gas sampled at the Watudakon field is essentially methane-dominated with a clear microbial isotopic signature ($\delta^{13}C_{CH_4}$ and δD_{CH_4} are -62.4‰ and -190.1‰ , respectively; Figures 3b and 3c). This

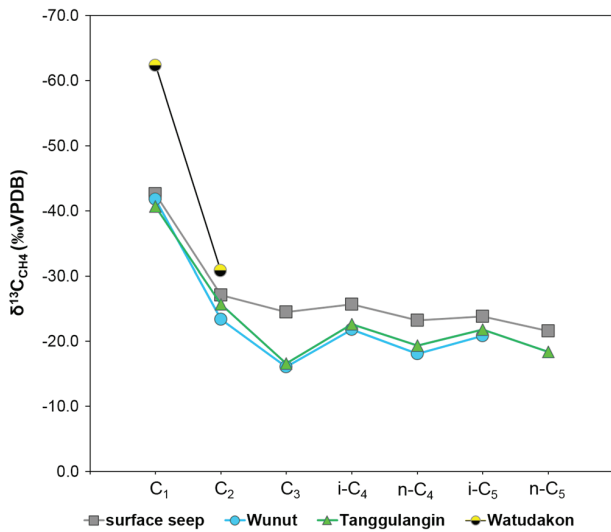


Figure 4. Carbon isotope distribution of the methane homologues in the samples from the Tanggulangin, Wunut, and Watudakon fields and surface seep. The plot indicates the occurrence of the hydrocarbon biodegradation processes in the Tanggulangin and Wunut reservoirs. Gas sampled at the surface seep above the Wunut field does not show the evidence of significant biodegradation.

indicates either (1) biodegradation processes of thermogenic HCs (gaseous and liquid), earlier generated by thermocracking process, or (2) ongoing microbial methanogenesis in the shallow organic-rich clays that interbed the porous media hosting the gas. According to the well log data from the Watudakon 20 well, there is no record of oil shows or other oil traces in the well. The trace amount of C₂₊ gases (lower than 0.1%) also supports a primary microbial origin of the methane. These data may suggest that the migration of HCs from the Ngimbang source rock did not occur in this peripheral part of the basin and that more recent microbial processes are currently very active.

6.2. Migration of the Mantle-Derived Fluids in the Sedimentary Basin

He isotopes represent a powerful tool for recognizing the occurrence of mantle-derived fluids in sedimentary HC reservoirs and in continental region away from volcanism (e.g., O’Nions & Oxburgh, 1988; Prinzhofer, 2013). He is an inert gas, highly mobile, physically stable, it has two stable isotopes (³He and ⁴He), and their isotopic signatures in the pristine reservoirs (atmosphere, crust and mantle) are strongly different: ³He has a primordial origin and is usually degassed from the mantle (Ozima & Podosek, 2002); ⁴He is produced by U and Th decay. Three major He reservoirs have distinct ³He/⁴He isotope ratios: (1) crust 0.01 R_A (R_A = ³He/⁴He of air, 1.4 × 10⁻⁶); (2) atmosphere 1 R_A; and (3) mantle from ~8 ± 1 R_A (Mid-Ocean Ridge Basalts mantle reservoir; Ozima & Podosek, 2002).

Our results (Table 2) reveal that all the samples from the HC reservoirs have a high ³He/⁴He isotope ratios (R/R_A as high as 6.7). Argon isotope composition (^{40/36}Ar) in the collected fluids shows that these fluids have low air contamination. This is confirmed by the values of the ⁴He/²⁰Ne ratios that are higher than the same ratio in the atmosphere (⁴He/²⁰Ne_{AIR} = 0.318, Table 2).

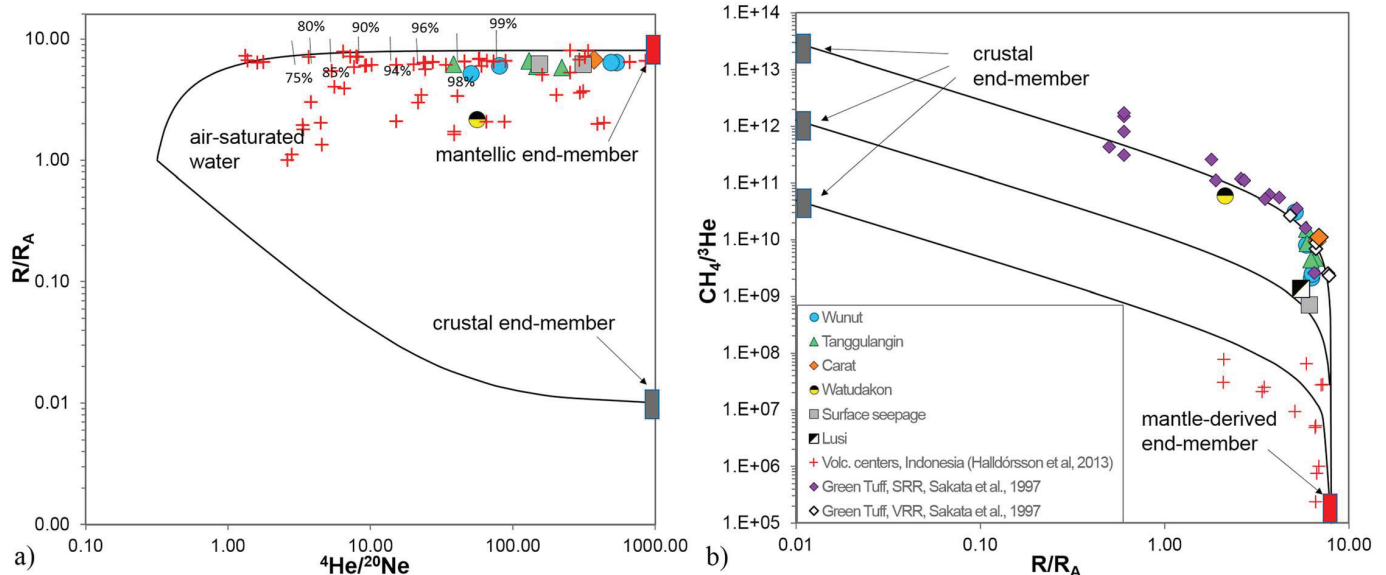


Figure 5. (a) Plot of the measured He isotopes versus ⁴He/²⁰Ne ratio showing the integrity of the He isotope results. The curves represent mixing between air-saturated water (1 R_A), Mid-Ocean Ridge Basalts (8 R_A), and crust (0.01 R_A); (b) plot of the CH₄/³He ratio versus He isotopes (R/R_A). Black lines indicate two-component mixing of the mantle-derived end-member (CH₄/³He = 1.0 × 10⁵ and ³He/⁴He = 8 R_A) and crustal end-member with three possible compositions (CH₄/³He = 5.0 × 10¹⁰, 1.3 × 10¹², and 3.0 × 10¹³ with a common ³He/⁴He = 0.01 R_A), adopted after Halldórsson et al. (2013) and Jenden et al. (1993). The plot demonstrates that even in the systems with high CH₄ abundance, He could have low crustal contamination.

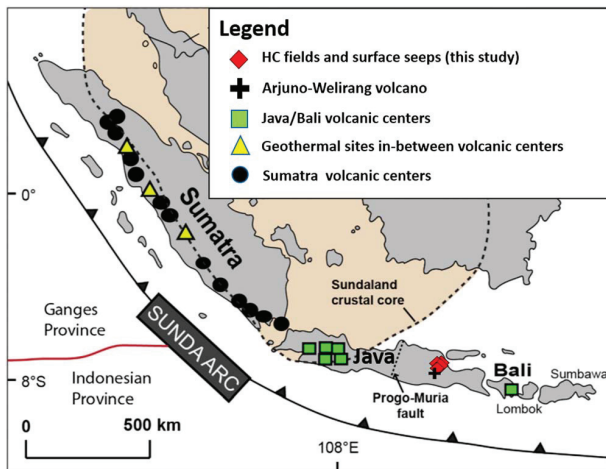


Figure 6. Map of Indonesia, modified after Halldórsson et al. (2013), showing measured He isotopes distribution through the Sunda arc (Halldórsson et al., 2013), at the Arjuno-Welirang volcano (Inguaggiato et al., 2018), and in the southern part of the East Java sedimentary basin (this study, red diamonds). HC = hydrocarbon.

The ranges of the measured He-isotope compositions and $^4\text{He}/^{20}\text{Ne}$ ratios in the collected gases can be explained in terms of mixing between three sources of He (Sano et al., 1997): atmosphere, mantle, and crust (Figure 5a). Since the investigated systems are located in a continental region, we assumed a Mid-Ocean Ridge Basalts mantle source in the area with a He-isotope ratio of $8 \pm 1 R_A$, as suggested by Halldórsson et al. (2013). We then computed the contributions of atmospheric, radiogenic, and mantle-derived He on the basis of the analytical $^3\text{He}/^4\text{He}$ and $^4\text{He}/^{20}\text{Ne}$ ratios (Sano et al., 1997). The fluids associated with the investigated HCs contain mantle He contributions from ~98% to ~99.9% (Figure 5a).

In order to constrain the possible origin of CH_4 in the HC reservoirs, we used the approach proposed by Poreda et al. (1988) that is based on a two component crust-mantle mixing model, $\text{CH}_4/^3\text{He}$ ratios versus He isotopes (Figure 5b). We used three possible crustal end-members with $\text{CH}_4/^3\text{He} = 5.0 \times 10^{10}$, 1.3×10^{12} , and 3.0×10^{13} , with common $^3\text{He}/^4\text{He} = 0.01 R_A$, and a mantle-derived end-member with $\text{CH}_4/^3\text{He} = 1 \times 10^5$ and $^3\text{He}/^4\text{He} = 8 R_A$ (Halldórsson et al., 2013). The proposed mixing model reveals that crustal end-member with $\text{CH}_4/^3\text{He} = 3.0 \times 10^{13}$ is the most suitable for our data set. Although the investigated reservoirs are methane-dominated, the measured $\text{CH}_4/^3\text{He}$ ratios are similar to those in the geothermal systems of subduction zones (Snyder et al.,

2003, and references therein) and those measured in the volcanic rock reservoirs of natural gas fields in the Green Tuff basin, Japan (Sakata et al., 1997; Figure 5b). However, $\text{CH}_4/^3\text{He}$ ratio in the HC reservoirs is 2 to 3 orders of magnitude higher than in the volcanic centers along the western Sunda Arc (Halldórsson et al., 2013). These findings confirm the presence of a specific setting where methane-dominated reservoirs are heavily affected by the migration of mantle-derived He. This situation presents new questions and scenarios regarding the migration of magmatic fluids that are typically CO_2 -dominated.

6.3. Noble Gas Distribution Through the Sunda Arc

Our data fit well with those from previous investigations in natural fluids emitted in volcanic and hydrothermal systems in the western and central Sunda Arc (Halldórsson et al., 2013), where the outgassing volatiles are dominated by CO_2 . Here the majority of the He isotopes ratios range from 5.3 to 8.1 R_A (Figure 6). Hence, at regional scale, the mantle wedge is considered to be the principal source of He at volcanic centers. However, a minor radiogenic contamination from the subducted crust can also be inferred, particularly in the western part of the Sunda Arc, where thicker and older crust is present, decreasing the typical mantle-derived He signature in the emitted volatiles. However, the large database described by Halldórsson et al. (2013) contains a gap in the central and eastern part of Java. Our novel data together with the He data from the Arjuno-Welirang volcanic system (Inguaggiato et al., 2018) and those from the Lusi crater (Mazzini et al., 2012) contribute to the filling of this gap and to the reconstruction of the general distribution of the magmatic volatile sources along the eastern Sunda Arc. Furthermore, our results demonstrate a propagation of the mantle-derived volatiles from the volcanic complex to the sedimentary basin around the Lusi system.

6.4. The Fate of Magmatic CO_2

CO_2 , CH_4 , and H_2O are considered as the main He carriers for migration through the crust in sedimentary and volcanic settings. Previous results and modeling indicate that CO_2 is the major magmatic volatile migrating through the East Java Basin, particularly at and around the Lusi eruption site (Mazzini et al., 2012; Sciarra et al., 2018; Svensen et al., 2018; Vanderkluyzen et al., 2014). Therefore, in our study case, CO_2 is assumed to be the carrier for the migration of the mantle-derived He in the sedimentary basin and the HC reservoirs. Nevertheless, the gas sampled in the HC reservoirs (Group 1) reveals very low CO_2 concentrations, varying from 0.02 to 0.37 vol.% (except for the well TG5), and concurrently high R/R_A values (Tables 1 and 2). Furthermore, the carbon isotopic composition of CO_2 is extremely positive (from +18.9‰ to +22.8‰) and significantly different from the typical composition of the mantle-derived CO_2

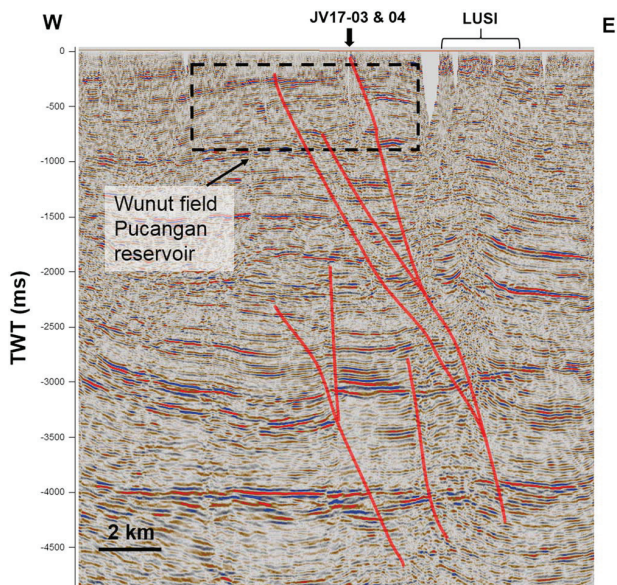


Figure 7. W-E-oriented seismic profile from 2003, with indicated location of the sampled surface seepage site, Lusi, the conditional location of the shallow hydrocarbon reservoirs of the Wunut field and several faults as part of the Watukosek Fault System (highlighted in red). Faults act as migration pathway for the fluids. Profile location indicated in Figure 1b. TWT represents two-way travel time.

($-8‰ < \delta^{13}\text{C}_{\text{CO}_2} < -4‰$; Clark & Fritz, 1997; Deines, 2002). Hence, mantle-derived CO_2 seems to be decoupled from the mantle-derived He. There are two potential mechanisms able to mask the CO_2 as carrier gas: (1) CO_2 transformation to CH_4 by microbial activity and (2) CO_2 dissolution in the water. The first hypothesis is that large part of the CO_2 is transformed by microbial activity operated by methanogens (as described in the section 6.1). An additional hypothesis is that during the migration of mantle-derived He and CO_2 , the latter gets mainly dissolved in formation water. This process is able to reduce the amount of CO_2 in the gas phase and preserve the pristine isotopic ratio of He that does not dissolve into water (Caracausi et al., 2003). This mechanism is not applicable for ongoing focused and vigorous seepage. For example, deep and hot CO_2 -rich fluids at Lusi are flushed rapidly toward the surface without cooling. When instead diffused fluids migration occurs at slower rates through gradually colder sedimentary rock formations, the dissolution of CO_2 takes place. Furthermore, it is recognized that the transport of He could be decoupled from that of carbon gases in the areas away from the active volcanism (Giggenbach et al., 1993). The depicted scenario is further supported by the significant concentration of dissolved CO_2 in the water (8.28 and $28.15 \text{ cm}^3/\text{l}$ STP at the Watudakon and Wunut fields, respectively, Group 4). Here the amount of the dissolved CO_2 is higher than in the water in equilibrium with the atmosphere ($0.31 \text{ cm}^3 \text{ SPT/l}$; Capasso & Inguaggiato, 1998), indicating that part of CO_2 can be dissolved in the shallow formation waters.

6.5. The Subsurface Plumbing System

To investigate potential fluid migration pathways, we compared the fluid geochemistry at different sites and complemented these data with available subsurface geophysical data. Gas compositions of the fluids emitted at the surface seepage sites above the Wunut reservoir (Group 2) are distinctively different from those recorded at the adjacent WU1 well (Tables 1 and 2). However, the origin of the HC gases is always thermogenic ($\delta^{13}\text{C}_{\text{CH}_4}$ as high as $-42.5‰$ and $\delta\text{D}_{\text{CH}_4}$ as high as $170.4‰$ $\text{C}_1/(\text{C}_2 - \text{C}_3) = 15$; Table 2 and Figures 3b and 3c). Furthermore, these seeps contain 5–10 times more CO_2 than samples of Group 1 (where CO_2 is almost absent) with a different isotopic signature (i.e., $\delta^{13}\text{C}_{\text{CO}_2}$ between $1.2‰$ and $2.7‰$). These marked differences suggest that a diverse source of fluids is present at this locality or that some processes (i.e., mixing) may occur during the transfer of the fluids toward the surface.

Insights about the subsurface plumbing system are provided by seismic profiles acquired during the 1990–2000s in this part of the basin. Geophysical data highlight the occurrence of the WFS that extends from the Arjuno-Welirang volcanic complex, intersects Lusi, and progresses toward the northeast Java (Moscarello et al., 2018). The authors describe the presence of this deep-rooted fault system that splits laterally at shallower depths and creates a network of fractures. These faults either stop within the topmost kilometer of sediments or can be traced all the way to the surface. This type of features can also be observed on the seismic lines crossing the Wunut field, sampled seepage zone (Group 2), and Lusi (Figure 7). Here one of these faults reaches the surface exactly at the Group 2 seepages locality. Additional faults can also be observed ending below, and sometimes within, the Wunut field. Therefore, these fractured zones represent ideal pathways for the transfer of fluids due to their high permeability within the reservoir and at the surface.

An additional fluids source that is feeding the surface seeps at the Wunut locality (Group 2) is potentially provided through broad caldera collapse and diffused fracturing ongoing around the neighboring Lusi crater, located 3.5 km to the east (Mauri et al., 2018; Panzera et al., 2018). These newborn fractures represent additional active pathways for radial transfer of the Lusi fluids in the shallow surface. Here thousands of active seeps are scattered around the Lusi vent and have CO_2 and CH_4 signatures similar to those measured for Group 2 (Tables 1 and 2; Mazzini et al., 2012; Sciarra et al., 2018). Further, the authors also describe the presence of ~W-E-oriented systems of newborn antithetic fractures that are interpreted to result from the sinistral strike-slip activity of the WFS. These fractures, similarly to the NE-SW-oriented WFS, are proven

to be an active advective pathway for the migration of fluids (Sciarra et al., 2018). Gravimetry data (Mauri et al., 2018) also confirm the presence of these structures that are likely recycled by the radial fluids expulsion from the over pressured Lusi conduit.

6.6. HC Reservoirs, Lusi, and the Volcanic System

Our results indicate that mantle-derived fluids not only migrate from the volcanic complex at focused localities such as the Lusi site (Inguaggiato et al., 2018; Mazzini et al., 2012) but also disperse over a broader area within the sedimentary basin through which the WFS extends. The highest He isotope signature was measured in the fluids trapped in the Carat field ($6.7 R_A$), the closest field to the volcanic complex. (Figures 1b and 2). In contrast, the lowest He isotope ratio was distinguished in the Watudakon field ($2.1 R_A$), located on the outskirts of the magmatic complex (Figures 1b and 2) but in a part of the basin that is not intersected by the WFS (i.e. ~36 km west of Lusi). This lower He isotope signature indicates that here the crustal He component (^4He due to U and Th decay in the crust) is higher (Figures 5a and 5b). The migration pathway of the mantle-derived volatiles toward the Watudakon field is less developed than the one existing for the fields located along the WFS. It is worth noting that the Watudakon field also has a different CH_4 signature indicated as primary microbial origin (Figures 3b and 3c). Hence, this reservoir contains volatiles that are very distinct with respect to those in the Wunut, Tanggulangin, and Carat reservoirs. This observation strengthens the hypothesis that the migration of mantle-derived fluids mainly occurs in the region around the volcanoes but that enhanced migration is promoted in the NE-SW-oriented corridor crossed by the WFS. This observation is also consistent with the thermal gradient measured from these fields based on the available shallow boreholes. The data indicate a gradient of 2.8–4.8 °C/100 m from Wunut field, 3.8–4.8 °C/100 m from Tanggulangin, and 4.9 °C/100 m from Carat. These values are remarkably similar to the gradient measured at the BJP-1 well (4.2 °C/100 m; Mazzini et al., 2007) drilled prior to the occurrence of the Lusi eruption. The evidence of a widespread high thermal gradient is in agreement with the broadly diffused migration of mantle-derived fluids.

Our new data also help to refine the fluids migration imaged by the ambient noise tomography acquired in the region that indicates the migration of hydrothermal fluids from the volcanic arc toward the sedimentary basin (Fallahi et al., 2017). The major migration pathway is linked to the WFS as well as W-E-oriented systems of antithetic fractures present around Lusi. Considering the remarkable variation of the geochemical composition of the C-rich gases (i.e., CO_2 and CH_4) sampled from the HC fields (this study) and the Lusi system (Mazzini et al., 2012), we can conclude that these two systems are essentially compartmentalized and input of fluids from the Lusi system to reservoirs is limited. The slow migration of mantle-derived He in the HC reservoirs occurs independently from the focused one occurring at the Lusi crater. We cannot rule out the possibility that fluids (i.e., CO_2 and CH_4) outgassing from the Lusi system may also move laterally toward the HC reservoirs (Wunut, Carat, and Tanggulangin) and are later modified by secondary processes (i.e., biodegradation). However, the collected data do not support this scenario.

6.7. Basinal Fluids Migration

Based on the findings and observations reported herein, merged with the known regional studies, we have developed a schematic model describing the fluids migration in the studied petroleum system (Figure 8).

1. *Deposition of petroleum system elements:* (a) Ngimbang Fm. HC source rock; (b) reservoir (volcaniclastic sands and sandstones); and (c) seals (intercalating shales) both within the Pucangan Fm. HC generation within the Ngimbang Fm., offshore northeast Java.
2. Late Pleistocene-Holocene HC fluid *migration to shallow reservoirs* of the Pucangan Fm., following the collapse of the Porong trap (7 km to the east).
3. *Alteration* of the gas and oil via HC biodegradation process.
4. *Magmatic and hydrothermal fluids migration* toward the organic-rich shales of the deep-seated Ngimbang Fm. (>3,800-m depth) generated additional HCs and CO_2 , creating overpressure within the Ngimbang Fm., enriching the gas with mantle-derived trace noble gases (^3He and ^{36}Ar).
5. These fluids migrated the surface through fractured and weak zones and are present today in the producing HC reservoirs and at the Lusi eruption site.

The gas geochemistry survey described herein corroborates all the previously collected geophysical, petrographic, geochemical, and modeling evidences (Collignon et al., 2018; Fallahi et al., 2017; Malvoisin et al.,

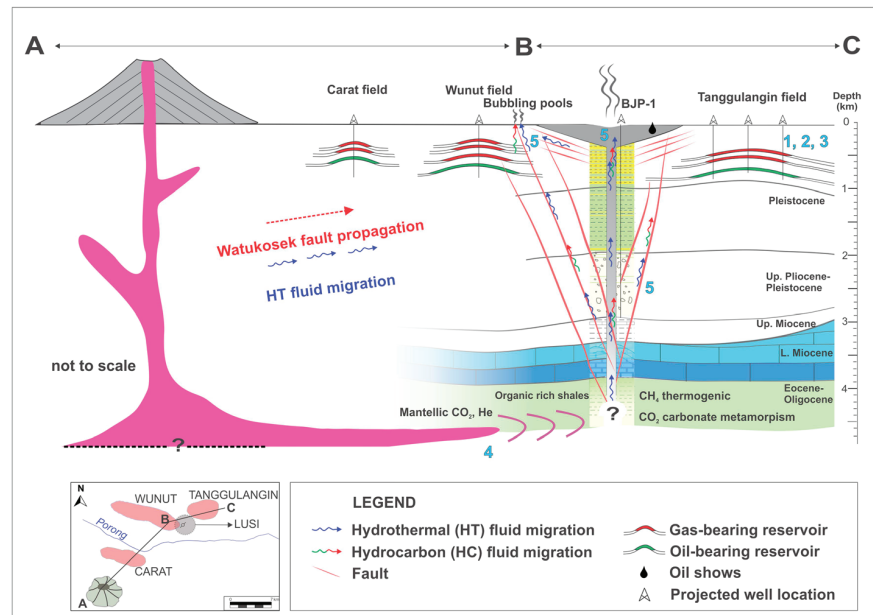


Figure 8. Conceptual geological model depicting the development of the petroleum system and the migration pathways of the mantle-derived and HC fluids in the study area. The major events are marked with Numbers 1–5, described in the section 6.7.

2018; Mazzini et al., 2012; Mazzini et al., 2018; Samankassou et al., 2018; Svensen et al., 2018). These converging data indicate that prior to the Lusi eruption and prior to the drilling of the BJP-1 well, an overpressured zone in the deeply buried Ngimbang Fm. (>4 km) already existed. Here the migration of magma and hydrothermal fluids from the neighboring volcanic arc generated significant overpressure confined in this prolific source rock buried more than 1 km below the bottom of the BJP-1 well. Therefore, the presence of this naturally overpressured system and its final manifestation at the surface appear to be unrelated to the drilling of the BJP-1 well.

7. Conclusions

We report the results of a gas geochemistry survey conducted in the southern part of the East Java sedimentary basin. Here several HC fields and adjacent surface seepage sites are located near the Arjuno-Welirang volcanic complex and around the Lusi eruption site. The samples collected from the shallow (200–1,000 m) HC fields (Group 1) reveal the presence of predominantly dry thermogenic gas ($-58.3 < \delta^{13}\text{C}_{\text{CH}_4} < -40.7$). Ongoing biodegradation processes are confirmed by the CO_2 signature with $+18.9 < \delta^{13}\text{C}_{\text{CO}_2} < +22.8$. The surface seepages (Group 2) located above the reservoirs reveal a remarkably different geochemical signature where less molecularly and isotopically fractionated and recently generated thermogenic gas is mixed with CO_2 with $+1.2 < \delta^{13}\text{C}_{\text{CO}_2} < +2.7$. All the analyzed samples reveal the presence of noble gases with a clear mantle-derived He signature that is comparable to that in the fluids emitted at the Lusi and Arjuno-Welirang fumaroles. Only a moderate decrease in $^3\text{He}/^4\text{He}$ ratio is observed along a NE-oriented transect from the Arjuno-Welirang fumaroles ($R = 7.3 R_A$), through the neighboring Carat HC reservoir ($R = 6.7 R_A$), Lusi (R up to $6.5 R_A$), and the surrounding HC fields that still display remarkably high values (R up to $6.3 R_A$).

The study region is intersected by the WFS that originates from the Arjuno-Welirang volcanic complex, hosting Lusi and the sampled HC fields. Previous studies revealed that this fault system provided the pathway for the magmatic fluids fueling the Lusi eruption. Our new results show that this system of faults also allows the ongoing migration of mantle-derived fluids over a larger region of the sedimentary basin hosting the HC fields. Potential migration of the shallow Lusi fluids to the reservoirs followed by alteration processes (i.e., biodegradation) cannot be totally excluded. However, the distinct signature of the C gases (i.e., CO_2 and

CH₄) observed at the Lusi eruption site and in the HC fields indicates that this input should be limited. Additional fluids expelled at the thousands of seeps around the Lusi crater (including those from Group 2) are migrating from the Lusi conduit through a network of fractures antithetic to the Watukosek strike slip fault system and through the caldera collapse shallow fractures that extend over kilometers around the main Lusi vent.

This study highlights that continuous monitoring of noble gas composition in HC fields neighboring volcanic centers could represent an efficient and logistically simple tool to distinguish perturbations of adjacent magmatic complexes.

Acknowledgments

The work was funded by the European Research Council under the European Union's Seventh Framework Programme Grant agreement 308126 (LUSI LAB project, A. Mazzini). We acknowledge the support from the Research Council of Norway through its Centres of Excellence funding scheme, Project 223272 (CEED). The authors would like to thank the management of Lapindo Brantas Indonesia and PT. Kimia Farma for providing access to the subsurface data and for the authorization to publish the results of this study. BPLS is thanked for their support during the field operations. Federal Institute for Geosciences and Natural Resources (BGR) is thanked for helping with TOC measurements. The interpretation and model presented in this paper reflect solely the view of the authors at the stage of the manuscript preparation. We are grateful to the Editor and two Reviewers who made insightful comments and contributed to improve the quality of the manuscript. The data supporting the paper is represented in the Tables 1 and stored at the NIRD database (<https://archive.sigma2.no/pages/public/datasetDetail.jsf?id=C9898994-C249-4190-84B4-13334E9E7B59>).

References

- Bernard, B., J. M. Brooks, and W. M. Sackett (1977). A geochemical model for characterization of hydrocarbon gas sources in marine sediments, paper presented at 9th Annual OTC Conference.
- Blumenberg, M., Lutz, R., Schlömer, S., Krüger, M., Scheeder, G., Berglar, K., et al. (2016). Hydrocarbons from near-surface sediments of the Barents Sea north of Svalbard—Indication of subsurface hydrocarbon generation? *Marine and Petroleum Geology*, 76, 432–443. <https://doi.org/10.1016/j.marpetgeo.2016.05.031>
- Capasso, G., & Inguaggiato, S. (1998). A simple method for the determination of dissolved gases in natural waters. An application to thermal waters from Vulcano Island. *Applied Geochemistry*, 13(5), 631–642. [https://doi.org/10.1016/S0883-2927\(97\)00109-1](https://doi.org/10.1016/S0883-2927(97)00109-1)
- Caracausi, A., Italiano, F., Paonita, A., Rizzo, A., & Nuccio, P. M. (2003). Evidence of deep magma degassing and ascent by geochemistry of peripheral gas emissions at Mount Etna (Italy): Assessment of the magmatic reservoir pressure. *Journal of Geophysical Research*, 108(B10), 2463. <https://doi.org/10.1029/2002JB002095>
- Caracausi, A., Paternoster, M., & Nuccio, P. M. (2015). Mantle CO₂ degassing at Mt. Vulture volcano (Italy): Relationship between CO₂ outgassing of volcanoes and the time of their last eruption. *Earth and Planetary Science Letters*, 411, 268–280. <https://doi.org/10.1016/j.epsl.2014.11.049>
- Caracausi, A., & Sulli, A. (2019). Outgassing of mantle volatiles in compressional tectonic regime away from volcanism: The role of continental delamination. *Geochemistry, Geophysics, Geosystems*, 20, 2007–2020. <https://doi.org/10.1029/2018GC008046>
- Chung, H. M., Gormly, J. R., & Squires, R. M. (1988). Origin of gaseous hydrocarbons in subsurface environments: Theoretical considerations of carbon isotope distribution. *Chemical Geology*, 71(1-3), 97–104. [https://doi.org/10.1016/0009-2541\(88\)90108-8](https://doi.org/10.1016/0009-2541(88)90108-8)
- Clark, I., & Fritz, P. (1997). *Environmental isotopes in hydrogeology*. Boca Raton, FL: CRC Press/Lewis Publishers.
- Collignon, M., Mazzini, A., Schmid, D. W., & Lupi, M. (2018). Modelling fluid flow in active clastic piercements: Challenges and approaches. *Marine and Petroleum Geology*, 90, 157–172. <https://doi.org/10.1016/j.marpetgeo.2017.09.033>
- Correale, A., Martelli, M., Paonita, A., Rizzo, A., Brusca, L., & Scribano, V. (2012). New evidence of mantle heterogeneity beneath the Hyblean Plateau (southeast Sicily, Italy) as inferred from noble gases and geochemistry of ultramafic xenoliths. *Lithos*, 132-133, 70–81. <https://doi.org/10.1016/j.lithos.2011.11.007>
- Deines, P. (2002). The carbon isotope geochemistry of mantle xenoliths. *Earth-Science Reviews*, 58(3-4), 247–278. [https://doi.org/10.1016/S0012-8252\(02\)00064-8](https://doi.org/10.1016/S0012-8252(02)00064-8)
- Devi, E. A., Rachman, F., Satyana, A. H., Fahrudin, F., & Setyawan, R. (2018). Paleofacies of Eocene Lower Ngimbang source rocks in Cepu Area, East Java Basin based on biomarkers and carbon-13 isotopes. *IOP Conference Series: Earth and Environmental Science*, 118, 012009. <https://doi.org/10.1088/1755-1315/118/1/012009>
- Doust, H., & Noble, R. A. (2008). Petroleum systems of Indonesia. *Marine and Petroleum Geology*, 25, 103–129. <https://doi.org/10.1016/j.marpetgeo.2007.05.007>
- Etiopie, G., Feyzullayev, A., Milkov, A. V., Waseda, A., Mizobe, K., & Sun, C. H. (2009). Evidence of subsurface anaerobic biodegradation of hydrocarbons and potential secondary methanogenesis in terrestrial mud volcanoes. *Marine and Petroleum Geology*, 26, 1692–1703. <https://doi.org/10.1016/j.marpetgeo.2008.12.002>
- Fallahi, M. J., Obermann, A., Lupi, M., Karyono, K., & Mazzini, A. (2017). The plumbing system feeding the Lusi eruption revealed by ambient noise tomography. *Journal of Geophysical Research: Solid Earth*, 122, 8200–8213. <https://doi.org/doi:10.1002/2017JB014592>
- Giggenbach, W. F., Sano, Y., & Wakita, H. (1993). Isotopic composition of helium, and CO₂ and CH₄ contents in gases produced along the New Zealand part of a convergent plate boundary. *Geochimica et Cosmochimica Acta*, 57(14), 3427–3455. [https://doi.org/10.1016/0016-7037\(93\)90549-C](https://doi.org/10.1016/0016-7037(93)90549-C)
- Global Volcanism Program (2013). In E. Venzke (Ed.), *Volcanoes of the World*, v. 4.8.1. Smithsonian Institution. <https://doi.org/10.5479/si.GVP.VOTW4-2013>
- Gutsalo, L. K., and A. M. Plotnikov (1981). Carbon isotopic composition in the CH₄-CO₂ system as a criterion for the origin of methane and carbon dioxide in Earth natural gases (in Russian), paper presented at Doklady Akademii Nauk SSSR (Proceedings of the USSR Academy of Science).
- Hall, R. (2002). Cenozoic geological and plate tectonic evolution of SE Asia and the SW Pacific: Computer-based reconstructions, model and animations. *Journal of Asian Earth Sciences*, 20(4), 353–431. [https://doi.org/10.1016/S1367-9120\(01\)00069-4](https://doi.org/10.1016/S1367-9120(01)00069-4)
- Hall, R. (2013). The palaeogeography of Sundaland and Wallacea since the Late Jurassic. *Journal of Limnology*, 72, –1, 17. <https://doi.org/10.4081/jlimnol.2013.s2.e1>
- Hall, R., Cottam, M. A., & Wilson, M. E. J. (2011). Australia–SE Asia collision: Plate tectonics and crustal flow. In M. A. C. R. Hall, & M. E. J. Wilson (Eds.), *The SE Asian gateway: history and tectonics of Australia-Asia collision*, edited by, *Special Publications*, (Vol. 355, pp. 75–109). London: Geological Society. <https://doi.org/10.1144/SP355.5>
- Halldórsson, S. A., Hilton, D. R., Troll, V. R., & Fischer, T. P. (2013). Resolving volatile sources along the western Sunda arc, Indonesia. *Chemical Geology*, 339, 263–282. <https://doi.org/10.1016/j.chemgeo.2012.09.042>
- Head, I. M., Jones, D. M., & Larter, S. R. (2003). Biological activity in the deep subsurface and the origin of heavy oil. *Nature*, 426(6964), 344–352. <https://doi.org/10.1038/nature02134>
- Inguaggiato, S., Mazzini, A., Vita, F., & Sciarra, A. (2018). The Arjuno-Welirang volcanic complex and the connected Lusi system: Geochemical evidences. *Marine and Petroleum Geology*, 90, 67–76. <https://doi.org/10.1016/j.marpetgeo.2017.10.015>

- Ishibashi, J.-I., Sato, M., Sano, Y., Wakita, H., Gamo, T., & Shanks, W. C. (2002). Helium and carbon gas geochemistry of pore fluids from the sediment-rich hydrothermal system in Escanaba Trough. *Applied Geochemistry*, 17(11), 1457–1466. [https://doi.org/10.1016/S0883-2927\(02\)00112-9](https://doi.org/10.1016/S0883-2927(02)00112-9)
- Istadi, B., Wibowo, H. T., Sunardi, E., Hadi, S., & Sawolo, N. (2012). Mud volcano and its evolution. *Earth Sciences, Imran Ahmad Dar, IntechOpen*, 375–434, 861–888. <https://doi.org/10.5772/24944>
- Istadi, B. P., Pramono, G. H., Sumintadireja, P., & Alam, S. (2009). Modeling study of growth and potential geohazard for LUSI mud volcano: East Java, Indonesia. *Marine and Petroleum Geology*, 26, 1724–1739. <https://doi.org/10.1016/j.marpetgeo.2009.03.006>
- Jenden, P. D., Hilton, D. R., Kaplan, I. R., & Craig, H. (Eds.) (1993). *Abiogenic hydrocarbons and mantle helium in oil and gas fields, United States Geological Survey, Professional Paper* (Vol. 1570, pp. 31–56).
- Kamenskiy, I. L., Yakutseni, V. P., Mamyrin, B. A., Anufriyev, S. G., & Tolstikhin, I. N. (1971). Helium isotopes in nature. *Geochemistry International*, 8, 575–589.
- Kusumastuti, A., Darmoyo, A.B., Suwarlan, W., Sosromihardjo, S.P.C. (1999), The Wunut field: Pleistocene volcanoclastic gas sands in East Java, *Proceedings, Indonesian Petroleum Association, Twenty Seventh Annual Convention & Exhibition, October 1999*.
- Lee, H., Muirhead, J. D., Fischer, T. P., Ebinger, C. J., Kattenhorn, S. A., Sharp, Z. D., & Kianji, G. (2016). Massive and prolonged deep carbon emissions associated with continental rifting. *Nature Geoscience*, 9, 145–149. <https://doi.org/10.1038/ngeo2622>
- Malvoisin, B., Mazzini, A., & Miller, S. A. (2018). Deep hydrothermal activity driving the Lusi mud eruption. *Earth and Planetary Science Letters*, 497, 42–49. <https://doi.org/10.1016/j.epsl.2018.06.006>
- Martha, A. A., Cummins, P., Saygin, E., Sri, W., & Masturyono (2017). Imaging of upper crustal structure beneath East Java–Bali, Indonesia with ambient noise tomography. *Geoscience Letters*, 4(1), 14. <https://doi.org/10.1186/s40562-017-0080-9>
- Mauri, G., Husein, A., Mazzini, A., Irawan, D., Sohrabi, R., Hadi, S., et al. (2018). Insights on the structure of Lusi mud edifice from land gravity data. *Marine and Petroleum Geology*, 90, 104–115. <https://doi.org/10.1016/j.marpetgeo.2017.05.041>
- Mazzini, A., & Etiope, G. (2017). Mud volcanism: An updated review. *Earth-Science Reviews*, 168, 81–112. <https://doi.org/10.1016/j.earscirev.2017.03.001>
- Mazzini, A., Etiope, G., & Svensen, H. (2012). A new hydrothermal scenario for the 2006 Lusi eruption, Indonesia, Insights from gas geochemistry. *Earth and Planetary Science Letters*, 317–318, 305–318. <https://doi.org/10.1016/j.epsl.2011.11.016>
- Mazzini, A., Nermoen, A., Krotkiewski, M., Podladchikov, Y., Planke, S., & Svensen, H. (2009). Strike-slip faulting as a trigger mechanism for overpressure release through piercement structures. Implications for the Lusi mud volcano, Indonesia. *Marine and Petroleum Geology*, 26(9), 1751–1765. <https://doi.org/10.1016/j.marpetgeo.2009.03.001>
- Mazzini, A., Scholz, F., Svensen, H. H., Hensen, C., & Hadi, S. (2018). The geochemistry and origin of the hydrothermal water erupted at Lusi, Indonesia. *Marine and Petroleum Geology*, 90, 52–66. <https://doi.org/10.1016/j.marpetgeo.2017.06.018>
- Mazzini, A., Svensen, H., Akhmanov, G. G., Aloisi, G., Planke, S., Malthe-Sørensen, A., & Istadi, B. (2007). Triggering and dynamic evolution of the LUSI mud volcano, Indonesia. *Earth and Planetary Science Letters*, 261(3–4), 375–388. <https://doi.org/10.1016/j.epsl.2007.07.001>
- Milkov, A. V. (2010). Methanogenic biodegradation of petroleum in the West Siberian Basin (Russia): Significance for formation of giant Cenomanian gas pools. *AAPG Bulletin*, 94(10), 1485–1541. <https://doi.org/10.1306/01051009122>
- Milkov, A. V. (2011). Worldwide distribution and significance of secondary microbial methane formed during petroleum biodegradation in conventional reservoirs. *Organic Geochemistry*, 42(2), 184–207. <https://doi.org/10.1016/j.orggeochem.2010.12.003>
- Milkov, A. V. (2018). Secondary microbial gas. In H. Wilkes (Ed.), *Hydrocarbons, oils and lipids: Diversity, origin, chemistry and fate*, edited by, (pp. 1–10). Cham: Springer International Publishing. https://doi.org/10.1007/978-3-319-54529-5_22-1
- Milkov, A. V., & Etiope, G. (2018). Revised genetic diagrams for natural gases based on a global dataset of >20,000 samples. *Organic Geochemistry*, 125, 109–120. <https://doi.org/10.1016/j.orggeochem.2018.09.002>
- Miller, S. A., & Mazzini, A. (2018). More than ten years of Lusi: A review of facts, coincidences, and past and future studies. *Marine and Petroleum Geology*, 90, 10–25. <https://doi.org/10.1016/j.marpetgeo.2017.06.019>
- Moreira, M. A., & Kurz, M. D. (2013). Noble gases as tracers of mantle processes and magmatic degassing. In P. Burnard (Ed.), *The Noble Gases as Geochemical Tracers* (pp. 371–391). Berlin, Heidelberg: Springer-Verlag.
- Moscariello, A., Do Couto, D., Mondino, F., Booth, J., Lupi, M., & Mazzini, A. (2018). Genesis and evolution of the Watukosek fault system in the Lusi area (East Java). *Marine and Petroleum Geology*, 90, 125–137. <https://doi.org/10.1016/j.marpetgeo.2017.09.032>
- Obermann, A., Karyono, K., Diehl, T., Lupi, M., & Mazzini, A. (2018). Seismicity at Lusi and the adjacent volcanic complex, Java, Indonesia. *Marine and Petroleum Geology*, 90, 149–156. <https://doi.org/10.1016/j.marpetgeo.2017.07.033>
- O’Nions, R. K., & Oxburgh, E. R. (1988). Helium, volatile fluxes and the development of continental crust. *Earth and Planetary Science Letters*, 90(3), 331–347. [https://doi.org/10.1016/0012-821X\(88\)90134-3](https://doi.org/10.1016/0012-821X(88)90134-3)
- Ozima, M., & Podosek, F. A. (2002). *Noble gas geochemistry*. Cambridge: Cambridge University Press.
- Panzera, F., D’Amico, S., Lupi, M., Mauri, G., Karyono, K., & Mazzini, A. (2018). Lusi hydrothermal structure inferred through ambient vibration measurements. *Marine and Petroleum Geology*, 90, 116–124. <https://doi.org/10.1016/j.marpetgeo.2017.06.017>
- Peters, K. E., Walters, C. C., & Moldovan, J. M. (2005). *The biomarker guide*. Cambridge: Cambridge University Press.
- Poreda, R. J., Jeffrey, A. W. A., Kaplan, I. R., & Craig, H. (1988). Magmatic helium in subduction-zone natural gases. *Chemical Geology*, 71(1–3), 199–210. [https://doi.org/10.1016/0009-2541\(88\)90115-5](https://doi.org/10.1016/0009-2541(88)90115-5)
- Poreda, R. J., Jenden, P. D., Kaplan, I. R., & Craig, H. (1986). Mantle helium in Sacramento basin natural gas wells. *Geochimica et Cosmochimica Acta*, 50(12), 2847–2853. [https://doi.org/10.1016/0016-7037\(86\)90231-0](https://doi.org/10.1016/0016-7037(86)90231-0)
- Prinzhofer, A. (2013). Noble gases in oil and gas accumulations. In P. Burnard (Ed.), *The noble gases as geochemical tracers* (pp. 225–248). Berlin, Heidelberg: Springer.
- Procesi, M., Ciotoli, G., Mazzini, A., & Etiope, G. (2019). Sediment-hosted geothermal systems: Review and first global mapping. *Earth-Science Reviews*, 192, 529–544. <https://doi.org/10.1016/j.earscirev.2019.03.020>
- Sakata, S., Sano, Y., Maekawa, T., & Igari, S.-I. (1997). Hydrogen and carbon isotopic composition of methane as evidence for biogenic origin of natural gases from the Green Tuff Basin, Japan. *Organic Geochemistry*, 26(5–6), 399–407. [https://doi.org/10.1016/S0146-6380\(97\)00005-3](https://doi.org/10.1016/S0146-6380(97)00005-3)
- Samankassou, E., Mazzini, A., Chiaradia, M., Spezzaferri, S., Moscariello, A., & Do Couto, D. (2018). Origin and age of carbonate clasts from the Lusi eruption, Java, Indonesia. *Marine and Petroleum Geology*, 90, 138–148. <https://doi.org/10.1016/j.marpetgeo.2017.11.012>
- Sano, Y., & Fischer, T. P. (2013). The analysis and interpretation of noble gases in modern hydrothermal systems. In P. Burnard (Ed.), *The noble gases as geochemical tracers*, edited by, (pp. 249–317). Berlin, Heidelberg: Springer Berlin Heidelberg. https://doi.org/10.1007/978-3-642-28836-4_10

- Sano, Y., Gamo, T., & Williams, S. N. (1997). Secular variations of helium and carbon isotopes at Galeras volcano, Colombia. *Journal of Volcanology and Geothermal Research*, 77(1-4), 255–265. [https://doi.org/10.1016/S0377-0273\(96\)00098-4](https://doi.org/10.1016/S0377-0273(96)00098-4)
- Sano, Y., & Wakita, H. (1985). Geographical distribution of $^3\text{He}/^4\text{He}$ ratios in Japan: Implications for arc tectonics and incipient magmatism. *Journal of Geophysical Research*, 90(B10), 8729–8741. <https://doi.org/10.1029/JB090iB10p08729>
- Satyana, A. H., & Purwaningsih, M. E. M. (2003a). Geochemistry of the East Java Basin: New observations on oil grouping, genetic gas types and trends of hydrocarbon habitats. *Proceedings of the 29th IAGI Annual Convention and Exhibition*.
- Satyana, A. H., Purwaningsih, M. E. M. (2003b). Oligo-Miocene carbonates of Java: Tectonic setting and effects of volcanism. *Proceedings of the 32nd IAGI and 28th HAGI Annual Convention and Exhibition*.
- Schoell, M. (1983). Genetic characterization of natural gases. American Association of Petroleum Geologists Bulletin paper presented at American Association of Petroleum Geologists Bulletin.
- Sciarra, A., Mazzini, A., Inguaggiato, S., Vita, F., Lupi, M., & Hadi, S. (2018). Radon and carbon gas anomalies along the Watukosek Fault System and Lusi mud eruption, Indonesia. *Marine and Petroleum Geology*, 90, 77–90. <https://doi.org/10.1016/j.marpetgeo.2017.09.031>
- Sharaf, E., Simo, J. A., Carroll, A. R., & Shields, M. (2005). Stratigraphic evolution of Oligocene–Miocene carbonates and siliciclastics, East Java basin, Indonesia. *AAPG Bulletin*, 89(6), 799–819. <https://doi.org/10.1306/01040504054>
- Smyth, H. R., Hall, R., & Nichols, G. J. (2008). Cenozoic volcanic arc history of East Java, Indonesia: The stratigraphic record of eruptions on an active continental margin. In A. E. Draut, P. D. Clift, & D. W. Scholl (Eds.), *Formation and Applications of the Sedimentary Record in Arc Collision Zones* (pp. 199–222). Boulder, CO: Geological Society of America.
- Snyder, G., Poreda, R., Fehn, U., & Hunt, A. (2003). Sources of nitrogen and methane in Central American geothermal settings: Noble gas and ^{129}I evidence for crustal and magmatic volatile components. *Geochemistry, Geophysics, Geosystems*, 4(1), 9001. <https://doi.org/10.1029/2002GC000363>
- Sutrisna, E. (2009). “Can LUSI be stopped?—A case study and lessons learned from the relief wells”, *Eos Transactions American Geophysical Union*, 90(52), Fall Meet. Suppl., Abstract NH51A-1053. <https://doi.org/10.1029/eost2009eo52>
- Svensen, H. H., Iyer, K., Schmid, D. W., & Mazzini, A. (2018). Modelling of gas generation following emplacement of an igneous sill below Lusi, East Java, Indonesia. *Marine and Petroleum Geology*, 90, 201–208. <https://doi.org/10.1016/j.marpetgeo.2017.07.007>
- Tingay, M. (2015). Initial pore pressures under the Lusi mud volcano, Indonesia. *Interpretation*, 3(1), SE33–SE49. <https://doi.org/10.1190/int-2014-0092.1>
- Van Noorden, R. (2006). Mud volcano floods Java. In *Nature News*. Italy: University of Padua. <https://doi.org/10.1038/news060828-1>
- Vanderkluyzen, L., Burton, M. R., Clarke, A. B., Hartnett, H. E., & Smekens, J.-F. (2014). Composition and flux of explosive gas release at LUSI mud volcano (East Java, Indonesia). *Geochemistry, Geophysics, Geosystems*, 15, 2932–2946. <https://doi.org/10.1002/2014gc005275>
- Wenger, L. M., Davis, C. L., & Isaksen, G. H. (2002). Multiple controls on petroleum biodegradation and impact on oil quality. *SPE Reservoir Evaluation and Engineering*, 5(05), 375–383. <https://doi.org/10.2118/80168-PA>
- Whiticar, M. J., Faber, E., & Schoell, M. (1986). Biogenic methane formation in marine and freshwater environments: CO_2 reduction vs. acetate fermentation—Isotope evidence. *Geochimica et Cosmochimica Acta*, 50(5), 693–709. [https://doi.org/10.1016/0016-7037\(86\)90346-7](https://doi.org/10.1016/0016-7037(86)90346-7)
- Xu, S., Nakai, S. I., Wakita, H., Xu, Y., & Wang, X. (1995). Helium isotope compositions in sedimentary basins in China. *Applied Geochemistry*, 10(6), 643–656. [https://doi.org/10.1016/0883-2927\(95\)00033-X](https://doi.org/10.1016/0883-2927(95)00033-X)

Erratum

In the originally published version of this article, several values in Table 1 were incorrect due to a typesetter error during production. The errors have been corrected, and this may be considered the official version of record.

Manuscript 2: Recent magmatism drives hydrocarbon generation in north-east Java, Indonesia

A. Zaputlyeva, A. Mazzini, M. Blumenberg, G. Scheeder, W. M. Kürschner, J. Kus M.T. Jones, J. Frieling

Published in *Scientific Reports*, vol.10, issue 1

<https://doi.org/10.1038/s41598-020-58567-6>

OPEN

Recent magmatism drives hydrocarbon generation in north-east Java, Indonesia

Alexandra Zaputlyeva^{1*}, Adriano Mazzini¹, Martin Blumenberg², Georg Scheeder², Wolfram Michael Kürschner³, Jolanta Kus², Morgan Thomas Jones¹ & Joost Frieling⁴

Conventional studies of petroleum basins associate oil generation with the gradual burial of organic-rich sediments. These classical models rely on the interplay between pressure, temperature, and the time required for organic matter transformation to oil and gas. These processes usually occur over geological timescales, but may be accelerated by rapid reactions when carbon-rich sediments are exposed to migrating magmatic fluids. The spectacular Lusi eruption (north-east Java, Indonesia) is the surface expression of the present-day deep interaction between volcanic and sedimentary domains. Here we report the ongoing generation of large amounts of hydrocarbons induced by a recent magmatic intrusion from the neighbouring Arjuno-Welirang volcanic complex. We have investigated a unique suite of oil and clast samples, and developed a detailed conceptual model for the complex hydrocarbon migration history in this part of the basin by integrating multidisciplinary techniques. Our results show that palynology, organic petrology, and chlorite microthermometry are the most sensitive geothermometers for basins affected by recent magmatic activity. These findings further our understanding of the driving mechanisms fueling the world's largest active mud eruption and provide a unique dataset to investigate modern hydrocarbon generation processes.

Hydrocarbons (HCs) stored in the sedimentary basins are predominantly of biotic origin, i.e. they are derived through the alteration of buried organic matter (OM)¹. The deposited OM experiences various alteration stages during diagenesis, catagenesis and metacatagenesis leading to HC generation. Some HCs (mostly methane) form at relatively modest temperatures (below 60–80 °C) due to microbial activity. In contrast, a larger variety of HCs (especially oil) are generated at higher temperatures (>60 °C) during thermocracking processes of kerogens^{2–5}. Oil generation typically occurs at significant burial depths (commonly 1.5–4 km, depending on the geothermal gradient and OM type) over timescales of thousands to millions of years. However, regardless the burial history and temperature conditions, rapid oil generation can be triggered if the source rocks are exposed to anomalously high heat induced by magmatic/hydrothermal activity. This phenomenon has been documented at several localities worldwide including the Guaymas Basin, Escanaba Trough, Lake Tanganyika, Neuquén Basin, Rockall Trough, Vøring-Møre basins, Salton Sea, and Faroe-Shetland basins^{6–9}. The overpressure produced by thermo-metamorphic reactions of organic matter exposed to high temperatures may lead to the formation of piercements that reach the surface, forming the so-called sediment-hosted geothermal systems (SHGSs)¹⁰. The largest documented SHGS on Earth is the ongoing Lusi mud eruption (named after LUmpur, “mud” in Indonesian, and SIdoarjo, the Local Regency), active since May 2006 in the East Java sedimentary basin, Indonesia (Fig. 1a). The study area is located just 10 km from the active Sunda volcanic arc. Several studies, including gas and water geochemical surveys and ambient noise tomography, show that the volcanic complex and Lusi plumbing system are connected through a fault system (Watukosek fault system) at a depth of ~4.5 km^{11–16}.

Lusi is surrounded by three hydrocarbon fields: Wunut, Tanggulangin, and Carat (Fig. 1b). These fields contain oil and gas accumulations within the shallow (200–1000 m depth) volcanoclastic reservoirs of the Pleistocene Pucangan Formation (Fm.). The Tanggulangin and Wunut fields are currently producing gas, and the oil production has ceased. Lusi is continuously erupting water, gas, rock clasts, mud and oil. The sources of water, gas and mud are relatively well constrained^{12–17}. In order to distinguish the source of oil and identify the potential

¹Centre for Earth Evolution and Dynamics (CEED), University of Oslo, Oslo, Norway. ²Federal Institute for Geosciences and Natural Resources (BGR), Hannover, Germany. ³Department of Geosciences, University of Oslo, Oslo, Norway. ⁴Department of Earth Sciences, Utrecht University, Utrecht, Netherlands. *email: alexandra.zaputlyeva@geo.uio.no

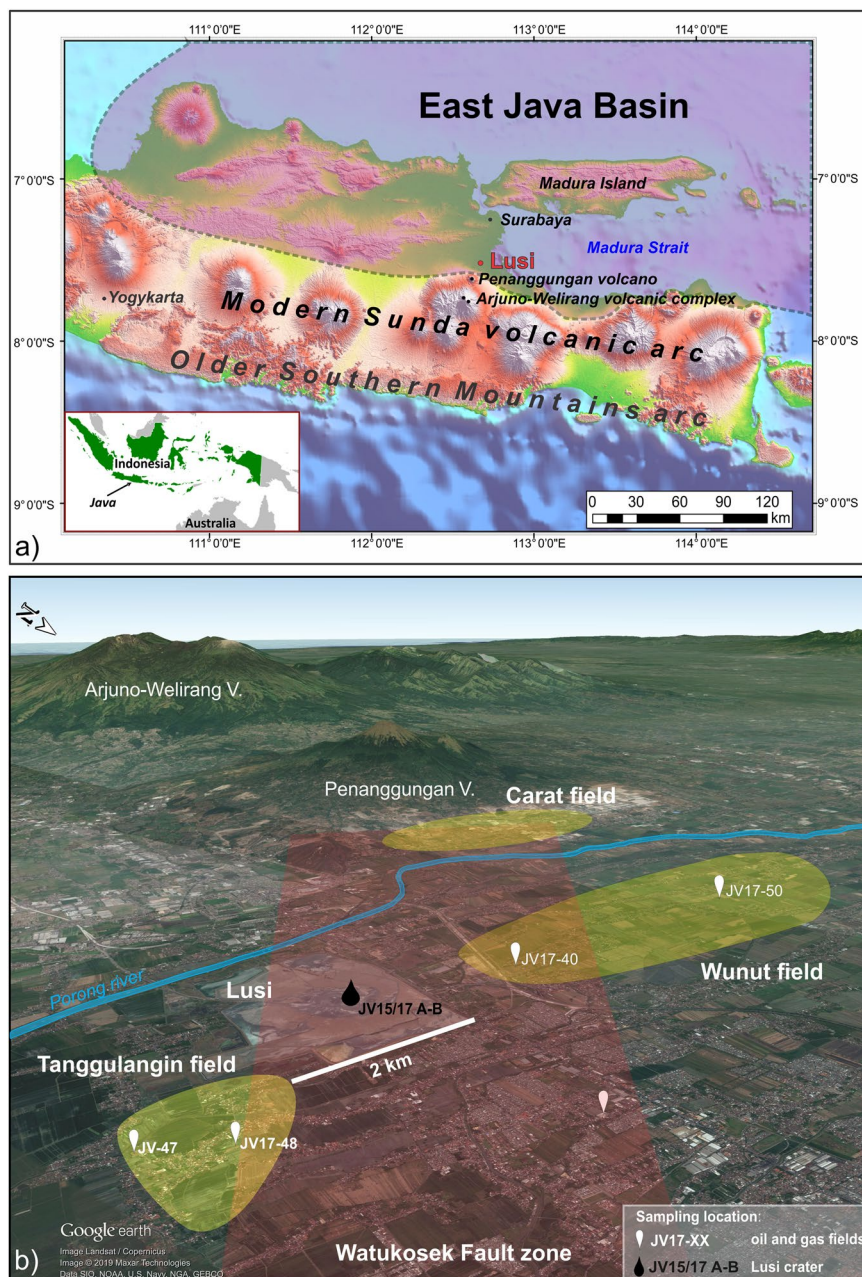


Figure 1. (a) Topography of the central and eastern Java, showing the location of Lusi mud eruption. The East Java sedimentary basin is highlighted by the purple-shaded area. Map of Indonesia in the inset. Topographic data is from the USGS SRTM (Shuttle Radar Topography Mission 1 Arc-Second Global, Source: Global Land Cover Facility). Map created using ArcGIS v10.5 (www.arcgis.com). (b) 3D Google Earth view of the study area, indicating the locations of the sampled Wunut and Tanggulangin hydrocarbon fields and Lusi crater. The red shaded area indicates the Watukosek fault system. Map data: Google, Image Landsat/Copernicus, Maxar technologies, SIO, NOAA, U.S. Navy, NGA, GEBCO.

migration pathways, we present new geochemical, palynological, and petrographical data acquired from oil films and rocks clasts erupted at the Lusi vent and compare them with those obtained from oil samples from the neighbouring HC fields.

The East Java sedimentary basin is located on the south-eastern margin of the Sunda plate, in the back-arc of the Sunda volcanic arc that has been active since the Miocene (ca. 12–10 Ma). The older Southern Mountain arc, located 50 km further south, was active between ca. 45–20 Ma and was also formed due to northward-directed subduction of the Indian-Australian Plate under the Sunda plate^{18,19}. The Penanggungan and Arjuno-Welirang volcanoes are located 10 and 25 km, respectively, to the south-west of the Lusi mud eruption site (Fig. 1).

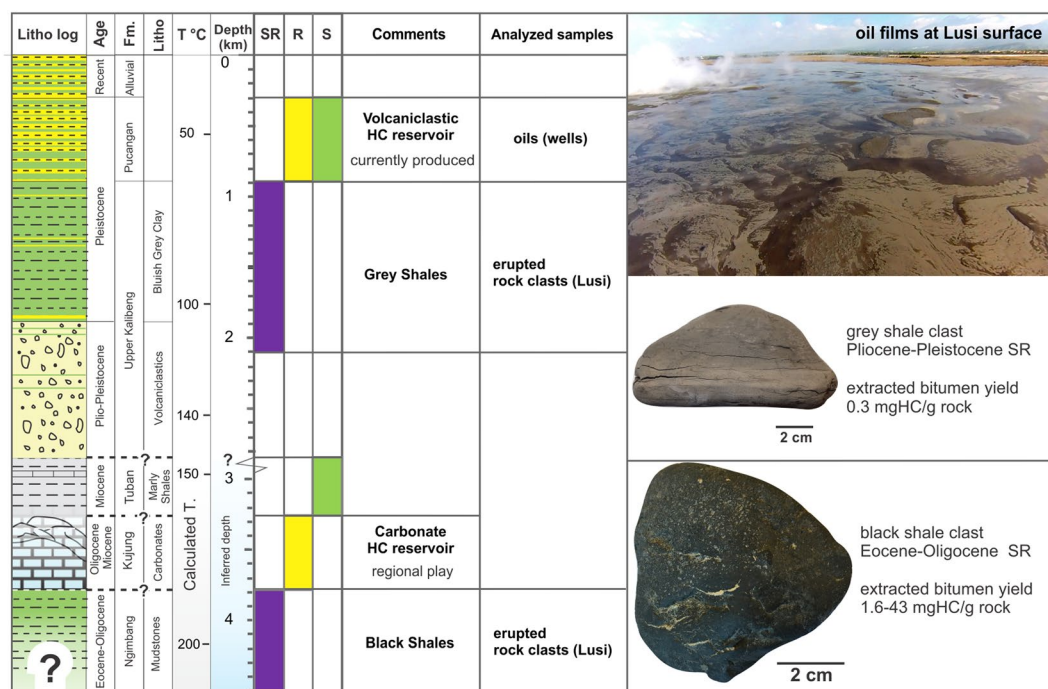


Figure 2. Petroleum systems of the southern part of the East Java petroleum basin, highlighting the main HC source rocks (SR), reservoirs (R), seals (S) and examples of the analysed samples with corresponding formation origin. Temperature gradient was measured in the well BJP-1 (located at the Lusi site) and inferred below 2.8 km²⁰. Lithostratigraphy log is from Samankassou *et al.*¹⁷.

In the study area the basin consists of a >5 km thick sedimentary section that overlies Pre-Cenozoic basement (Fig. 2). The lithostratigraphy of the region is constrained by the drilled boreholes and seismic surveys acquired in 1990's-2000's^{13,17,20-22}. The sedimentary section contains (from bottom to top): Middle Eocene-Lower Oligocene organic-rich black shales of the Ngimbang Fm. (>3800 m), Upper Oligocene-Lower Miocene carbonates of the Kujung Fm. (from ~3800 to ~3250 m), Lower-Upper Miocene marls and shales of the Tuban Fm. (from ~3250 to ~2830 m), Upper Pliocene-Pleistocene Upper Kalibeng Fm. containing tight volcanic and volcanoclastic units in the lower part (~2830 to 1870 m) and bluish grey shales and marls in the upper part (1870–900 m), Pleistocene volcanoclastic shales and sands of the Pucangan Fm. (900–290 m), and recent alluvial sediments (290–0 m). This part of the basin is characterized by high sedimentation rates (0.7 km/Myr) since Late Pliocene, which caused the rapid burial and preservation of the semi-lithified deposits.

The East Java sedimentary basin is a petroleum-rich region, with a total estimated reserves of 1830 Million Barrels of Oil Equivalent²³. The hydrocarbon accumulations in the basin were discovered in Pleistocene volcanoclastic reservoirs of the Pucangan Fm., Miocene sands of the Ngrayong Fm. and Woncolo Fm., Upper Oligocene-Lower Miocene carbonates of the Kujung Fm., and the carbonates and sands of the Ngimbang Fm.^{23,24}. The organic-rich shales are confined to the Middle Eocene-Lower Oligocene Ngimbang Fm., Miocene Tuban Fm., Upper Pliocene-Pleistocene Upper Kalibeng Fms. The major HC source rock is the Ngimbang Fm., consisting of organic-rich shales, coals and coaly shales^{22,25}.

In the study area, the producing reservoir intervals are confined to the Pucangan Fm., 200–1000 m depth, consisting of fine-grained lithologies (up to 80% of net shales) and interbedded with 3–50 m thick layers of sandstones²⁶ (Fig. 2). The intercalating shales seal the HC accumulations. The gas accumulations have an oil leg in the lower intervals of the Pucangan Fm.

Results

The dataset was gathered from a suite of samples collected during yearly sampling campaigns conducted in the study area since the beginning of the Lusi activity. Lithoclasts erupted at the crater site include carbonates, lahar, grey shales, and black shales. Among those, specimens of potential source rocks (grey and black shales) were selected for this study (30 rock clasts). In addition, 4 oil film samples collected from the Lusi crater and 4 oils samples from the Wunut and Tanggulangin oil and gas fields were analysed.

Oils. Organic geochemical analyses of the oil films collected from the Lusi crater (Supplementary Table S1) reveal that they are composed of 53–64% of saturated HCs, 13–15% of aromatic HCs, and 21–34% of polar compounds (i.e. resins and asphaltens). *n*-Alkane distributions demonstrate the predominance in high-molecular-weight zone (*n*-C₂₃ – *n*-C₂₇) (Fig. 3), Pristane/Phytane (Pr/Ph) ratios vary from 2.6 to 3.9. Carbon preference index ranges from 1.02 to 1.03 ($CPI = (n-C_{23} + n-C_{25} + n-C_{27}) / (n-C_{25} + n-C_{27} + n-C_{29}) / 2 \times (n-C_{24} + n-C_{26} + n-C_{28})$) (Fig. 3). The oleanane index, indicating contributions to the organic matter of the

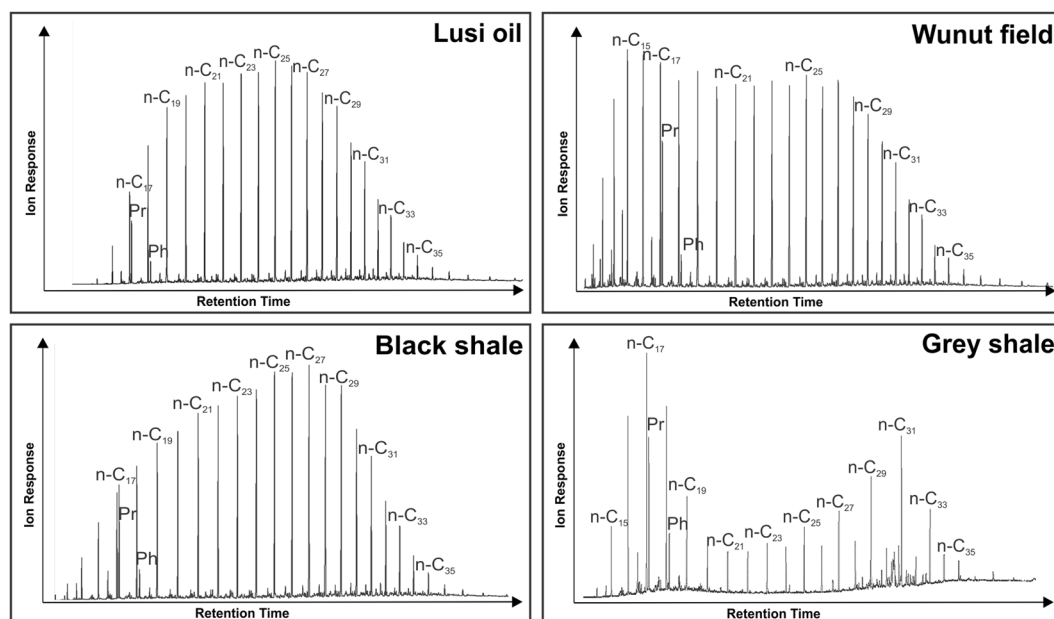


Figure 3. Gas chromatography results of the aliphatic fractions of the Lusi oil films, oil from the Wunut field, black and grey shale bitumen extracts. Normal and *iso*-alkane distribution of the Lusi oil films, oil from the Wunut HC field and bitumen extract of the black shales (Ngimbang Fm.) share similar distribution patterns, indicating that both oils originate from the clasts of the Ngimbang Fm. Low n -C₁₃–C₁₇ peaks in the black shale bitumen extracts and Lusi oil are due to the loss of light oil fraction in the Lusi vent, that was subjected to the temperatures greater than 100 °C. Alkane distribution in the bitumen extracts of the grey shales indicates that OM is immature and differs from that of black shales.

source rock from certain angiosperms²⁷, varies from 0.18 to 0.20, and 2- methylhopanoid index ranges from 0.05 to 0.06, and 3-methylhopanoid index in the samples is 0.03. The methylphenanthrene index [$MPI-1 = 1.5 \times (3- + 2-MPhenanthrene)/(Phenanthrene + 1- + 9-MPhenanthrene)$]²⁸ ranges from 0.55 to 0.62, methylphenanthrene ratio ($MPR = 2-MPhenanthrene/1-MPhenanthrene$)²⁹ equals to 1.18.

The oil sample from the Wunut field (JV17–40) is composed of 81% saturated HCs, 14% aromatic HCs, and 5% polar compounds. Normal and *iso*-alkane distributions are bimodal, with a predominance in lower molecular-weight zone (n -C₁₅) and higher molecular-weight zone (n -C₂₃ – n -C₂₇) (Fig. 3). This sample was not affected by biodegradation processes. In contrast, oils from the other wells feature evidence of biodegradation occurring in the reservoirs, resulting in the reduction of the *n*-alkanes and increase of the *iso*-alkanes. Pr/Ph ratios of the 4 analysed oil samples vary from 4.1 to 4.34, while CPIs range from 0.94 to 1.06. The oleanane index ranges from 0.17 to 0.24, and 2- and 3-methylhopanoid indices vary from 0.056 to 0.059 and from 0.031 to 0.033, respectively. MPI-1 and MPR vary from 0.73 to 0.82 and from 1.19 to 1.22, respectively (Supplementary Table S1).

Rock clasts. Rock clast samples were divided into 2 groups based on lithology: **grey shales (GS) and black shales (BS)**. GS group contains light grey-coloured shales and marls with no obvious HC odour, often laminated, and poorly lithified. The BS group consists of black-coloured clasts, well-lithified, often laminated and with a strong HC odour.

Palynological analysis revealed that the GS clasts can be assigned to stratigraphical units ranging from Miocene to Late Pliocene-Pleistocene, corresponding to the Tuban and Upper Kalibeng Fms., respectively (Fig. 4, Supplementary Table S2). The shortage of quantitative palynological data and the long stratigraphic range of most palynomorphs do not allow a more detailed biostratigraphic correlation to regional palynological zonation schemes^{30–32}. However, GS samples contain both marine and terrestrial palynomorphs, including the long-ranging dinoflagellate cysts (dinocysts) species *Lingulodinium machaerophorum*, *Spiniferites* spp., *Operculodinium* spp. and diverse spores and angiosperm pollen, including mangrove palm pollen (*Nypa*). The occurrence of dinocysts with a more limited range, such as *O. piaseckii* and *Dapsilidinium* sp. indicates a Miocene and pre-Pleistocene age for GS samples JV14B-02 and JV17-01–40, respectively (Supplementary Table S2). Additional constraints regarding the age of the samples can be provided using the colour of the palynomorphs that show 2 distinctive groups: a) yellow-orange, indicating the lowest thermal maturity, TAS (Thermal Alteration Scale³³) = 1–2, < 65 °C, likely Late Pliocene-Pleistocene; and b) dark brown colours indicating a higher thermal maturity (TAS = 5–6, 150–180 °C), likely of Miocene age.

Palynological residue of the BS samples only contains highly thermally-altered and degraded/oxidized organic particles of black colour; identifiable palynomorphs were lacking (TAS = 7, >250 °C, Fig. 4, Supplementary Table S2). Bleaching of the organic residue revealed a terrestrial palynofacies with charcoals, leaf cuticles, highly degraded amorphous OM, some highly corroded spores, and remains of fresh water algae. The high thermal maturity and the extensive degree of alteration observed in these remains hampered an age assignment

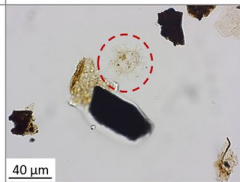

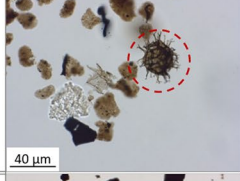
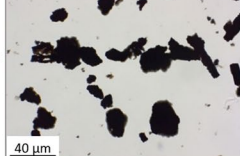

Clasts	Age	Palynological preparation	TAS, Temp.	Palynofacies description	Petrographical photomicrograph	Petrographical description	Ro (%) Temp.	RSCM Temp.	T _{max} Temp.	TOC, (%)
Grey shales	L. Pliocene - Pleistocene		1-2 <65 °C	Dinoflag. cyst (<i>Spiniferites</i>), algae fragm., diverse plant debris (wood and cuticle particles).		Pyrite-rich, abundant thermally unaltered dispersed organic matter. Macerals of the huminite and liptinite groups.	0.45 ~60-80°C		423-442 °C ~60-100 °C	0.3-2.0
	Miocene		5-6 150-180 °C	Dinoflag. cyst (<i>Spiniferites</i>), plant debris (cuticle), charcoal, amorphous organic matter	Not analysed	Not analysed				0.5-0.8
Black shales	Eocene-Oligocene		7 >250 °C	Corroded, degraded plant debris (wood, cuticle?), charcoal, amorphous organic matter.		Macerals display high temperature imprint, represented by anisotropic vitrinite and cutinite with distinct degasification pores.	2.5-2.7 >230 °C	~260°C chlorite >300 °C carbonate	433-446°C ~75-120 °C	1.6-14.6

Figure 4. Summary chart of the identified lithostratigraphy groups with main observations and analysed thermal maturity parameters. TAS - Thermal Alteration Scale³³, Temp. – estimated temperature, Ro – vitrinite reflectance measurements, T_{max} – Rock-Eval parameter characterizing the maturity of the samples, RSCM – Raman spectroscopy (from Malvoisin, *et al.*¹³), TOC – Total Organic Carbon. The shallow Upper Pliocene-Pleistocene grey shales (Up. Kalibeng Fm.) have lower maturity than the Eocene-Oligocene black shales (Ngimbang Fm.). Although black shales feature high temperature imprints (>300 °C), they consistently show high organic carbon content and moderately low T_{max} parameters, suggesting the temperatures lower than 120 °C. This discrepancy is ascribed to the migration of magmatic fluids within the Ngimbang Fm. that occurred only recently (possibly Holocene) and enhanced OM maturation.

using biostratigraphic events. However, the palynofacies of the BS samples consistently indicate a terrestrial, fluvial-lacustrine depositional environment, which suggests that the BS lithoclasts originate from the lower terrestrial units of the Eocene–Oligocene Ngimbang Fm. Previous studies showed that the lower part of Ngimbang Fm. was deposited in a terrestrial to coastal marine setting with sands, coals and lacustrine shales, overlain by marine shales and limestones in the upper part^{31,34}. While younger lithostratigraphic units (the Upper Kalibeng and Tuban Fms) were deposited predominantly in a marine environment. This is supported by the regular occurrences of open marine dinocyst genera, such as *Spiniferites* and *Operculodinium*³⁵ in the GS samples, which are correlated to the Upper Kalibeng and Tuban Fms.

Mercury concentrations in Upper Pliocene-Pleistocene GS samples range from 5 to 47 ppb (mean 20.9 ppb, Fig. 5), in Miocene GS samples from 2 to 3 ppb (mean 2.3 ppb), in the Eocene–Oligocene BS samples is from 1 to 9 ppb (mean 2.8 ppb). There is a strong positive correlation between Hg and TOC in modern sediments as OM is usually the dominant depositional pathway for Hg into sediments³⁶. Mercury concentrations are therefore often normalised to TOC concentrations to account for variations in OM deposition³⁷. After normalisation, there is a distinctive and consistent difference between the BS clasts of the Eocene–Oligocene Ngimbang Fm. (Hg/TOC = 0.1 to 1.2 ppb/wt.%) and both the Miocene Tuban Fm. (Hg/TOC = 3.5 to 4 ppb/wt.%) and Upper Pliocene-Pleistocene Upper Kalibeng Fm. (Hg/TOC = 12 to 49 ppb/wt.%) GS clasts.

Organic petrography. The investigated Upper Pliocene-Pleistocene GS sample is a pyrite-rich marly shale with abundant thermally unaltered dispersed organic matter (Fig. 4). Macerals of the huminite and liptinite maceral groups were observed, among others ulminite, gelinite, as well as lamalginite, telalginite, sporinite, cutinite, lip-todetrinite, and interodetrinite. Mean random vitrinite reflectance measurements show Ro = 0.45%. In contrast, the investigated Eocene–Oligocene BS samples are identified as silty shales with some inclusions of coarse crystalline quartz or dolomite. The groundmass encloses fine-pored structures characterised by pale inner reflections of unknown origin, possibly of a relict character. The encountered macerals display clear high temperature imprint and are represented by anisotropic vitrinite and cutinite with distinct degasification pores. The secondary particles embrace fly ash-like particles and pyrolytic carbons with characteristic spherulitic domains. Thermal maturity analyses based on the random vitrinite reflectance method show Ro = 2.47–2.69%.

Organic geochemistry. The Miocene-Pleistocene GS samples have low to moderate OM content (TOC from 0.3 to 2 wt.%), low generative potential (S₁ peaks vary from 0.01 to 0.3 mg HC/g rock, S₂ from 0.04 to 1.2 mg HC/g rock) and extracted bitumen amounts ranging between 0.26 to 0.28 mg/g rock (Fig. 6, Supplementary Table S3). The T_{max} is 419–444 °C. The extracted bitumens contain 7–15% saturated HCs, 24–34% aromatic HCs, 59–61% polar compounds. C_{27–29} sterane distributions indicate that the OM is of II-III type, fluvio-deltaic – shallow

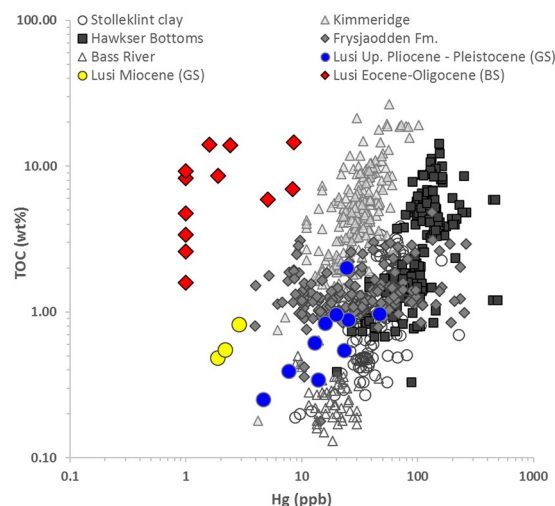


Figure 5. The distribution of mercury and TOC concentrations in the black shales (BS) and grey shales (GS) samples from the Lusi eruption site. The grey data points correspond to the shale sections from published datasets from the Paleocene-Eocene Stolleklint clay in Fur island (Denmark), Paleocene-Eocene Frysjaodden Fm. (Svalbard), Paleocene-Eocene Bass River locality (USA), Upper Jurassic Kimmeridge clay (UK), and Low Jurassic Hawkser Bottoms (UK)^{59,60} showing the known range of Hg/TOC values in clays and shales. Note that Hg concentrations <1 ppb are below the instrumental detection limit and are here given a value of 1 for illustration purposes.

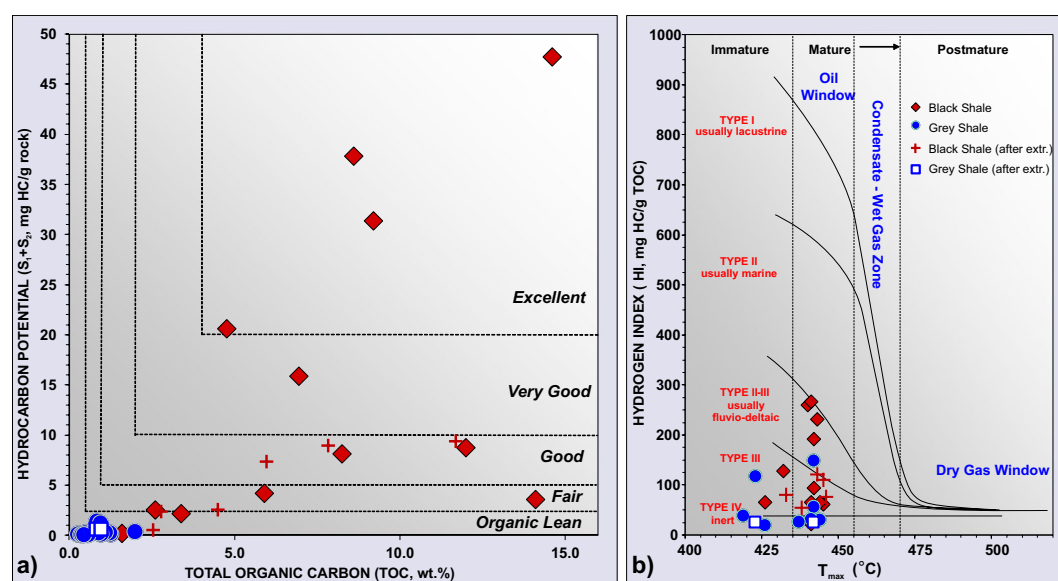


Figure 6. (a) Source rock characterization based on Rock-Eval parameters. TOC - Total Organic Carbon and $S_1 + S_2$ - hydrocarbon generative potential. Black shales have fair to excellent HC potential, while grey shales could be treated as organic lean (classification is based on Peters *et al.*⁴). (b) Maturity of the HC source rocks, suggesting that both grey and black shales fall within the oil window zone.

marine origin, which is in line with HI values up to 148 mg HC/g TOC (Fig. 6). Gas chromatography of the aliphatic fractions shows bimodal peak distributions reaching maximums in the lowmolecular-weight zone ($n-C_{17}$) and high molecular-weight zone ($n-C_{31}$) (Fig. 3). The Pr/Ph ratios are 0.5–2.5, with CPI values between 1.4–1.6. The oleanane indices range from 0.32 to 0.47, and 2- and 3-methylhopanoid indices vary from 0.025 to 0.026 and from 0.023 to 0.026, respectively. MPI-1 ranges from 0.41 to 0.56, MPR varies from 1.06 to 1.17 (Supplementary Table S1).

All Eocene-Oligocene BS clasts show distinct characteristics. The rocks have high OM contents (TOC from 1.6 to 14.6 wt.%, mean 7.7 wt.%), high generative potential (S_1 from 0.1 to 19.8, mean 5.3 mg HC/g rock, S_2 from 0.2 to 27.9 mg HC/g rock, mean 10 mg HC/g rock) and high extractable bitumen amounts (from 1.6 to 43.4 mg/g rock, mean 24.6 mg/g rock) (Fig. 6, Supplementary Table S3). The bitumens contain 53–91% (average

82%) saturated HCs, 7–24% aromatic HCs, 0.01–22% polar compounds. The OM is a II-III kerogen type with HI up to 267 mg HC/g TOC, which points to a fluvio-deltaic origin. The T_{\max} is 433–446 °C and aliphatic fractions show unimodal peak distribution with maxima in the higher molecular-weight zone ($n\text{-C}_{25}$ – $n\text{-C}_{29}$) (Fig. 3). The Pr/Ph ratios are 2.6–3.7, with CPI values between 1.02–1.04. The oleanane index varies from 0.16 to 0.23, and 2- and 3-methylhopanoid indices vary from 0.051 to 0.060 and from 0.033 to 0.039, respectively. MPI-1 ranges from 0.63 to 0.9, MPR varies from 1.03 to 1.57 (Supplementary Table S1).

Discussion

High temperatures (~100 °C) at the surface of the Lusi mud vent may have caused partial leaching of the light oil fraction (particularly C_7 – C_{16} compounds) from the oil films and bitumens in the rock clasts. Nevertheless, oil-films from Lusi and oils from the HC fields share similar biomarker compositions with the bitumen extracts from the BS rock samples, including: a) unimodal *normal* and *iso*-alkane distribution (CPI ranging from 0.94 to 1.06); b) regular C_{27} , C_{28} , C_{29} sterane homologues distributions; c) oleanane index; d) 2- and 3-methylhopanoid indices; e) as well non-biomarker dibenzothiophene/phenanthrene ratio (DBT/Phen) (Figs. 3 and 7a,b, Supplementary Table S1 and Fig. S4). These biomarkers and aromatic compounds ratio are commonly used for source-oil and oil-oil correlations^{27,38–40}. Extractable organic matter from the Miocene-Pleistocene GS samples have remarkably different characteristics, which include: a) bimodal alkane distribution, with predominance of the odd over even alkanes (CPI ranges from 1.4 to 1.6); b) higher oleanane index than in the oils and BS bitumen extracts; c) lower 2- and 3-methylhopanoid indices; d) lower DBT/Phen (Figs. 3 and 7a,b, Supplementary Table S1 and Fig. S4). Rock-Eval analysis reveals that GS samples have poor hydrocarbon generative potential⁴, implying that these formations can generally only negligibly contribute to petroleum systems in this part of the basin (Fig. 6a). In contrast, BS clasts have high OM content, and the hydrocarbon generative potential for most of the samples is good to excellent. These observations suggest that all the oils, both vented at Lusi and trapped in the HC reservoirs, share a common origin pointing to the Eocene–Oligocene BS clasts of the Ngimbang Fm. as the major HC source rock.

The high occurrences of oleanane, as well as high Pr/Ph ratios, DBT/Phen ratio lower than 1 (Fig. 7a,b, Supplementary Table S1), combined with results from palynology, clearly indicate a dominant terrestrial source of the organic matter of the HC source rock. These characteristics along with the lithology and the high OM content match the geochemical results obtained from the wells penetrating the Ngimbang Fm. source rock²⁵, the dominant source rock in the East Java Basin^{22,23}.

The thermal maturity of the OM from BS samples (Ngimbang Fm.), evaluated using the Rock-Eval method, corresponds to the oil window zone (T_{\max} 433–446 °C after extraction) (Fig. 6b, Supplementary Table S3). Recalculating the T_{\max} parameter to the R_o equivalent using the formula by Jarvie *et al.*⁴¹ (R_o eq. (%) = $0.0180 \times T_{\max} - 7.16$) suggests a R_o eq. varying between 0.63 to 0.87%. In contrast, the measured vitrinite reflectance values of the same BS clasts ($R_o = 2.5$ – 2.7%) are significantly higher than the estimated R_o using T_{\max} . This suggests that in the catchment area of the Lusi site the Ngimbang Fm. was exposed to temperatures significantly greater than 230 °C, based on the chemical kinetic model of vitrinite maturation proposed by Burnham and Sweeney⁴². Maceral analysis also revealed the presence of high temperature imprints, which typically take place between 400 to 1000 °C^{43–45}. Palynological analyses confirm a high maturity level of the samples from the Ngimbang Fm. with spores, which were typically poorly preserved, altered cell shapes and dark brown to black colour, indicating the palynomorphs have been subjected to paleo temperatures above 250 °C^{42,46}. This is consistent with chlorite and carbonate Raman microthermometry measured on the similar set of the erupted Ngimbang Fm. clasts, which indicates this formation had been exposed to conditions > 260 °C¹³.

Most sedimentary basins worldwide are characterized by relatively gradual burial, which typically leads to the coherent thermal alteration of the OM and progressive changes of the maturity-related parameters (i.e. vitrinite reflectance, T_{\max} , biomarker isomerisations, spore and pollen alterations). Rapid heating events induced by magmatic activity and/or hydrothermal fluid circulation may enhance the maturation of OM and unevenly modify it, leading to maturity estimate inconsistencies. For instance, comparisons of extractable organic matter (EOM) compounds in Scottish Carboniferous coals affected by contact and burial metamorphism showed that reversals in the trend of molecular-maturity parameters stem from different reaction rates of organic components in the areas subjected to rapid heating events⁴⁷. A geochemical study of Jurassic sediments affected by Paleogene dykes also show that different maturity-related proxies show varying sensitivity to short temperature pulses⁴⁸. Therefore, only certain proxies for OM maturation follow the expected heating rate in contact metamorphic zones, while other parameters used for basins with gradual burial do not keep pace with the thermal effects. For example, sterane and hopane maturation appears to lag behind the alteration of vitrinite macerals during short-lived temperature anomalies⁴⁹, acquired during experimental maturation. Moreover, studies of shales affected by sill intrusions have scatter T_{\max} measurements that do not follow the maturation trend estimated by vitrinite reflectance data^{50,51}. Overall, multiple studies on the coal/organic matter maturation impacted by the magmatic intrusions imply that several parameters strongly affect the maturation in those specific geological settings: the lithological type of the host rock, initial maturation level of the OM prior to the intrusion, heating rate, duration, sill thickness, temperature and pressure regimes^{52–55}. Therefore, the discrepancies in the maturity/temperature estimations using various maturity-related parameters mirror the short-termed high temperature anomaly occurring in the LUSI system.

Our data clearly demonstrates a complex geological setting of the southern East Java basin. Lusi is located 10 km to the NE from the active Quaternary volcanic arc. Ambient noise tomography investigations highlighted the connection between the magma chamber of the nearest volcano and the Lusi conduit at a depth of ~ 4.5 km¹¹. This suggests the presence of a magmatic intrusion penetrating the organic-rich sediments of the Ngimbang Fm. and associated hydrothermal fluid migration¹¹. These conclusions are supported by the gas geochemical parameters, such as presence of the mantle-derived volatiles in the gas vented at Lusi^{12,14}. Furthermore, the erupted HC gases have quite different molecular and isotopic composition ($\delta^{13}C_{CH_4}$ up to –35.7‰) compared to the

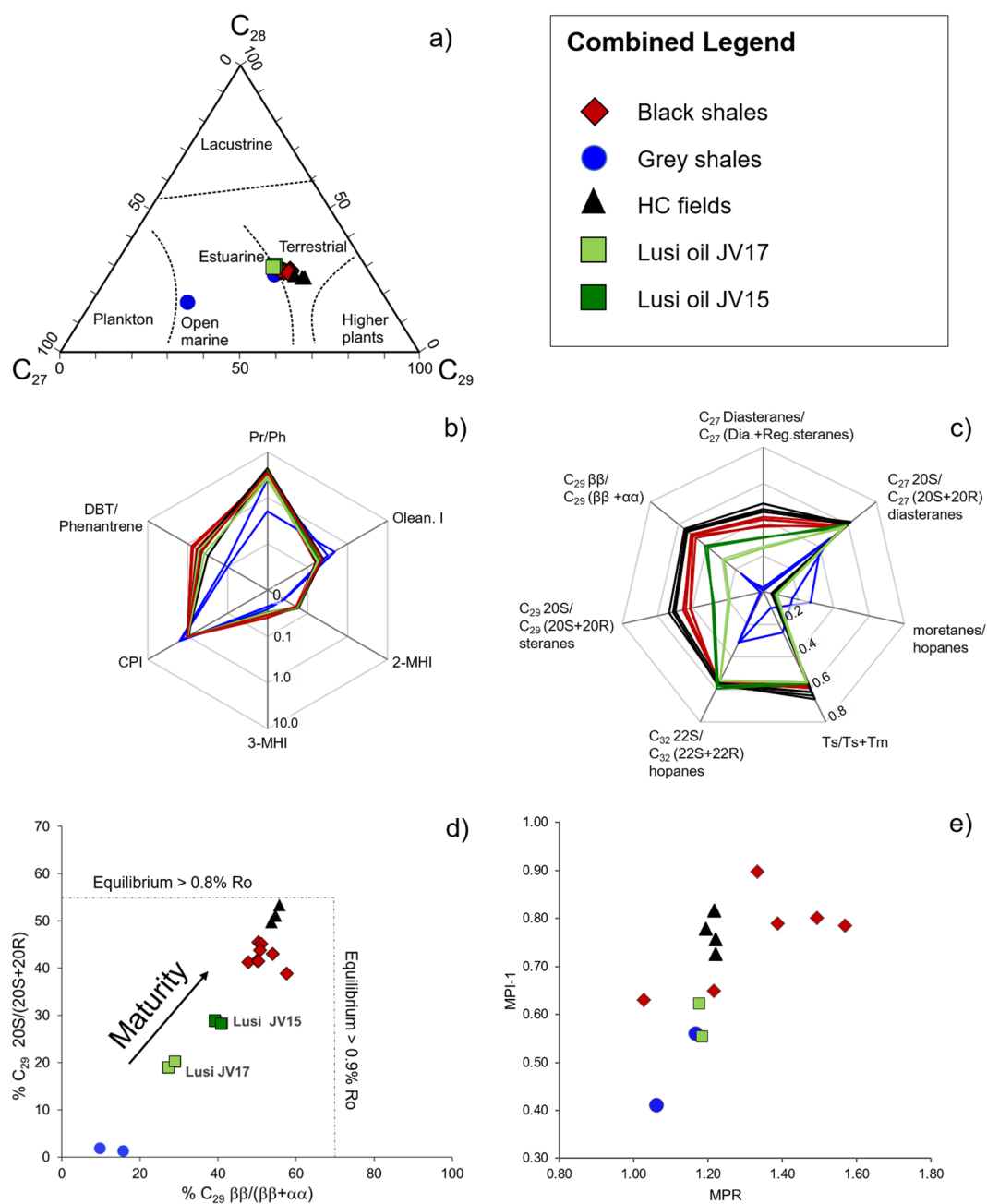


Figure 7. Biomarker and aromatic compounds distribution of the oil films from the Lusi, HC fields and bitumen extracts of the black and grey shale rock clasts. **(a)** Ternary diagram of the C_{27} , C_{28} and C_{29} sterane distribution, indicating fluvio-deltaic – shallow marine depositional settings for most of the samples. **(b)** Star diagram of the major source-related biomarkers and aromatic compounds, suggesting that all Lusi oil films and oils in the HC fields are sourced by the black shales of the Ngimbang Formation (Eocene-Oligocene). 2-MHI and 3-MHI correspond to 2- and 3-methylhopanoid indices, Olean. I - oleanane index, DBT - dibenzothiophene. **(c)** Star diagram of maturity-related biomarkers shows that grey shales have the lowest maturity, while the oils from the hydrocarbon fields have the highest maturity; **(d)** C_{29} sterane isomer distribution indicates that Lusi oil films and oils from the HC fields form different clusters, underscoring recent HC generation for the oil erupted at Lusi; **(e)** methylphenanthrene index (MPI-1 = $1.5 \cdot (2\text{-MP} + 3\text{-MP}) / (P + 1\text{-MP} + 9\text{-MP})$) and methylphenanthrene ratio (MPR = $2\text{-MP} / 1\text{-MP}$) suggest the lowest maturity for the Lusi oil, but the highest for the bitumen extracts of the BS samples.

gas stored in the adjacent HC fields ($\delta^{13}C_{CH_4}$ range from -58.3 to -40.7%), hence suggesting that these two systems are compartmentalised^{12,16}. These lines of evidence, together with the geochemical results from the rock clasts and oils presented here, indicate that the erupted HCs have been recently generated within the Ngimbang Fm. that is affected by a recent (Holocene?) magmatic intrusion and hydrothermal fluid migration. These rapid

heating events are thus interpreted to be the reason of the discrepancies observed in the BS maturity-related parameters. Furthermore, if HC reservoirs or source rock intervals are exposed to high temperatures (>200 °C) over a geological time span, bitumen (and/or oil) is usually totally converted to gas and pyrobitumen due to secondary cracking processes^{56,57}. The investigated BS samples of the Ngimbang Fm. are oversaturated with the bitumen phase (up to 43 mg HC/g rock of the extracted bitumen). Therefore, the exposure of these samples to high temperatures (>200 °C) must have taken place over a short period of time, insufficient to cause total secondary cracking of all bitumen and oil.

Our results highlight the importance of the timing effect in the maturation of the source rock. More specifically, multiple lines of evidence suggest that organic-rich sediments have been recently exposed to high temperatures (geochemically corresponding to the late gas window-overmature zone). This implies that the source rocks did not fully release their hydrocarbon potential and are essentially still prone to generate oil. Therefore, the methods to estimate thermal maturity, such as Rock-Eval and maturity-related biomarkers, will not accurately represent true paleo-temperatures in sedimentary successions affected by magmatic intrusions. Indeed, the Rock-Eval analysis and aliphatic compounds of the bitumen extracts from BS indicate that in the study area the Ngimbang Fm. was generally exposed to temperatures not higher than 120 °C (middle oil window). This would result in a thermal gradient 22–25 °C/km prior to magmatic/hydrothermal activity. A similar low gradient is also measured in the wells of the KE structure (40 km east of Lusi). In contrast, the geothermal gradient estimated at the Lusi site (42 °C/km, based on the BJP1 well²⁰) implies that the Ngimbang Fm. reaches temperatures between 186–236 °C (3.8–5 km depth, 26 °C at the surface) even when applying a linear curve gradient (Fig. 2). These temperature estimates are indeed consistent with random vitrinite reflectance data and microthermometry measurements conducted on the BS clasts. The combined observations support the conclusion that a recent increase of the heat flow is localized in the southern part of the East Java sedimentary basin affected by Quaternary volcanism. The kinetic model for the BS kerogen suggests that HC generation starts at ~105 °C, and the transformation ratio of the kerogen is less than 10% at 120 °C⁵⁸. Therefore, we cannot exclude the scenario where the HC generation processes have started prior to the migration of the magmatic/hydrothermal fluids in the study area. However, we suggest that recent magmatic activity has largely enhanced the maturation of OM and HC formation is very likely ongoing.

The distinctive difference in Hg/TOC ratios between BS and GS clasts further support the stratigraphical assessment of the clasts using biostratigraphical and geochemical methods, as well as our conclusion on the exposure of the Ngimbang Fm. to hydrothermal/magmatic activity. Elevated Hg/TOC ratios have been used as a proxy for enhanced volcanic activity in the geological record due to Hg deposition through other avenues such as clay particles^{37,59}. As a result, there is now a wealth of data on Hg/TOC ratios in shales, both during periods of elevated global volcanic activity and relative global quiescence^{59,60} (Fig. 5). Compared to these data sets, BS clasts of the Ngimbang Fm. are extremely depleted in mercury, even though the study area has been located close to the volcanic arc since the Eocene. In contrast, GS samples of Miocene-Pleistocene age plot within the field of previously measured Hg/TOC ratios (Fig. 5). We suggest that preferential Hg loss occurs in the BS samples due to the volatilization and escape of Hg at high temperatures due to the recent volcanic activity. Organic-bound Hg release occurs at the temperature window of 150–400 °C, with the highest intensity at ~300 °C⁶¹. This provides further support for the presence of the high temperature anomaly affecting the Ngimbang Fm. at depths greater than 4 km.

Our dataset reveals also the striking maturity discrepancies between the oil present in the HC reservoirs and that erupted at Lusi. Maturity-related biomarker parameters (C_{29} sterane $\beta\beta/(\beta\beta + \alpha\alpha)$ and 20S/(20S + 20R) isomer ratios, C_{27} dia- and regular steranes ratio, Ts/Ts + Tm hopanes, moretanes/hopanes) indicate that Lusi oil films are less mature than the oil trapped in the production fields (Fig. 7c,d, Supplementary Table S1 and Fig. S1). The ratios of aromatic compounds MPI-1 and MPR (methylphenanthrene index and methylphenanthrene ratio), that are less susceptible to degradation and evaporation loss, also suggest the lowest maturity for the Lusi oil, but in contrast indicate the highest maturity for the bitumen extracts of the BS samples. Recalculated vitrinite reflectance of the BS from MPI-1 equals to 1.76 to 1.92%^{29,62}. However, the reversal trend for MPI-1 may differ due to rapid heating⁴⁷, indicating potentially higher recalculated value. Maturity estimates based on phenanthrene ratios thus result in high uncertainty.

Our multidisciplinary study provides insights into understanding the Lusi plumbing system and the HC migration mechanisms at regional scale. Specifically, the maturity differences imply that: a) HC accumulations of Wunut and Tanggulangin fields are not the source of the large volume of oil erupted from the Lusi system; and b) the oils from the HC fields and Lusi were likely generated at different depositional areas of the Ngimbang Fm. and therefore most probably had different migration pathways. Integrating all the geological and geochemical observations, we propose a conceptual model of the hydrocarbon migration in the southern part of the NE Java Basin (Fig. 8a–d):

- (a) Late Miocene-Pliocene HC generation initiated within the organic-rich shales of the Ngimbang Fm. deposited in the deepest parts of the East Java sedimentary basin where the South Madura depositional centre resides (Fig. 8b). Gravity anomalies and well data show that in this part of the basin (located ~40 km to the east of Lusi) the sedimentary cover is thicker and hence Ngimbang Fm. is buried at least 1 km deeper^{63,64}. Therefore, deep burial induced HC generation most likely occurred in the South Madura region.
- (b) HC migration to the carbonates of the Kujung Fm., forming the accumulation within the Porong reefal structure, located 7 km to the north-east of Lusi⁶⁴. The Porong-1 exploration well penetrated the top part of this potential reservoir revealing the presence of oil shows²⁶ (Fig. 8b).
- (c) Late Pleistocene-Holocene witnessed the triggering and collapse of the Porong paleo-vent. The breach of the seal led to secondary HC migration from the Porong trap to the shallow clastic units of the Pucangan Fm.⁶⁴, forming the shallow accumulations of the Tanggulangin, Wunut and Carat fields (Fig. 8c).

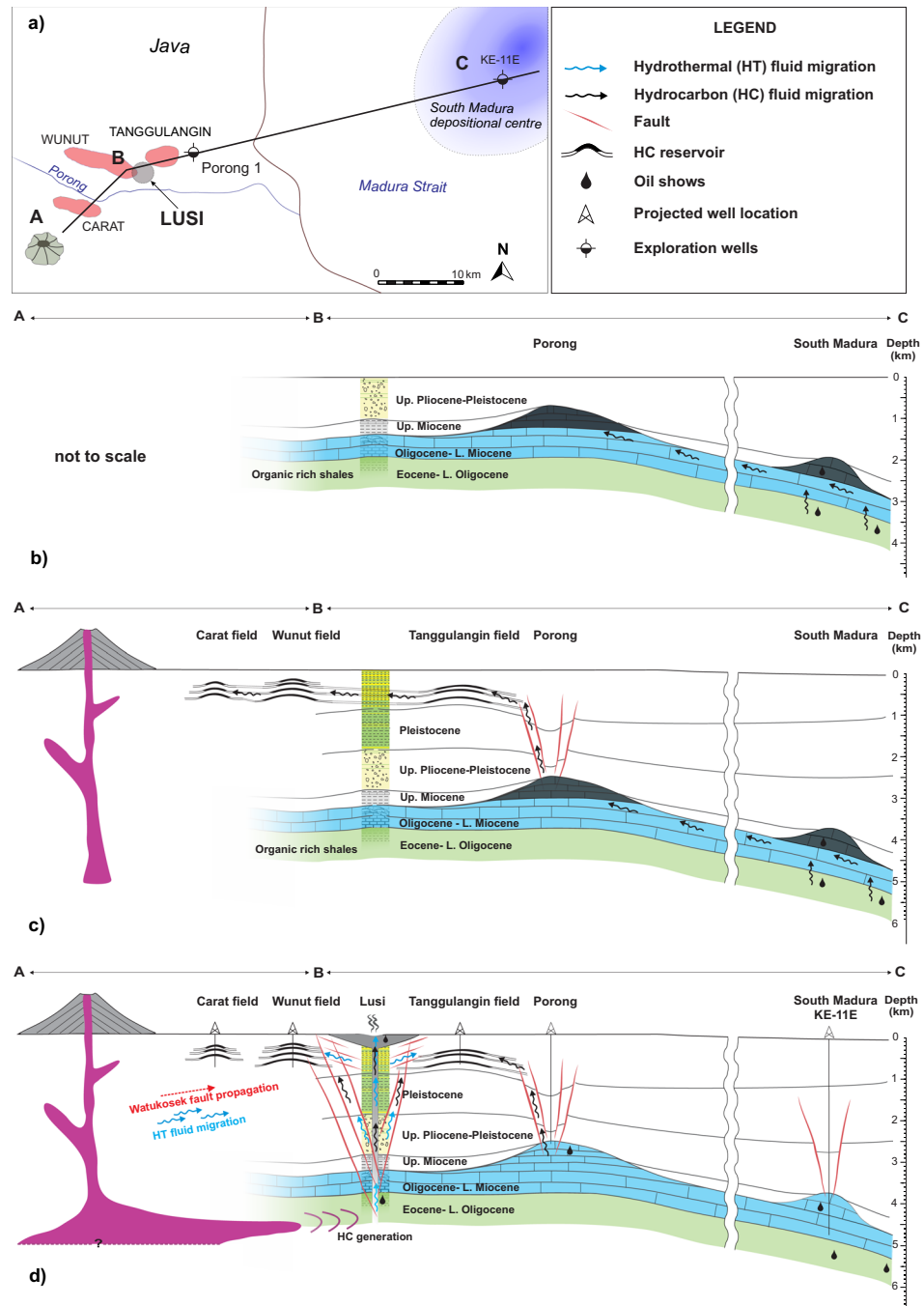


Figure 8. Conceptual geological model depicting the development of the petroleum system in the study area: (a) location of the profile ABC, crossing HC fields, Lusi eruption site, Porong paleovent and South Madura depositional center; (b) HC generation in the subsided South Madura region (on the east) and migration to the Porong reefal carbonates during Late Miocene-Pliocene; (c) collapse of the Porong trap in Pleistocene or recent, followed by the secondary migration of the HCs to the shallow Pleistocene reservoirs (Tunggulangi, Wunut, Carat fields); (d) Holocene magmatic intrusion penetrates organic-rich deposits (>4 km depth), triggering HC and CO₂ generation below Lusi and overpressure buildup. Reactivation of the Watukosek fault system was followed by the occurrence of the Lusi piercement and surface migration of the brecciated sediments, water, hydrocarbons and mantle-derived fluids.

(d) Holocene migration of magmatic fluids within the organic-rich Ngimbang Fm. triggered thermo-metamorphic reactions, greatly enhancing the generation of the HCs, CO₂ and leading to overpressure buildup. The recent reactivation of the Watukosek fault system⁶⁵ facilitated the trigger of the Lusi system and the release of HC at the surface (Fig. 8d).

The Lusi eruption represents an excellent opportunity to investigate the impact of the recent activity of volcanic systems on petroleum sedimentary basins and enhanced HC generation. The study highlights the relevance of time factor for source rock maturation, and the importance of specific geochemical and microscopy methods (i.e. palynology, organic petrology, and chlorite microthermometry) to estimate the temperatures in sedimentary basins affected by volcanic activity.

Methods

Bulk analyses (C_{org}, Rock-Eval). Bulk rock analyses were performed at the Federal Institute for Geosciences and Natural Resources (BGR, Hannover, 12 samples), and at the Applied Petroleum Technology (APT, Oslo, 18 samples) laboratories. Both laboratories used the same Rock-Eval 6 analyzer standard procedures.

Aliquots of the dried (at 40 °C for 48 h) clasts samples were crushed and ground (grain size <200 μm) using a mortar grinder mill. Rock-Eval pyrolysis was performed on a Rock-Eval 6 analyzer using a standard program^{66,67}: start isothermal with 300 °C for 3 min, then applying a heating rate of 25 °C/min up to 650 °C. Initial sample weights were between 10 and 200 mg depending on the expected S₂ yield to prevent oversaturation of the FID for highly productive samples. Hydrocarbons, released isothermally at 300 °C are presented as S₁ and between 300 and 650 °C as S₂ yields. Precision of the hydrocarbon determination was better than 5%. T_{max} values represent the maxima of the S₂ peak and correspond to the evaluation of the thermal maturity of the organic matter. For better estimation of the residual generative potential of the kerogen Rock-Eval analyses were as well performed on the extracted samples.

Organic carbon was measured with Rock-Eval 6 analyzer at APT labs. At BGR labs. organic carbon was measured with LECO CS-230 (Leco Instrumente, Germany). The samples were primarily decalcified (acidification with 10% hydrochloric acid; HCl at 80 °C) and dried (50 °C for 18 h). About 180 mg of each sample was burned in a high-frequency induction furnace in an oxygen atmosphere by use of the absorption signal at the IR detector. The instrument was calibrated using commercially available standards (LECO). Reproducibility of the measurements (organic and carbonate carbon content) was ± 0.02%.

Extraction and biomarker analysis. Analyses of mid- to high-molecular-weight hydrocarbons were performed at the BGR labs. Organic compounds were extracted from the grounded clast samples (3–10 g) 3 times using a 10–30 ml mixture of dichloromethane-methanol (DCM:MeOH, 8:2; volume:volume) for 15 min in an ultrasonic bath. All triplicate extracts were combined. The oil films from the Lusi crater mud samples (40–120 g) were extracted with 20 ml DCM by shaking for 5 min and subsequent separation of the organic phase. All extracts were dried under a nitrogen stream at 40 °C and weighed. All extracts were transferred to a chromatographic column filled with activated silica gel (240 °C for 12 h) and fractionated into an aliphatic and aromatic fraction using isohexane and DCM respectively. All fractions were dried under a nitrogen stream and weighed.

The oil-field samples were stabilised at 40 °C for 18 h and subjected to a fractionation procedure. Prior to this, asphaltenes in the oils were precipitated by adding 2 mL DCM and 60 mL petroleum ether to (at maximum) 100 mg of oil (reaction time 12 h). Subsequently, the solutions were centrifuged at 3000 rpm for 15 min. The supernatant solution containing maltenes and resins was collected and the solvent removed through evaporation in a nitrogen atmosphere at 40 °C. Parallel preparation and asphaltene precipitation of a sample of known composition (Norwegian Geochemical Standard NSO-1 oil) assured reproducibility control of the method. The residual maltenes and resins (up to 100 mg) were separated into aliphatic and aromatic fractions as well as into hetero-compounds (NSO-compounds) on silica gel (activated at 240 °C for 12 h) by mid-pressure liquid chromatography (BESTA-Technik für Chromatographie GmbH, using a sequence of organic solvents of different polarity (iso-hexane, iso-hexane/DCM (mix 2:1; v-v), DCM/MeOH (mix 2:1; v-v)).

The distribution of compounds contained in the aliphatic fractions was determined with an Agilent 7890 gas chromatograph (GC) equipped with a 50 m Ultra 1 column (Agilent; 0.2 mm inner diameter; 0.11 μm film thickness) and connected to a flame ionization detector (FID). Individual biomarkers were analysed after gas chromatographic separation (Agilent 7890) with a mass spectrometer system (MS; Agilent QQQ 7000). Measurements of aliphatic fractions were carried out as multiple-reaction-monitoring using parent-daughter-scans. The aromatic fractions were analysed in the full-scan mode (scanning from *m/z* 50 to 700). Compounds were identified by comparison of mass spectra and retention times with own and published data. Sterane and hopane biomarkers ratios were calculated from individual peak areas.

Organic petrography. The preparation of polished particulate blocks was conducted by LAOP, Tübingen, Germany following the German Standard Methods DIN22020-2:1998-08⁶⁸ and the guidelines published in Taylor *et al.*⁶⁹. Random huminite and vitrinite reflectance measurements were carried out in accordance to German National Standard DIN22020-5:2005-02⁷⁰, under non-polarized light, at magnification of 500× and room temperature of 23 °C ± 1 °C using a Leica DMRX incident-light microscope equipped with a MPV Compact 2 microphotometer photomultiplier tube (PMT), halogen lamp (12 V, 100 W), HBO[®] Lamp (103 W/2, 12 V), and Leica Oil P 50×/0.85 oil immersion objective. Leica Type F immersion oil *n_D* = 1.518 (23 °C). Up to twenty five random reflectance measurements were performed on the rock samples using Leica MPV Measure software. The filters used for analysis in fluorescence mode were Leica excitation filter BP 355–425, dichroic mirror RKP 455, and barrier filter LP 460. Photomicrographs were captured under incident white and blue light excitation using a Leica digital fluorescence camera DC 300 F at format of 1.300 × 1030 pixels and were stored using imaging software Image Access Premium 09. The maceral nomenclature applied in this paper follows ICCP System 1994, as it is adopted by the International Committee for Coal and Organic Petrology^{71–73}.

Palynological preparations. Samples preparation and analyses were carried out at the Department of Geosciences, University of Oslo. About 10 g of sediment was crushed and treated with acids to remove the

rock-mineral components according to palynological standard protocols adopted from Traverse⁷⁴. 10% HCl at room temperature to dissolve the carbonate fraction. To dissolve the silicates, the samples were treated with hot concentrated HF (65 °C) in a water bath for two days. The organic residue was washed and rinsed sieved with a 250 µm and a 15 µm mesh. Slides were mounted using epoxy resin (Entellan) as a mounting medium.

The organic residue of the highly thermally altered BS samples was treated in a series of experiments in test tubes with 3 different bleaching agents to extract and lighten recognizable palynomorphs or any other particulate present in the dark-coloured organic matter fraction. The tested bleaching reagents included: a) NaOCl solution (5%), b) concentrated nitric acid HNO₃ and c) Schulze's solution (saturated K₂ClO₃+ concentrated HNO₃). On selected samples an additional treatment with NaOCl solution (5%) was applied at 40 °C for 10 h. Among the applied bleaching methods, only the samples treated with Schulze's solution released small organic particles.

Photographs were taken with a Zeiss Imager and Zeiss digital camera at 400x magnification. The organic residues are stored at the Department of Geosciences, University of Oslo, Norway.

Mercury analysis. Mercury analyses were conducted at the University of Oxford using a Lumex RA-915 Portable Mercury Analyzer with an attached PYRO-915 pyrolyzer⁷⁵. Analytical procedures followed established in-house protocols^{60,76} and calibrated using the NIMT/UOE/FM/001 peat standard with a known Hg concentration of 169 ± 7 ppb. Between 50 to 100 mg of powdered sample was weighed before being inserted into the pyrolyzer. The samples were heated to >700 °C and left for up to 120 seconds to allow full volatilization of the Hg present. The machine was recalibrated every ten samples to negate any influence of drift in the sensor. As such, individual sample analytical errors are only ±5%, although samples with Hg concentrations <5 ppb are subject to greater errors due to background noise affecting peak integration.

Data availability

All data generated or analysed during this study are included in this published article and its Supplementary Information files.

Received: 8 October 2019; Accepted: 17 January 2020;

Published online: 04 February 2020

References

- Sherwood Lollar, B., Westgate, T. D., Ward, J. A., Slater, G. F. & Lacrampe-Couloume, G. Abiogenic formation of alkanes in the Earth's crust as a minor source for global hydrocarbon reservoirs. *Nature* **416**, 522–524, <https://doi.org/10.1038/416522a> (2002).
- Tissot, B. P. & Welte, D. H. *Petroleum Formation and Occurrence*. (Springer Berlin Heidelberg, 1984).
- Hunt, J. M. *Petroleum Geochemistry and Geology* (Freeman (2nd ed.), 1996).
- Peters, K. E., Walters, C. C. & Moldowan, J. M. *The Biomarker Guide*. (Cambridge University Press, 2005).
- Vassoevitch, N., Korchagina, Y., Lopatin, N. & Chernyshev, V. Principal phase of oil formation. *Moscow Univ. Vestnik* **6**, pps 3–27 (*In Russian*). *Engl Translation in Geol. Rev.* (1970) **12**, 1276–1296 (1969).
- Senger, K. *et al.* Effects of igneous intrusions on the petroleum system: a review. *First Break* **35**, 47–56 (2017).
- Simoneit, B. R. T. In *Hydrocarbons, Oils and Lipids: Diversity, Origin, Chemistry and Fate* (ed Heinz Wilkes) 1–35 (Springer International Publishing, 2018).
- Simoneit, B. R. T. Petroleum generation, an easy and widespread process in hydrothermal systems: an overview. *Applied Geochemistry* **5**, 3–15, [https://doi.org/10.1016/0883-2927\(90\)90031-Y](https://doi.org/10.1016/0883-2927(90)90031-Y) (1990).
- Svensen, H. *et al.* Processes controlling water and hydrocarbon composition in seeps from the Salton Sea geothermal system, California, USA. *Geology* **35**, 85–88, <https://doi.org/10.1130/g23101a.1> (2007).
- Procesi, M., Ciotoli, G., Mazzini, A. & Etiope, G. Sediment-hosted geothermal systems: Review and first global mapping. *Earth-Science Reviews* **192**, 529–544, <https://doi.org/10.1016/j.earscirev.2019.03.020> (2019).
- Fallahi, M. J., Obermann, A., Lupi, M., Karyono, K. & Mazzini, A. The Plumbing System Feeding the Lusi Eruption Revealed by Ambient Noise Tomography. *Journal of Geophysical Research: Solid Earth* **122**, 8200–8213, <https://doi.org/10.1002/2017JB014592> (2017).
- Mazzini, A., Etiope, G. & Svensen, H. A new hydrothermal scenario for the 2006 Lusi eruption, Indonesia. Insights from gas geochemistry. *Earth and Planetary Science Letters* **317–318**, 305–318, <https://doi.org/10.1016/j.epsl.2011.11.016> (2012).
- Malvoisin, B., Mazzini, A. & Miller, S. A. Deep hydrothermal activity driving the Lusi mud eruption. *Earth and Planetary Science Letters* **497**, 42–49, <https://doi.org/10.1016/j.epsl.2018.06.006> (2018).
- Inguaggiato, S., Mazzini, A., Vita, F. & Sciarra, A. The Arjuno-Welirang volcanic complex and the connected Lusi system: Geochemical evidences. *Marine and Petroleum Geology* **90**, 67–76, <https://doi.org/10.1016/j.marpetgeo.2017.10.015> (2018).
- Mazzini, A., Scholz, F., Svensen, H. H., Hensen, C. & Hadi, S. The geochemistry and origin of the hydrothermal water erupted at Lusi, Indonesia. *Marine and Petroleum Geology* **90**, 52–66, <https://doi.org/10.1016/j.marpetgeo.2017.06.018> (2018).
- Zaputlyaeva, A., Mazzini, A., Caracausi, A. & Sciarra, A. Mantle-derived fluids in the East Java sedimentary basin, Indonesia. *Journal of Geophysical Research: Solid Earth* **124**, 7962–7977, <https://doi.org/10.1029/2018JB017274> (2019).
- Samankassou, E. *et al.* Origin and age of carbonate clasts from the Lusi eruption, Java, Indonesia. *Marine and Petroleum Geology* **90**, 138–148, <https://doi.org/10.1016/j.marpetgeo.2017.11.012> (2018).
- Hall, R. *The palaeogeography of Sundaland and Wallacea since the Late Jurassic*. Vol. 72 (2013).
- Smyth, H. R., Hall, R. & Nichols, G. J. In *Formation and Applications of the Sedimentary Record in Arc Collision Zones* (eds Amy E. Draut, Peter D. Clift, & David W. Scholl) (Geological Society of America, 2008).
- Mazzini, A. *et al.* Triggering and dynamic evolution of the LUSI mud volcano, Indonesia. *Earth and Planetary Science Letters* **261**, 375–388, <https://doi.org/10.1016/j.epsl.2007.07.001> (2007).
- Moscariello, A. *et al.* Genesis and evolution of the Watukosek fault system in the Lusi area (East Java). *Marine and Petroleum Geology* **90**, 125–137, <https://doi.org/10.1016/j.marpetgeo.2017.09.032> (2018).
- Satyana, A. H. & Purwaningsih, M. E. M. Geochemistry of the East Java Basin: new observations on oil grouping, genetic gas types and trends of hydrocarbon habitats. *Proceedings of the 29th IAGI Annual Convention and Exhibition* (2003).
- Doust, H. & Noble, R. A. Petroleum systems of Indonesia. *Marine and Petroleum Geology* **25**, 103–129, <https://doi.org/10.1016/j.marpetgeo.2007.05.007> (2008).
- Satyana, A. H. & Purwaningsih, M. E. M. Oligo-Miocene carbonates of Java: tectonic setting and effects of volcanism. *Proceedings of the 32nd IAGI and 28th HAGI Annual Convention and Exhibition* (2003).

25. Devi, E. A., Rachman, F., Satyana, A. H., Fahrudin & Setyawan, R. Paleofacies of Eocene Lower Ngimbang Source Rocks in Cepu Area, East Java Basin based on Biomarkers and Carbon-13 Isotopes. *IOP Conference Series: Earth and Environmental Science* **118**, <https://doi.org/10.1088/1755-1315/118/1/012009> (2018).
26. Kusumastuti, A., Darmoyo, A. B., Suwarlan, W. & Sosromihardjo, S. P. C. The Wunut field: Pleistocene volcanoclastic gas sands in East Java. *Proceedings, Indonesian Petroleum Association, Twenty Seventh Annual Convention & Exhibition, October 1999* (1999).
27. Moldovan, J. M. *et al.* The Molecular Fossil Record of Oleanane and Its Relation to Angiosperms. *Science* **265**, 768, <https://doi.org/10.1126/science.265.5173.768> (1994).
28. Radke, M., Welte, D. H. & Willsch, H. Geochemical study on a well in the Western Canada Basin: relation of the aromatic distribution pattern to maturity of organic matter. *Geochimica et Cosmochimica Acta* **46**, 1–10, [https://doi.org/10.1016/0016-7037\(82\)90285-X](https://doi.org/10.1016/0016-7037(82)90285-X) (1982).
29. Radke, M., Willsch, H., Leythaeuser, D. & Teichmüller, M. Aromatic components of coal: relation of distribution pattern to rank. *Geochimica et Cosmochimica Acta* **46**, 1831–1848, [https://doi.org/10.1016/0016-7037\(82\)90122-3](https://doi.org/10.1016/0016-7037(82)90122-3) (1982).
30. Morley, R. J. Tertiary stratigraphic palynology in South-East Asia; current status and new directions. *Bulletin Of The Geological Society Of Malaysia* **28**, 1–36 (1991).
31. Lelono, E. B. & Morley, R. J. Oligocene palynological succession from the East Java Sea. *Geological Society, London, Special Publications* **355**, 333–345, <https://doi.org/10.1144/sp355.17> (2011).
32. Besems, R. E. Dinoflagellate cyst biostratigraphy of Tertiary and Quaternary deposits of offshore NW Borneo. *Bulletin of the Geological Society of Malaysia* **33**, 65–93 (1993).
33. Batten, D. In *Palynology: principles and applications* Vol. 3 (eds J. Jansonius & D.C. McGregor) 1065–1084 (American Association of Stratigraphic Palynologists Foundation, 1996).
34. Yulianto, E., Martodjojo, S. & Zaim, Y. In *An Outline of the Geology of Indonesia. Ikatan Ahli Geologi, Indonesia* Vol. 192 (ed D. & Hasan Herman, S.) 45–68 (Ikatan Ahli Geologi, Indonesia, 2000).
35. Zonneveld, K. A. F. *et al.* Geographic distribution of dinoflagellate cysts in surface sediments, <https://doi.org/10.1594/PANGAEA.818280> (2013).
36. Outridge, P. M., Sanei, H., Stern, G. A., Hamilton, P. B. & Goodarzi, F. Evidence for Control of Mercury Accumulation Rates in Canadian High Arctic Lake Sediments by Variations of Aquatic Primary Productivity. *Environmental Science & Technology* **41**, 5259–5265, <https://doi.org/10.1021/es070408x> (2007).
37. Sanei, H., Grasby, S. E. & Beauchamp, B. Latest permian mercury anomalies. *Geology* **40**, 63–66, <https://doi.org/10.1130/G32596.1> (2012).
38. Eigenbrode, J. L., Freeman, K. H. & Summons, R. E. Methylhopane biomarker hydrocarbons in Hamersley Province sediments provide evidence for Neoproterozoic aerobicity. *Earth and Planetary Science Letters* **273**, 323–331, <https://doi.org/10.1016/j.epsl.2008.06.037> (2008).
39. Summons, R. E., Jahnke, L. L., Hope, J. M. & Logan, G. A. 2-Methylhopanoids as biomarkers for cyanobacterial oxygenic photosynthesis. *Nature* **400**, 554–557, <https://doi.org/10.1038/23005> (1999).
40. Hughes, W. B., Holba, A. G. & Dzou, L. I. P. The ratios of dibenzothiophene to phenanthrene and pristane to phytane as indicators of depositional environment and lithology of petroleum source rocks. *Geochimica et Cosmochimica Acta* **59**, 3581–3598, [https://doi.org/10.1016/0016-7037\(95\)00225-O](https://doi.org/10.1016/0016-7037(95)00225-O) (1995).
41. Jarvie, D. M., Claxton, B. L., Henk, F. & Breyer, J. T. In *AAPG National Convention* Vol. 85 A100 (AAPG Bull., Denver, CO, 2001).
42. Burnham, A. K. & Sweeney, J. J. A chemical kinetic model of vitrinite maturation and reflectance. *Geochimica et Cosmochimica Acta* **53**, 2649–2657, [https://doi.org/10.1016/0016-7037\(89\)90136-1](https://doi.org/10.1016/0016-7037(89)90136-1) (1989).
43. Chandra, D. & Taylor, G. H. In *Stach's textbook of coal petrology*. Stuttgart (eds E. Stach *et al.*) 206–218 (Gebrüder Borntraeger, 1982).
44. Stewart, A. K., Massey, M., Padgett, P. L., Rimmer, S. M. & Hower, J. C. Influence of a basic intrusion on the vitrinite reflectance and chemistry of the Springfield (No. 5) coal, Harrisburg, Illinois. *International Journal of Coal Geology* **63**, 58–67, <https://doi.org/10.1016/j.coal.2005.02.005> (2005).
45. Goodarzi, F., Gentzis, T., Grasby, S. E. & Dewing, K. Influence of igneous intrusions on thermal maturity and optical texture: Comparison between a bituminous marl and a coal seam of the same maturity. *International Journal of Coal Geology* **198**, 183–197, <https://doi.org/10.1016/j.coal.2018.09.013> (2018).
46. R. W. Jones, T. A. E. In *Low temperature metamorphism of kerogen and clay minerals* (ed D. F. Oltz) 1–12 (Society of Economic Paleontologists and Mineralogists Special Symposium, Los Angeles, California, 1978).
47. Raymond, A. C. & Murchison, D. G. Effect of igneous activity on molecular-maturation indices in different types of organic matter. *Organic Geochemistry* **18**, 725–735, [https://doi.org/10.1016/0146-6380\(92\)90098-1](https://doi.org/10.1016/0146-6380(92)90098-1) (1992).
48. Bishop, A. N. & Abbott, G. D. Vitrinite reflectance and molecular geochemistry of Jurassic sediments: the influence of heating by Tertiary dykes (northwest Scotland). *Organic Geochemistry* **22**, 165–177, [https://doi.org/10.1016/0146-6380\(95\)90015-2](https://doi.org/10.1016/0146-6380(95)90015-2) (1995).
49. Mißbach, H., Duda, J. P., Lünsdorf, N. K., Schmidt, B. C. & Thiel, V. Testing the preservation of biomarkers during experimental maturation of an immature kerogen. *International Journal of Astrobiology* **15**, 165–175, <https://doi.org/10.1017/S1473550416000069> (2016).
50. Hubred, J. H. *Thermal Effects of Basaltic Sill Emplacement in Source Rocks on Maturation and Hydrocarbon Generation*, University of Oslo (2006).
51. Spacapan, J. B. *et al.* Thermal impact of igneous sill-complexes on organic-rich formations and implications for petroleum systems: A case study in the northern Neuquén Basin, Argentina. *Marine and Petroleum Geology* **91**, 519–531, <https://doi.org/10.1016/j.marpetgeo.2018.01.018> (2018).
52. Rahman, M. W. & Rimmer, S. M. Effects of rapid thermal alteration on coal: Geochemical and petrographic signatures in the Springfield (No. 5) Coal, Illinois Basin. *International Journal of Coal Geology* **131**, 214–226, <https://doi.org/10.1016/j.coal.2014.06.020> (2014).
53. Quaderer, A. *et al.* Dike-induced thermal alteration of the Springfield Coal Member (Pennsylvanian) and adjacent clastic rocks, Illinois Basin, USA. *International Journal of Coal Geology* **166**, 108–117, <https://doi.org/10.1016/j.coal.2016.07.005> (2016).
54. Raymond, A. C. & Murchison, D. G. Development of organic maturation in the thermal aureoles of sills and its relation to sediment compaction. *Fuel* **67**, 1599–1608, [https://doi.org/10.1016/0016-2361\(88\)90202-5](https://doi.org/10.1016/0016-2361(88)90202-5) (1988).
55. Aarnes, I., Svensen, H., Polteau, S. & Planke, S. Contact metamorphic devolatilization of shales in the Karoo Basin, South Africa, and the effects of multiple sill intrusions. *Chemical Geology* **281**, 181–194, <https://doi.org/10.1016/j.chemgeo.2010.12.007> (2011).
56. Prinzhofer, A. A. & Huc, A. Y. Genetic and post-genetic molecular and isotopic fractionations in natural gases. *Chemical Geology* **126**, 281–290, [https://doi.org/10.1016/0009-2541\(95\)00123-9](https://doi.org/10.1016/0009-2541(95)00123-9) (1995).
57. Schenk, H. J., Di Primio, R. & Horsfield, B. The conversion of oil into gas in petroleum reservoirs. Part 1: Comparative kinetic investigation of gas generation from crude oils of lacustrine, marine and fluviodeltaic origin by programmed-temperature closed-system pyrolysis. *Organic Geochemistry* **26**, 467–481, [https://doi.org/10.1016/S0146-6380\(97\)00024-7](https://doi.org/10.1016/S0146-6380(97)00024-7) (1997).
58. Tegelaar, E. W. & Noble, R. A. Kinetics of hydrocarbon generation as a function of the molecular structure of kerogen as revealed by pyrolysis-gas chromatography. *Organic Geochemistry* **22**, 543–574, [https://doi.org/10.1016/0146-6380\(94\)90125-2](https://doi.org/10.1016/0146-6380(94)90125-2) (1994).
59. Percival, L. M. E. *et al.* Globally enhanced mercury deposition during the end-Pliensbachian extinction and Toarcian OAE: A link to the Karoo–Ferrars Large Igneous Province. *Earth and Planetary Science Letters* **428**, 267–280, <https://doi.org/10.1016/j.epsl.2015.06.064> (2015).

60. Jones, M. T. *et al.* Mercury anomalies across the Palaeocene–Eocene Thermal Maximum. *Clim. Past* **15**, 217–236, <https://doi.org/10.5194/cp-15-217-2019> (2019).
61. Guo, S. *et al.* Mercury release characteristics during pyrolysis of eight bituminous coals. *Fuel* **222**, 250–257, <https://doi.org/10.1016/j.fuel.2018.02.134> (2018).
62. Radke, M. & Welte, D. H. The Methylphenanthrene Index (MPI): A Maturity Parameter Based on Aromatic Hydrocarbons. *Advances in Organic Geochemistry*, 504–512 (1983).
63. Istadi, B. P., Pramono, G. H., Sumintadireja, P. & Alam, S. Modeling study of growth and potential geohazard for LUSI mud volcano: East Java, Indonesia. *Marine and Petroleum Geology* **26**, 1724–1739, <https://doi.org/10.1016/j.marpetgeo.2009.03.006> (2009).
64. Kusumastuti, A., Van Rensbergen, P. & Warren, J. K. Seismic Sequence Analysis and Reservoir Potential of Drowned Miocene Carbonate Platforms in the Madura Strait, East Java, Indonesia. *AAPG Bulletin* **86**, 213–232, <https://doi.org/10.1306/61eeda94-173e-11d7-8645000102c1865d> (2002).
65. Mazzini, A. *et al.* Strike-slip faulting as a trigger mechanism for overpressure release through piercement structures. Implications for the Lusi mud volcano, Indonesia. *Marine and Petroleum Geology* **26**, 1751–1765, <https://doi.org/10.1016/j.marpetgeo.2009.03.001> (2009).
66. Espitalié, J. *et al.* Méthode rapide de caractérisation des roches mères, de leur potentiel pétrolier et de leur degré d'évolution. *Rev. Inst. Fr. Pét.* **32**, 23–42 (1977).
67. Lafargue, E., Marquis, F. & Pillot, D. Rock-Eval 6 Applications in Hydrocarbon Exploration, Production, and Soil Contamination Studies. *Rev. Inst. Fr. Pét.* **53**, 421–437 (1998).
68. DIN22020-2:1998-08. in *Investigations of raw material in hard-coal-mining - Microscopical examination of hard coal, coke and briquettes - Part 2: Preparation of polished surface from lump material and particulate blocks.*
69. Taylor, G. H. *et al.* *Organic Petrology*. (Gebrüder Borntraeger, Berlin-Stuttgart, 1998).
70. DIN22020-5:2005-02. in *Investigations of the raw material in hard-coal-mining - Microscopical examinations of hard coal, coke and briquettes - Part 5: Reflectance measurements on vitrinites.*
71. Pickel, W. *et al.* Classification of liptinite – ICCP System 1994. *International Journal of Coal Geology* **169**, 40–61, <https://doi.org/10.1016/j.coal.2016.11.004> (2017).
72. Šykorová, I. *et al.* Classification of huminite—ICCP System 1994. *International Journal of Coal Geology* **62**, 85–106, <https://doi.org/10.1016/j.coal.2004.06.006> (2005).
73. The new inertinite classification (ICCP System 1994). *Fuel* **80**, 459–471, [https://doi.org/10.1016/S0016-2361\(00\)00102-2](https://doi.org/10.1016/S0016-2361(00)00102-2) (2001).
74. Traverse, A. *Paleopalynology*. Vol. 28 (Springer Netherlands, 2007).
75. Bin, C., Xiaoru, W. & Lee, F. S. C. Pyrolysis coupled with atomic absorption spectrometry for the determination of mercury in Chinese medicinal materials. *Analytica Chimica Acta* **447**, 161–169, [https://doi.org/10.1016/S0003-2670\(01\)01218-1](https://doi.org/10.1016/S0003-2670(01)01218-1) (2001).
76. Percival, L. M. E. *et al.* Mercury evidence for pulsed volcanism during the end-Triassic mass extinction. *Proceedings of the National Academy of Sciences* **114**, 7929, <https://doi.org/10.1073/pnas.1705378114> (2017).

Acknowledgements

The work was funded by the European Research Council under the European Union's Seventh Framework Programme Grant agreement n° 308126 (LUSI LAB project, PI A. Mazzini). We acknowledge the support from the Research Council of Norway through its Centres of Excellence funding scheme, Project Number 223272 (CEED). The Authors would like to thank the management of Lapindo Brantas Indonesia for providing access to the subsurface data and for the authorisation to publish the results of this study. BPLS is thanked for their support during the field operations. Morgan T. Jones is also supported by the Research Council of Norway Unge Forskeralenter project 'Ashlantic', project number 263000. Tamsin Mather (University of Oxford) and Monika Weiß (BGR) are thanked for their help and assistance.

Author contributions

A.Z. and A.M. performed the sampling and organized the field expeditions and coordination and designed the structure of the manuscript. M.B., G.S. and A.Z. performed organic geochemistry analyses. W.K., J.F. and A.Z. performed palynological analyses. J.K. performed vitrinite reflectance measurements. M.T.J. performed mercury content measurement. All authors contributed to the data interpretation, manuscript writing and revision.

Competing interests

The authors declare no competing interests.

Additional information

Supplementary information is available for this paper at <https://doi.org/10.1038/s41598-020-58567-6>.

Correspondence and requests for materials should be addressed to A.Z.

Reprints and permissions information is available at www.nature.com/reprints.

Publisher's note Springer Nature remains neutral with regard to jurisdictional claims in published maps and institutional affiliations.



Open Access This article is licensed under a Creative Commons Attribution 4.0 International License, which permits use, sharing, adaptation, distribution and reproduction in any medium or format, as long as you give appropriate credit to the original author(s) and the source, provide a link to the Creative Commons license, and indicate if changes were made. The images or other third party material in this article are included in the article's Creative Commons license, unless indicated otherwise in a credit line to the material. If material is not included in the article's Creative Commons license and your intended use is not permitted by statutory regulation or exceeds the permitted use, you will need to obtain permission directly from the copyright holder. To view a copy of this license, visit <http://creativecommons.org/licenses/by/4.0/>.

© The Author(s) 2020

Supplementary Material for the paper:

“Recent magmatism drives hydrocarbon generation in north-east Java, Indonesia”.

Alexandra Zaputlyaeva (1), Adriano Mazzini (1), Martin Blumenberg (2), Georg Scheeder (2),
Wolfram Michael Kürschner (3), Jolanta Kus (2), Morgan Thomas Jones (1), Joost Frieling (4)

- (1) Centre for Earth Evolution and Dynamics (CEED), University of Oslo, Norway
- (2) Federal Institute for Geosciences and Natural Resources (BGR), Hannover, Germany
- (3) Department of Geosciences, University of Oslo, Norway
- (4) Department of Earth Sciences, Utrecht University, Netherlands

Supplementary Table S1. Main biomarker parameters, methylphenanthrene index (MPI-1=1.5*(2-MP+3-MP)/(P+1-MP+9-MP) and methylphenanthrene ratio (MPR=2-MP/1-MP), and dibenzothiophene/phenanthrene ratio (DBT/Phen) of the studied bitumen extracts of the grey shale (GS), black shale (BS), and oil (O) samples. Oil was sampled from the Lusi crater and as well from Wunut and Tanggulangin oil fields, located close to the Lusi.

Sample ID	Sample type	Sampling location	Dia/Dia+Reg C ₂₇	20S/20S+20R dia C ₂₇	moretanes/hopanes	Ts/Ts+Tm	homohopane index	C ₃₂ hopane (22S/22S+22R)	C ₂₉ 20S(20S+20R)	C ₂₉ β/(β+αα)	CPI	Pi/Ph	Oil(O+Hop)	2-M/2-M+Hopan.	3-M/3-M+Hopan.	MPI-1	MPR	DBT/Phen
JV17-01-39	GS	Lusi crater	0.02	0.47	0.17	0.25	-	0.31	0.02	0.10	1.61	2.46	0.32	0.025	0.026	0.56	1.17	0.12
JV17-01-40	GS	Lusi crater	0.01	0.41	0.27	0.10	-	0.31	0.01	0.16	1.43	0.50	0.47	0.026	0.023	0.41	1.06	0.10
JV16-29-01	BS	Lusi crater	0.40	0.58	0.05	0.59	3.33	0.56	0.45	0.50	1.02	3.55	0.17	0.051	0.034	0.79	1.39	0.59
JV16-29-04	BS	Lusi crater	0.40	0.59	0.06	0.57	3.13	0.56	0.45	0.51	1.02	2.94	0.20	0.053	0.039	0.65	1.22	0.80
JV17-01-01	BS	Lusi crater	0.39	0.58	0.05	0.61	2.19	0.57	0.45	0.50	1.04	3.69	0.23	0.052	0.034	0.63	1.03	0.47
JV17-01-10	BS	Lusi crater	0.36	0.60	0.06	0.59	2.98	0.57	0.42	0.50	1.02	2.56	0.20	0.060	0.034	0.79	1.57	0.55
JV17-01-15	BS	Lusi crater	0.37	0.57	0.05	0.58	3.44	0.58	0.41	0.48	1.03	3.12	0.16	0.054	0.033	0.90	1.33	0.80
JV17-01-37	BS	Lusi crater	0.41	0.61	0.05	0.59	3.19	0.56	0.44	0.51	1.03	3.48	0.17	0.053	0.035	0.80	1.49	0.72
JV17-40	O	Wunut f.	0.44	0.62	0.05	0.62	3.63	0.56	0.50	0.54	1.03	4.13	0.18	0.058	0.031	0.73	1.22	0.31
JV17-47	O	Tang f.	0.46	0.62	0.05	0.62	3.39	0.57	0.51	0.55	1.00	4.26	0.17	0.057	0.033	0.76	1.22	0.55
JV17-48	O	Tang. f.	0.45	0.60	0.05	0.64	3.62	0.58	0.51	0.55	0.94	4.34	0.20	0.056	0.031	0.78	1.19	0.45
JV17-50	O	Wunut f.	0.49	0.60	0.05	0.66	3.47	0.57	0.53	0.56	1.06	4.31	0.24	0.059	0.031	0.82	1.22	0.48
JV15-A	O	Lusi crater	0.30	0.60	0.07	0.56	2.96	0.60	0.29	0.40	1.02	3.93	0.20	0.054	0.030	-	-	-
JV15-B	O	Lusi crater	0.30	0.57	0.07	0.56	3.18	0.58	0.28	0.41	1.02	3.93	0.19	0.057	0.034	-	-	-
JV17-A	O	Lusi crater	0.25	0.56	0.07	0.56	3.10	0.55	0.20	0.29	1.03	2.58	0.18	0.054	0.031	0.62	1.18	0.38
JV17-B	O	Lusi crater	0.24	0.58	0.08	0.56	3.11	0.54	0.19	0.27	1.03	2.92	0.18	0.053	0.033	0.55	1.18	0.54

Supplementary Table S2 Results of the palynological analyses of the rock clasts. Highly thermally-altered samples were bleached using NaOCl solution (5%), concentrated nitric acid (HNO₃), and Schulze's solution (saturated K₂ClO₃ + concentrated HNO₃). Original – preparations without bleaching procedure; bl. – bleached; TOC – Total Organic Carbon; TAS – Thermally Alteration Scale, developed by Batten³³; VR – Vitrinite Reflectance; AOM – Amorphous organic matter. Yellow, orange and grey colours highlight presence of 3 sample groups with various maturation, based on the spore and pollen colours.

Sample ID	Preparation type	Lithology	TOC, wt. %	Palynofacies	TAS (according to Batten, 1996)	Palynology	Stratigraphic age
JV14B-11-01	original	light grey shale	0.34	light brown plant debris (plenty cuticle and vitrinite), light brown AOM	1-2 (<50 °C) VR 0.2-0.3 %	<i>Lingulodinium machaerophorum</i> , <i>Tasmanites</i> , smooth walled spores, diverse angiosperm pollen, mangrove palm pollen (<i>Nyssa</i>)	Pleistocene?
JV14B-11-02	original	grey shale	0.35	light brown - brown plant debris (plenty cuticle and vitrinite), light brown AOM	1-2 (<50 °C) VR 0.2-0.3 %	no	no age assignment possible
	bl. Schulze's S.			light brown - light brownish plant debris (plenty cuticle and vitrinite), light brown AOM			
JV14B-11-11	original	grey shale	1.99	light brown plant debris (plenty cuticle and vitrinite), light brown AOM	1-2 (<50 °C) VR 0.2-0.3 %	no	no age assignment possible
JV17-01-39	original	grey marl, immature,	0.83		1-2 (<50 °C) VR 0.2-0.3 %		
JV17-01-40	original	grey marl, immature,	0.95	light brown plant debris (cuticle, vitrinite), foraminiferal linings, AOM	1-2 (<50 °C) VR 0.2-0.3 %	<i>Spiniferites</i> , <i>Lingulodinium</i> , <i>Selenopemphix armata</i> ?, <i>Diphyes</i> (or <i>Dapsilitidium</i> ?)	Late Pliocene-Pleistocene
JV14B-02-02	original	dark grey shale	0.5	light brown plant debris (plenty cuticle and vitrinite), light brown AOM	6 (170-180 °C) VR 1.5-2%	<i>Lingulodinium machaerophorum</i> , <i>Operculodinium centrocarpum</i> and <i>O. piaseckii</i> , <i>Polykrikos schwartzii</i> (or <i>kofoidii</i>), <i>Spiniferites</i> , <i>Stelladinium</i> (<i>Lejeunecesta</i>), spores, <i>Ruella</i> type pollen?	Middle - Late Miocene

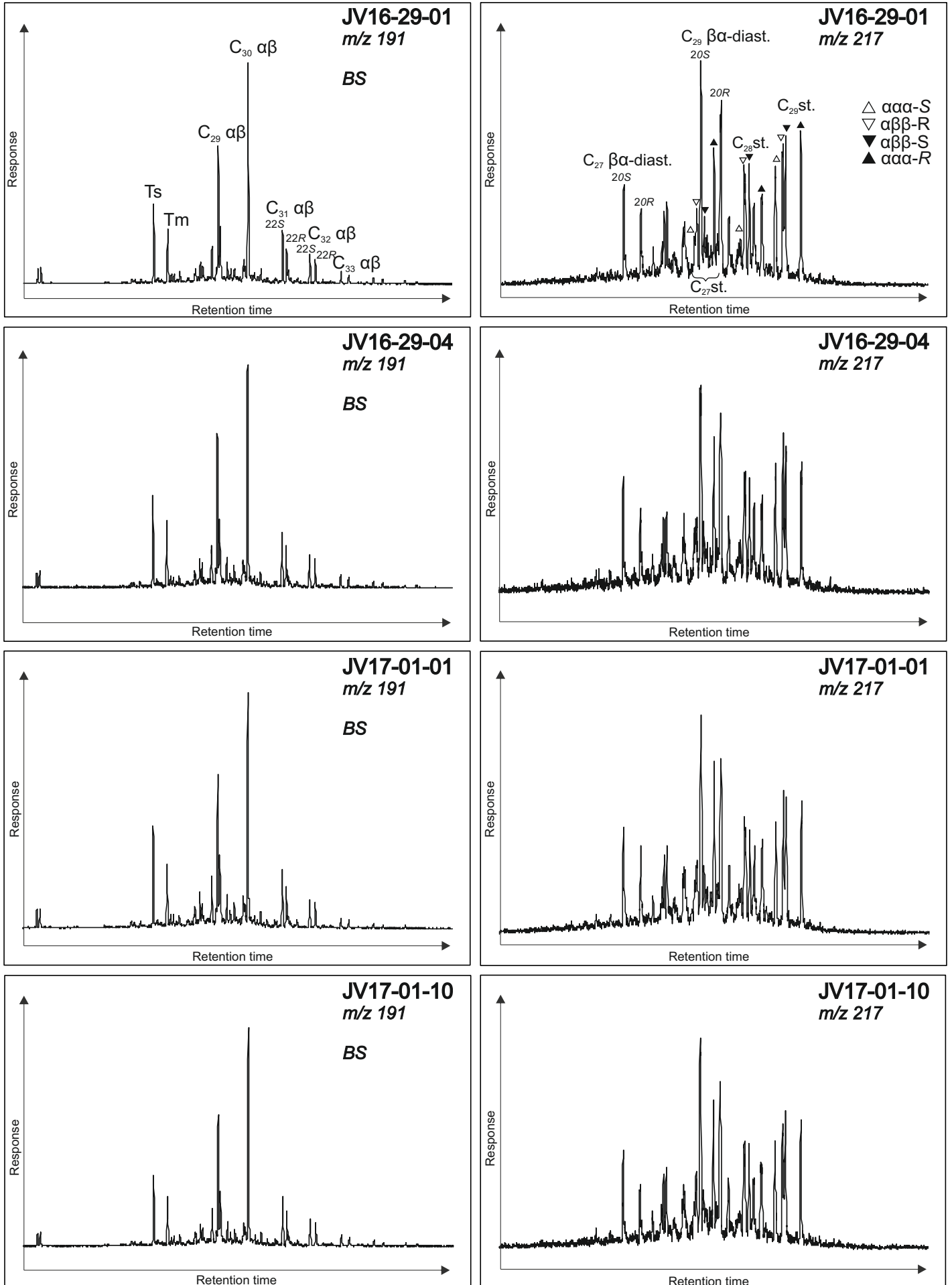
JV15-06-08	original	dark grey shale	1.27	dark brownish to black plant debris (vitrinite, cuticles), degraded dark AOM	6 (170-180 °C) VR 1.5-2%	lacking identifiable palynomorphs	Pleistocene or Miocene
	bl. Schulze's S.			<i>Spiniferites bentorii</i>			
JV17-01-02	original	grey breccia with volcanoclastics	0.48	dark brownish to black plant debris (vitrinite, cuticles)	5-6 (150-180 °C) VR 1.5-2%	no age assignment possible	
JV17-01-08	original	grey shale	0.82	dark brownish AOM, plant debris, foraminiferal linings	5-6 (150-180 °C) VR 1.5-2%	<i>Spiniferites, Operculodinium, Palambages?</i> , striate angiosperm pollen	Miocene?
JV17-01-34	original	grey shale	0.55	dark brownish to black plant debris (vitrinite, cuticles)	5-6 (150-180 °C) VR 1.5-2%	no	no age assignment possible
JV15-06-04	original	coal with leaf imprints	66.4	dark brownish and black AOM, droplets of resin	7 (>250 °C) VR 4%	lacking identifiable palynomorphs	no age assignment possible
	bl. Schulze's S.			dark brownish and black AOM, droplets of resin			
JV15-06-05	original	black shale	1.59	dark brownish to black plant debris (vitrinite, cuticles), degraded dark AOM	7 (>250 °C) VR 4%	lacking identifiable palynomorphs	no age assignment possible
	bl. Schulze's S.			dark brownish to black plant debris, dominating vitrinite			
JV16-29-01	original	black shale	9.21	black opaque plant debris, degraded dark grey AOM	7 (>250 °C) VR 4%	lacking identifiable palynomorphs	no age assignment possible
	bleached NaOCl			no visual difference from the original			
	bl. NaOCl+temp			yellow AOM, plant debris, vitrinite			
	bl. HNO3			black opaque or dark brownish plant debris (vitrinite, cuticle)			
JV16-29-04	bl. Schulze's S.	black shale	14.6	no visual difference from the original	7 (>250 °C) VR 4%	lacking identifiable palynomorphs	no age assignment possible
	original			no visual difference from the original			
	bleached NaOCl			brown plant debris (vitrinite, cuticle) <i>Botryococcus</i>			
	bl. NaOCl+temp			angiosperm pollen, spores			

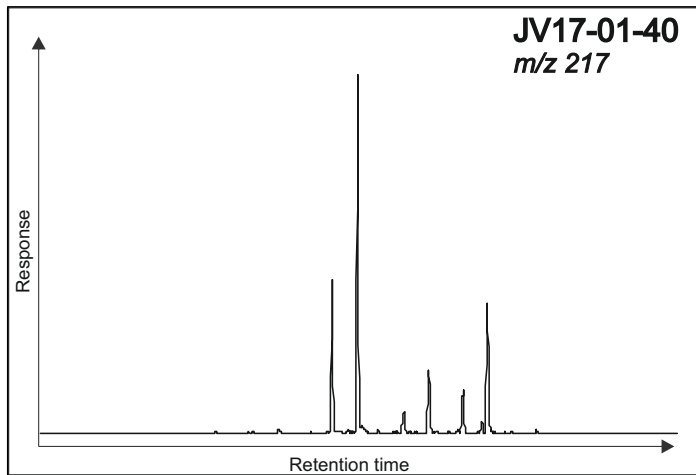
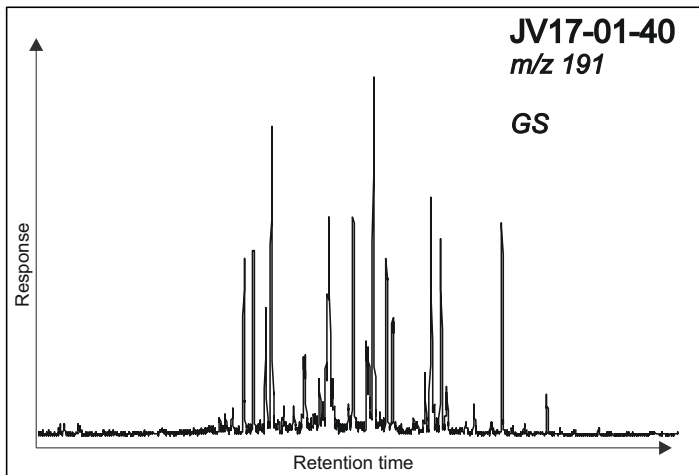
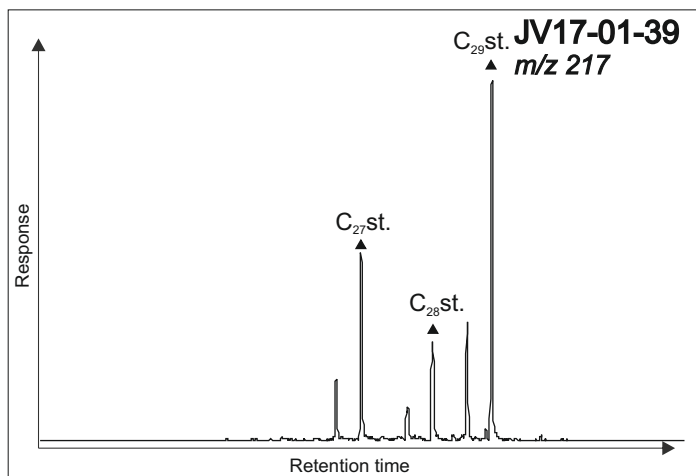
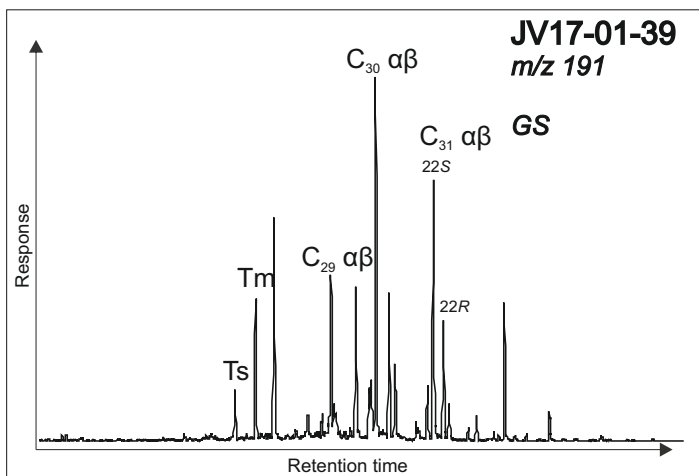
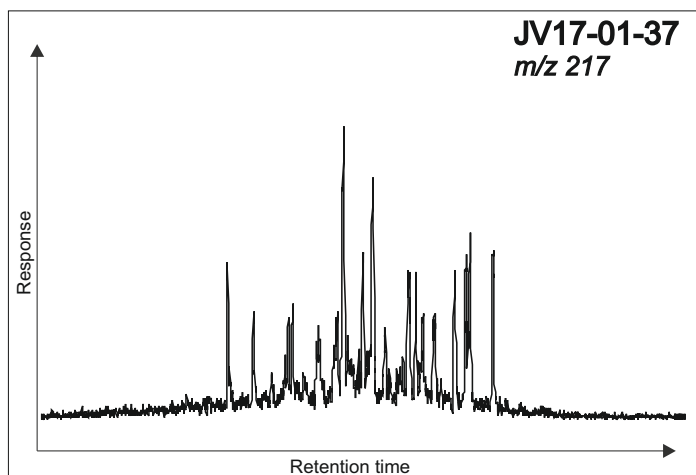
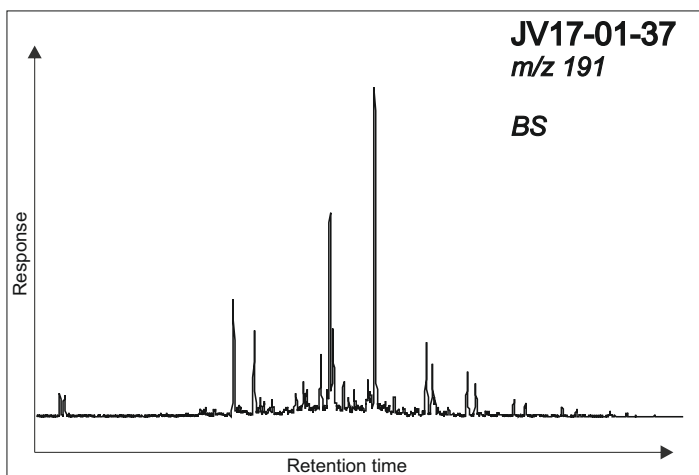
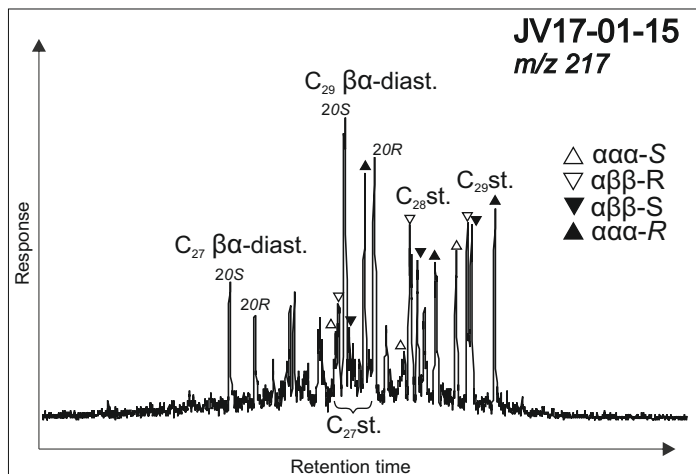
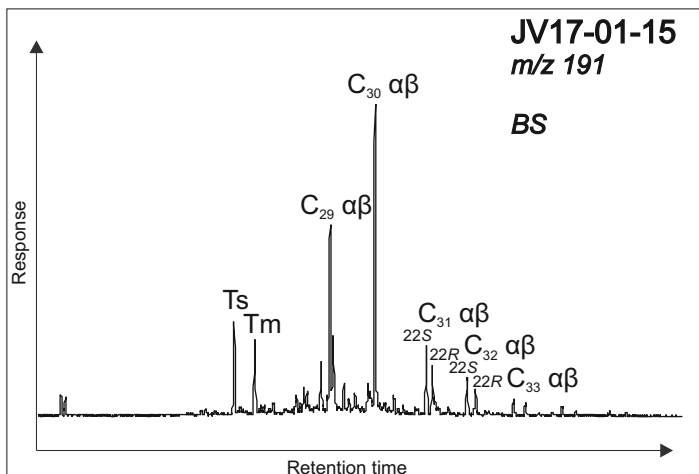
JV17-01-01	original	dark grey shale	2.6	dark brown plant debris (vitrinite, cuticles), no AOM light brown plant debris, mainly vitrinite and cuticles, no AOM	5-6 (150-180 °C) VR 1.5-2%	spores (smooth, spinous, faveolate)	no age assignment possible
	bl. Schulze's S.						
JV17-01-10	original	black shale	6.94	black plant debris (vitrinite, cuticle) and degraded AOM black plant debris (vitrinite, cuticle) and degraded AOM	7 (>250 °C) VR 4%	lacking identifiable palynomorphs	no age assignment possible
	bl. Schulze's S.						
JV17-01-15	original	black shale	8.61	dark brownish, black opaque plant debris (vitrinite) and AOM	7 (>250 °C) VR 4%	lacking identifiable palynomorphs	no age assignment possible
	bl. NaOCl						
	bl. NaOCl+temp						
	bl. HNO3						
bl. Schulze's S.	no visual difference from the original	dark brownish to black plant debris (vitrinite, cuticles), <i>Botryococcus</i>	algae remains?, mangrove palm pollen (<i>Nypa</i>),				
JV17-01-37	original	black shale	4.76	dark brownish to black plant debris (vitrinite, cuticles) dark brownish to black plant debris (vitrinite, cuticles)	7 (>250 °C) VR 4%	lacking identifiable palynomorphs	no age assignment possible
	bl. Schulze's S.						
JV15-06-04	original	coal with leaf imprints	66.4	dark brownish and black AOM, droplets of resin dark brownish and black AOM, droplets of resin	7 (>250 °C) VR 4%	lacking identifiable palynomorphs	no age assignment possible
	bl. Schulze's S.						
JV15-06-05	original	black shale	1.59	dark brownish to black plant debris (vitrinite, cuticles), degraded dark AOM dark brownish to black plant debris, dominating vitrinite	7 (>250 °C) VR 4%	lacking identifiable palynomorphs	no age assignment possible
	bl. Schulze's S.						

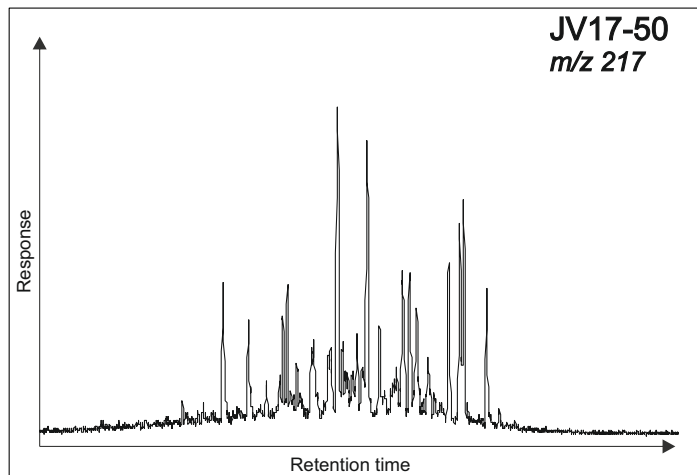
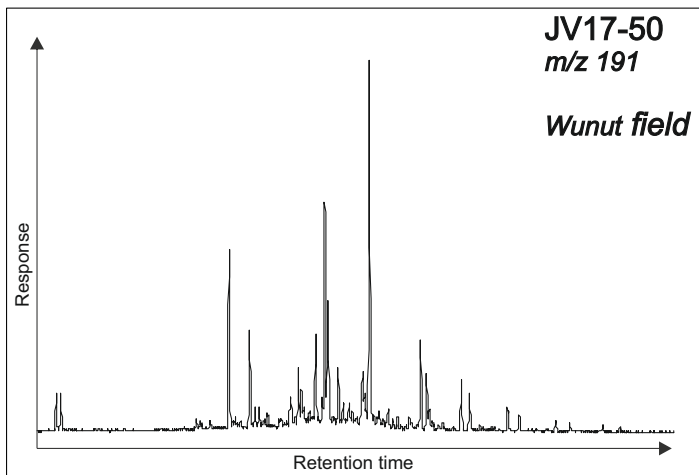
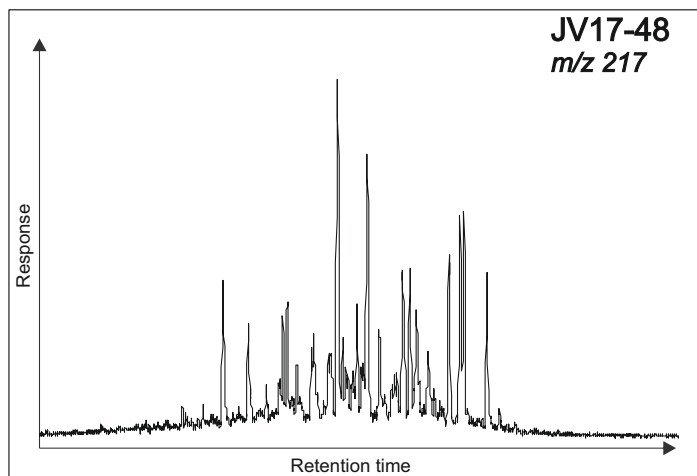
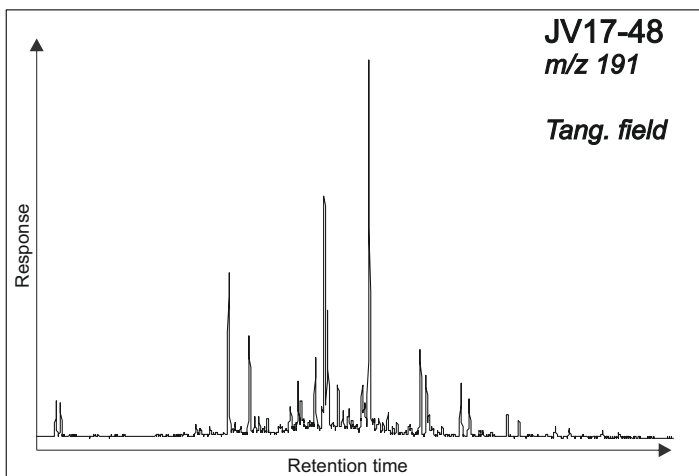
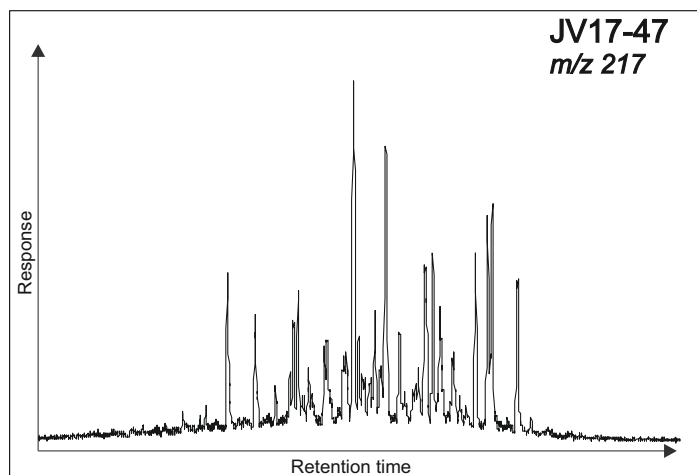
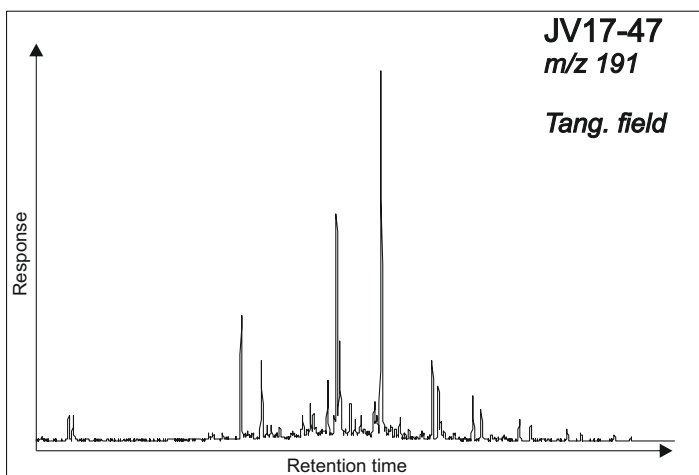
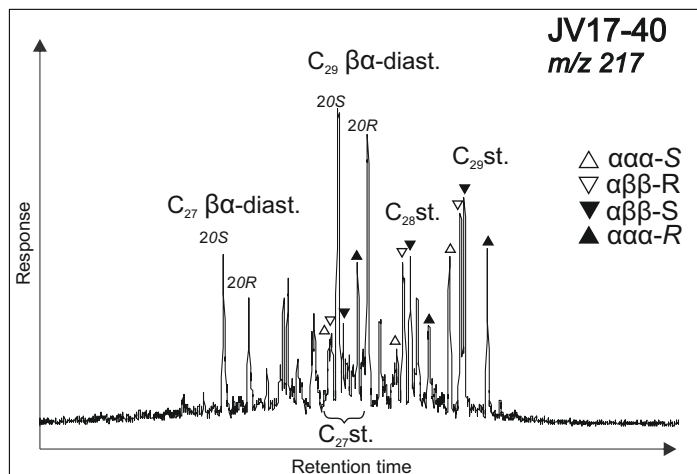
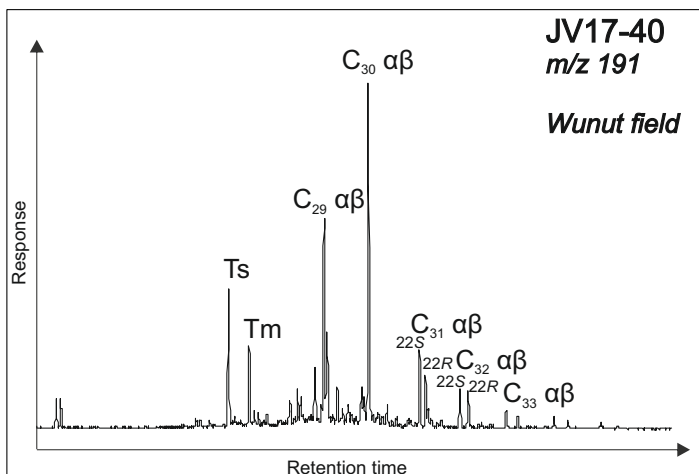
Supplementary Table S3. Results of the pyrolysis analysis, using Rock-Eval method, organic carbon content (C_{org}), measured by LECO, vitrinite reflectance (R_o), bitumen extraction yield, and mercury content (Hg). Analyses using Rock-Eval and Leco instruments were performed twice: before and after extraction. BS- black shale, GC-grey shale. Suggested age assignment is based on combined palynostratigraphical and geochemical methods.

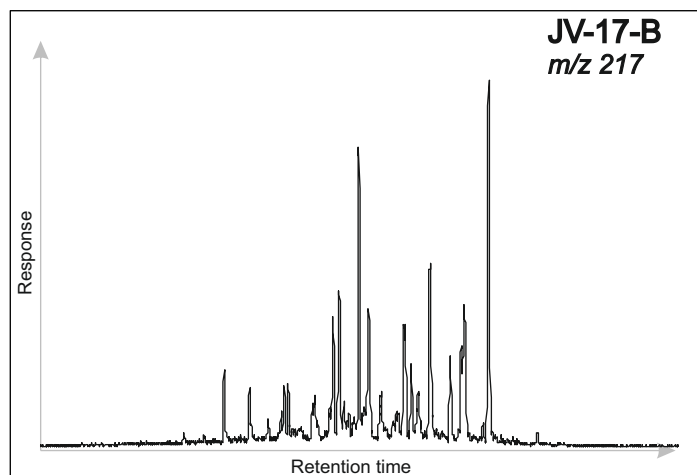
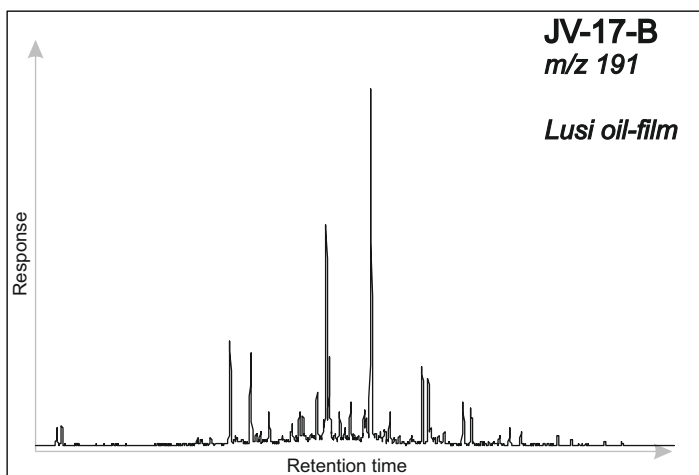
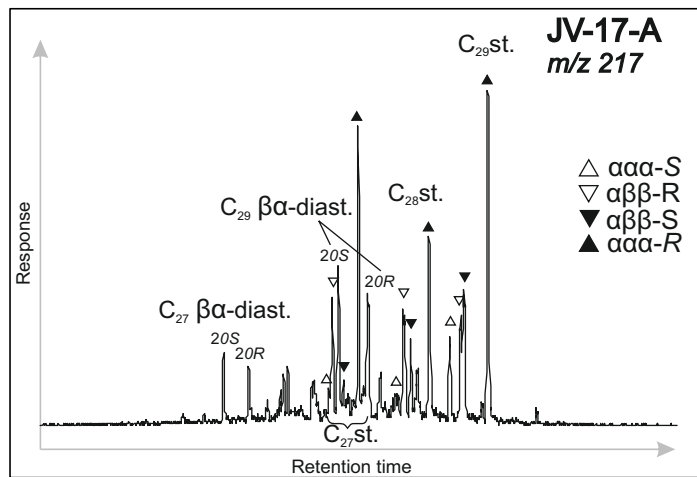
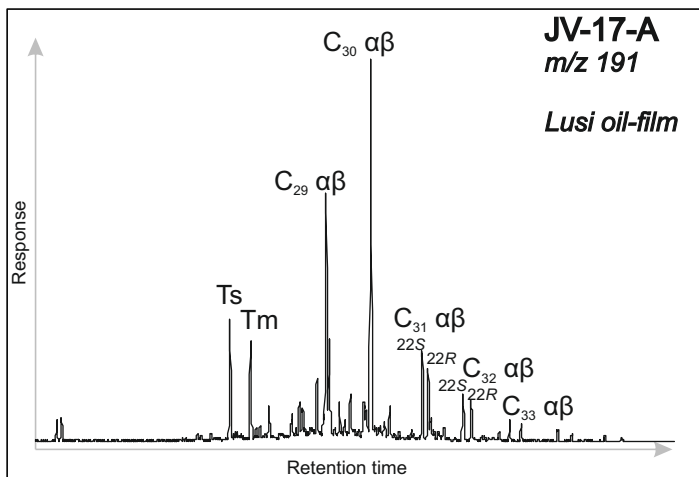
Sample ID	Group	Age	Before extraction						After Extraction						Ro, %	Bitum. extr-n yield (mg/g)	Lab	Hg (ppb)	Hg/TOC
			S_1 (mg/g)	S_2 (mg/g)	S_3 (mg/g)	T_{max} (°C)	PI	C_{org} (%)	C_{carb} (%)	S_1 (mg/g)	S_2 (mg/g)	S_3 (mg/g)	T_{max} (°C)	C_{org} (%)					
JV14B-11-01	GS	Plio.- Pleistocene	0.01	0.10	1.9	444	0.09	0.3								APT	14.0	41.2	
JV14B-11-03	GS		0.04	0.04	1.7		0.50	0.4								APT	7.8	20.0	
JV14B-11-04	GS		0.01	0.17	1.8	438	0.06	1.0								APT	47.0	49.0	
JV14B-11-05	GS		0.01	0.17	3.3	441	0.06	0.5								APT	23.5	43.5	
JV14B-11-06	GS		0.00	0.23	2.3	419	0.00	0.6								APT	13.0	21.3	
JV14B-11-09	GS		0.03	0.23	3.2	437	0.12	0.9								APT	25.5	29.0	
JV14B-11-10	GS		0.03	0.05	2.7		0.38	0.6								APT			
JV14B-11-11	GS		0.02	0.37	1.4	426	0.05	2.0								APT	24.5	12.3	
JV14B-02-01	GS		0.01	0.10	1.4		0.09	0.5								APT			
JV15-06-08	GS		0.04	0.10	0.5		0.29	1.3								APT			
JV15-06-09	GS		0.11	0.18	0.8		0.38	1.2								APT			
JV15-06-10	GS		0.07	0.25	0.6		0.22	1.1								APT			
JV15-GS	GS		0.01	0.14		442	0.07	0.3								BGR	4.7	18.8	
JV-17-01-39	GS		0.21	1.23	3.1	437	0.15	0.8								BGR	16.0	19.2	
JV-17-01-40	GS	Plio.- Pleistocene	0.13	1.11	1.3	423	0.10	1.0								BGR	20.0	21.0	
JV14B-02-02	GS	Miocene	0.00	0.11	1.9		0.00	0.5								APT			
JV17-01-02	GS	Miocene?	0.09	0.20	0.8		0.3	0.5								BGR	1.9	4.0	
JV17-01-08	GS	Miocene?	0.31	0.63	0.1		0.3	0.8								BGR	2.9	3.5	
JV15-06-02	BS		0.09	2.08	0.5	445	0.04	3.4								APT	1.0	0.3	
JV15-06-03	BS		0.47	3.12	1.1	441	0.13	14.1								APT	1.6	0.1	
JV15-06-05	BS		0.08	0.16	0.5		0.33	1.6								APT	1.0	0.6	
JV15-06-06	BS		0.38	7.79	0.5	442	0.05	8.3								APT	1.0	0.1	
JV15-06-07	BS		0.35	3.85	0.6	441	0.08	5.9								APT	5.1	0.9	
JV15-BS	BS	Eocene-	0.85	7.89		444	0.10	12.0								BGR	2.4	0.2	
JV-16-29-01	BS	Oligocene	10.16	21.24	0.2	443	0.32	9.2								BGR	1.0	0.1	
JV-16-29-04	BS		19.80	27.90	0.1	442	0.42	14.6								BGR	8.5	0.6	
JV-17-01-01	BS		0.89	1.69	0.1	426	0.34	2.6								BGR	1.0	0.4	
JV-17-01-10	BS		7.00	8.90	0.1	432	0.44	6.9								BGR	8.3	1.2	
JV-17-01-15	BS		15.52	22.33	0.2	440	0.41	8.6								BGR	1.9	0.2	
JV-17-01-37	BS		7.89	12.70	0.2	441	0.38	4.8								BGR	1.0	0.2	

Supplementary Figure S1. Reconstructed chromatograms of the Gas Chromatography – Mass Spectrometry (GC-MS) traces m/z 191 and m/z 217 for the bitumen extracts of the black shales (BS) and grey shales (GS), oils from the HC fields and Lusi oil films.









Manuscript 3: Extensive oil discharge ongoing at the Lusi mud eruption, Indonesia

A. Zaputlyeva, A. Mazzini, H. Svensen

(draft to be submitted)

